Grassland responses to global change: Diversity loss and compositional shifts across sites and scales

By

EVAN ELLIOT BATZER

DISSERTATION

Submitted in partial satisfaction of the requirements for the degree of

DOCTOR OF PHILOSOPHY

in

ECOLOGY

in the

OFFICE OF GRADUATE STUDIES

of the

UNIVERSITY OF CALIFORNIA
DAVIS

Approved:

(Valerie Eviner), Chair

(Susan Harrison)

(Andrew Latimer)

Committee in Charge

2020

Acknowledgements

All of the research I completed in pursuit of a PhD was conducted among a network of friends and mentors, without whom none of this work would have been possible.

I chose to attend Davis in response to the affability and enthusiasm that my advisor, Valerie Eviner, displayed in our first conversations In retrospect, I am very fortunate to have joined a lab that emphasized both scientific rigor and personal growth. Valerie's support was crucial to all elements of my graduate education, encouraging me to pursue research in subjects that I found compelling while also refocusing my wandering interests. Most importantly, Valerie was always an advocate for my individual pursuits. Her support was essential to the path I took through graduate school, which allowed me to focus on my own development as a researcher and scientist.

I am deeply grateful to the support offered by the rest of the Eviner lab. Ben Waitman, Joanne Heraty, Sherly Castro, Julia Michaels, Brianne Palmer, David Mitchell, and Maggie Shepherd were important sources of companionship and acted as sounding boards for many projects. Sara Gaffney, Julea Shaw, and Jonah Weeks – the Sisterhood of the Traveling Plants – have been an incredible source of support during much of my time in graduate school. I couldn't ask for better friends, collaborators, and travel companions.

Thank you to my guidance, qualifying exam, and dissertation committees — Susan Harrison, Andrew Latimer, Mary Cadenasso, Marcel Rejmanek, and Rick Karban – for their role in developing and refining my research ideas.

My work was strongly influenced by training provided by the UC Davis Statistics Department. The opportunity to pursue a statistics MS during my PhD was an invaluable source of knowledge that shaped many projects, ultimately making me a

better scientist. A big thanks to Chris Miller, who took a majority of these classes with me. I would have struggled greatly without our study sessions.

It's been a pleasure being part of the Graduate Group in Ecology at UC Davis. Holly Hatfield-Rogai, Elizabeth Sturdy, Matt Maelepeai, and JoAnna Lewis were a crucial to navigating all the technical aspects of the PhD program. A big thanks to Martha Wolfheil, Michael Culshaw-Maurer, and Ross Brennan for their work helping lead the Statistics Support Group, which was a highlight of the last couple years. To the whole of the GGE community, thank you so much for contributing to such a collegial and productive work environment.

Eric Seabloom, Elizabeth Borer, Ashley Asmus, Siddharth Bharath, and the rest of the Nutrient Network community were fantastic collaborators and field companions. I learned so much during sampling trips and annual meetings at the NutNet working group. The opportunity to work with such an engaged, collaborative group of researchers has been one of the highlights of my academic career.

I never would have been able to conduct my field research without the help of directors and staff at McLaughlin Reserve, Hopland REC, and Sierra Foothill REC. Cathy Koehler, Chuck Vaughn, and Dustin Flavell were instrumental in getting acquainted with California's grassland ecosystems. Thanks to Paul Aigner, Amber Shrum, John Bailey, Kim Rodrigues, and others for their assistance keeping my projects organized.

Generous funding support during my PhD was provided by the UC Davis Graduate Group in Ecology, Department of Plant Sciences, UC Natural Reserve System, Northern California Botanists, and the California Native Plant Society.

And finally, thank you to Alex McInturf, who has been a constant companion, editor, cycling partner, and general advocate for my own well-being. You have made these

last few years of my PhD among the most fun and rewarding. I will be forever grateful for your patience, kindness, and understanding.

To everyone that contributed to my time in graduate school – thank you.

Abstract

The recent history of the Earth's biosphere – the Anthropocene – is characterized by human activity. Increasingly, industrialization, land use change, fossil fuel combustion, and other drivers have altered key biological processes that govern the composition and function of natural communities. Among the two most impactful stressors are increased concentrations of limiting soil nutrients and shifting patterns of temperature and precipitation through climate change. Grasslands, like many plant ecosystems, are highly sensitive to these changes. Their widespread distribution and importance to both conservation and human enterprise underscores the need to understand how these global changes operate in grassland systems. However, climate change and nutrient deposition are known to produce complex effects on plant community structure; to effectively predict vegetation change, studies must integrate across multiple stressors, mechanisms, and scales of interest. This dissertation contributes to a deeper understanding of these complexities through a synthesis of large-scale experimentation and novel statistical methodology.

Chapter 1 uses data from a global experimental cooperative – the Nutrient Network – to test contrasting hypotheses about compositional change driven by soil nutrient enrichment. While traditional perspectives on resource competition suggest that nutrient enrichment controls plant species abundances through increasing limitation by light, experimental evidence indicates that other mechanisms related to trade-offs in the use of specific soil resources may also be an important driver. Across 49 experimental sites, there was strong support for a "neutral" model, where plants respond similarly to the increased availability of soil nitrogen, phosphorous, or potassium. However, I also find that responses to treatments were more varied in sites charac-

terized by higher average productivity and pre-treatment light limitation. Together, these findings indicate that grassland responses to fertilization tend to be driven by a trade-off between belowground and aboveground resource use, yet the predictability of these effects will depend on the inherent productivity and community structure of a given site.

Chapters 2 and 3 focus on California grasslands. Chapter 2 explores the effects of nitrogen enrichment on plant community diversity at multiple scales of organization, highlighting how shifts in community structure and distribution shape observed diversity loss at different sampling areas. Most nutrient addition studies have utilized small-scale plots ($1m^2$), though it has been shown that the area sampled can have significant impacts on the direction or magnitude of observed results. While a few studies have demonstrated scale-dependence in effects on species richness, I expand upon these findings by relating effects across scales to impacts on total community richness, community evenness, and spatial organization of vegetation. I find that nitrogen enrichment rarely produces large-scale species extirpation, but effects on evenness are nearly constant across sampling areas. While large-scale coexistence processes may facilitate species persistence at large spatial extents, fertilization also prompts increases in individual spatial aggregation, which may produce species extirpation in the long term.

In Chapter 3, I evaluate changes in California grassland community composition in response to interannual variation in temperature and precipitation. In Mediterranean systems, the quantity and timing of rainfall is hypothesized to control turnover between distinct species groups. A key challenge to the evaluation of these species-climate relationships, however, is historical contingency in vegetation composition –

non-independence between species abundances in a given year and the year previous, caused by local seed pools, plant-soil feedbacks, and other priority effects. To quantify how climate and prior community composition interact, I employ a novel application of multi-state modeling to a long-term dataset. This approach expands on traditional methods, which qualitatively describe variation among a priori species groups, to directly quantify the number of discrete vegetation states within a system and the probability of transition between them. When applied to ten years of community observation across a range of climatic conditions, this method produced a revised partitioning of vegetation states: one "classic" species group was split into two separate states based on performance under extreme drought. In turn, climate patterns interacted with the emergent properties of each vegetation state to control which community types were most likely to dominate. Invasive species, for example, were unlikely to persist under drought; yet low precipitation only tended to favor vegetation transitions to a native dominated state when these species were previously seeded.

It is increasingly understood that integration across interacting sets of processes is needed to effectively understand the effects of global change on the diversity and composition of plant communities. Together, these three chapters highlight how local environmental characteristics, the scale of observation, and prior vegetation type combine to structure grassland responses to environmental changes. In doing so, my work contributes to a more complete understanding of ecological dynamics that is needed to better conserve and manage ecosystems in a rapidly changing world.

Contents

Abstract v

List of Tables x

List of Figures xiii

1 The "Neutral Theory" of Niche Dimensionality 1

Abstract . . . 3

Introduction . . . 4

Methods . . . 7

Results . . . 17

Discussion . . . 25

2 Nitrogen enrichment has scale-dependent effects on plant diversity in California grasslands. 30

Abstract . . . 30

Introduction . . . 31

Methods . . . 35

Results . . . 41

Discussion . . . 49

3 Climate drives transitions between vegetation states in California grasslands. 54

Abstract 54

Introduction 56

Methods 60

Results 66

Discussion 75

A Chapter 1 Supporting Information 81

B Chapter 2 Supporting Information 85

C Chapter 3 Supporting Information 94

References 100

List of Tables

1.1 Summary of semi major axis (SMA) regression model fits to each of 3 pairwise comparisons of response to fertilization treatment. A majority of models captured significantly more variation ($P < 0.05$) in response than models assuming no correlation between treatment responses; models with non-significant fits are denoted by superscript "ns". . . . 21

1.2 Mean coordinate position of functional groups along 1:1:1 vector ($\bar{y}$) and residual components ($\bar{b_1}$,$\bar{b_2}$). Superscripts correspond to significant ($P < 0.05$) contrasts between functional group means in each dimension. 21

2.1 ANOVA of linear mixed-effects models used to estimate changes in total aboveground biomass in response to fertilization treatment. Degrees of freedom were calculated using Satterthwaite Approximation, often yielding non-integer denominator degrees of freedom. Coefficients with statistically significant effects ($P < 0.05$) are highlighted with "*". 41

2.2 ANOVA of linear mixed-effects models used to estimate changes in light interception in response to fertilization treatment. Degrees of freedom were calculated using Satterthwaite Approximation, often yielding non-integer denominator degrees of freedom. Coefficients with statistically significant effects ($P < 0.05$) are highlighted with "*". 43

3.1 Species mixtures used in initial plot seeding. Distinctions between "Native", "Naturalized", and "Invasive" species groups reflect species origins in California grasslands. 62

3.2 Results of indicator species analysis following K-medoids clustering. High values of the indicator species statistic reflect strong associations between a taxon and a given state assignment. P-values calculated using 1,000 permutations. 69

3.3 Parameter estimates of the best fit multi-state model (Model 6). For each state assignment, potential state assignments in subsequent years (Transitions) and their associated probabilities (with 95 percent confidence intervals) are reported. Covariate effects reported as hazard ratios, where superscripts correspond to statistical significance: ' = P < 0.1; * = P < 0.05; ** = P < 0.01. 73

A.1 Table of sites included in analysis. 83

A.2 Table of sites, pairwise correlations between community responses to different treatments (ρ), rate of community change in response to treatment (Δ), and estimated response dimensionality (D). Significant (P < 0.05) magnitudes of community response are labelled with *. . . . 84

B.1 Taxon abbreviations and functional types in pre-treatment sampling . 89

B.2 PERMANOVA of Compositional Variation – MCLA 89

B.3 PERMANOVA of Compositional Variation – SFREC 90

B.4 Summary of identified species, functional group, origin (native/introduced) mean cover in control plots, and average net change in treatment (+N) plot at MCLA. Sorted by mean relative cover in control plots in 2019 sampling. 92

B.5 Summary of identified species, functional group, origin (native/introduced) mean cover in control plots, and average net change in treatment (+N) plot at SFREC. Sorted by mean relative cover in control plots in 2019 sampling. 93

C.1 Permutational ANOVA (PERMANOVA) output of variance in plot community composition in the first year of sampling. 94

C.2 Rank summary table of performance across different clustering indices. 94

C.3 Contingency table of observed transitions between state assignments between 2008-2018. For each plot observation of a state assignment in year t (rows), data shows the frequency of state assignments (columns) of the same plot in a subsequent year (t + 1). Diagonal values represent the frequency of a given state retaining its assignment (persistence), while off-diagonal values represent transitions in state assignment. Changes in assignment frequency were highly non-random (χ^2 = 392.017, df = 9, P < 0.001). 96

C.4 AIC model comparison used to select the best fit multi-state model from a series of candidates. Covariates include "Priority Effects" – the effect of initial seeding mixture representation of indicator species correlated with cluster assignments – and "1-", "2-", and "3-year SPEI" – a standardized measure of drought stress computed over 1, 2, and 3 cumulative water year intervals, respectively. DF corresponds to the number of parameters estimated within the transition matrix, including baseline transition probabilities and effects of covariates. 96

List of Figures

1.1 Conceptual diagram illustrating the method used to assess dimensionality of community enrichment response.
(a) *Bivariate relationships between responses*: In this hypothetical example, a community of 3 species is subject to enrichment by three different resources. Estimated responses to these nutrients are standardized such that the total magnitude of community response to each nutrient is of unit length.
(b) *Three-dimensional representation of responses*: The responses above are presented as a three-dimensional plot, with the vector y representing the null hypothesis. The vector of responses estimated for each species, x, is projected onto y, producing the projection, a, and rejection, b In this community, strong positive correlation across all three treatment dimensions yielded low overall response dimensionality, D = 0.04.
(c) *Two-dimensional plot of rejection vectors*: Residual elements of the response vector not captured by projection onto y may be visualized in two dimensions, b_1 and b_2. 11

1.2 (a) Frequency of sites exhibiting significant ($P < 0.05$) effects of nutrient (N, P, or Kμ) fertilization on plant community composition. Of 49 total sites, 37 showed significant compositional changes to at least one of three fertilization treatments, while 12 sites showed non-significant compositional responses to all nutrient manipulations.
(b) Rate of estimated fertilization-driven change in species composition, prior to standardization of response coefficients. The rate of total compositional change was calculated as the magnitude of the vector of estimated species response coefficients, as net Euclidean change in log_2_-transformed community cover per year of treatment. Higher values indicate greater overall rate of compositional change. 18

1.3 Visualization of pairwise relationships between plant responses to nutrient addition treatments. Each point refers to a unique site x species combination, colored by functional group. Lines correspond to results of semi major axis (SMA) regression applied to each functional group. 20

1.4 (a) Three-dimensional visualization of species responses to nutrient enrichment across all sites, with line corresponding to 1:1:1 vector (y) assuming proportionally equal responses.
(b) Residual deviation from 1:1:1 vector displayed in two dimensions (b1, b2) orthogonal to y. Points are colored by functional group with 95% confidence ellipses centered on group means. 22

1.5 Visual representation of structural equation model (SEM) used to evaluate pre-treatment site factors that explain variation in community response dimensionality (D) following multiple nutrient enrichment. All statistically significant ($P < 0.05$) pathways are presented. Solid lines correspond to positive effects, while dashed lines correspond to negative effects. Chi-square test statistic = 23.408 on 20 degrees of freedom indicates close model-data fit ($P = 0.269$; Comparative Fit Index = 0.943). 24

2.1 Study site locations and sampling design. Site 1: McLaughlin Natural Reserve (MCLA). Site 2: Sierra Foothill Research and Extension Center (SFREC). In each site, we established 4 blocks consisting of 10x10m paired plots randomly subject to nitrogen enrichment (+N). Within each plot, we constructed a grid of sixty-four 0.5x0.5m subplots with a 1m boundary to plot edges. 36

2.2 Effects of fertilization on (a) total aboveground biomass and (b) canopy light interception, colored by treatment. Large points correspond to mean values across all plots with associated Bonferroni-adjusted 95% confidence intervals. Small points reflect plot-level means. Statistically significant differences in means ($P < 0.05$) are highlighted with "*". 42

2.3 Species accumulation curves (SACs) depicting the cumulative number of observed species as a function of sampling effort, presented on untransformed (a) and log scales (b). Accumulation curves presented were generated through spatially explicit sample accumulation ("empirical" SACs), where samples are accumulated in order of proximity to the starting sample. Bolded lines represent the mean SAC across all treatment and control plots in each year; standard lines correspond to individual plots across all sites in each year. 44

2.4 Changes in community diversity at α (subplot), β, and γ (plot) scales using multiplicative diversity partitioning using Hill diversity indices. Diversity was calculated as function of species richness ($Q = 0$) and abundance-weighted diversity ($Q = 2$). Effects are presented as log response ratios of each diversity metric within blocks. Black points correspond to mean effect across all blocks, with Bonferroni-corrected 95% confidence intervals generated using 10,000 bootstrap samples. Colored points correspond to estimated effects within each block. Statistically significant effects are highlighted, "*", when 95% confidence intervals do not overlap 0. 46

2.5 Effect of fertilization on the proportion of subplots occupied by species, relative to average subplot cover. Lines correspond to mean relationship reported by mixed-effects logistic regression, after accounting for random variance across species and blocks within sites (2018 data not shown). Treatment effects indicate significant decreases in occupancy relative to cover in the second and third year of treatment (2018: $Z = -0.274$, $P < 0.001$; 2019: $Z = -0.288$, $P < 0.001$). Effects on occupancy were not significant in the first year of treatment (2017: $Z = -0.008$, $P = 0.803$). 47

2.6 Effect of fertilization on species richness and spatial aggregation as a function of sampling scale in 2019, presented as a log response ratio. In subplot 5a, the solid black line corresponds to mean estimated effects under spatially explicit ("empirical") sample accumulation, while dashed line reflects the median value of mean diversity effects under randomized sample accumulation. Shaded areas correspond to Bonferroni-adjusted 95% confidence intervals of mean diversity response across 10,000 random sample accumulation curves. Colored lines denote individual responses of each block. In subplot 5b, lines correspond to the net effects of spatial aggregation on estimated response, calculated as the observed log-response ratio relative to the median value across bootstrap samples. The shaded area depicts Bonferroni-adjusted 95% confidence intervals of aggregation effects on mean diversity response across 10,000 random sample accumulation curves. 48

3.1 Visualization of clustering assignments following K-medoids clustering. Non-metric multidimensional scaling (NMDS) ordination was conducted on all community observations from 2008 – 2018 (n=560). Pairwise community distance was calculated using Bray-Curtis dissimilarity index. Species vectors correspond to taxa that were found to be significantly associated ($P < 0.05$) with state assignments using indicator species analysis. 68

3.2 Variation in total water year drought severity (A) and frequencies of state assignments (B) from 2008-2018. Average drought stress (SPEI = 0) between 1983-2008 is presented as a dotted line in panel A. Drought in California from 2012-2016 included several years of substantially below-average water availability, including a single year with recorded drought stress greater than two standard deviations beyond historic norms (SPEI < -2). 70

3.3 State-transition representation of fitted multi-state model coefficients at baseline, assuming no effects of seeding composition and average drought stress (SPEI = 0). Labels refer to the probability a plot transitions between 2 different state assignments (arrows) or the probability a plot retains its assignment (circles) in consecutive years. Circles and arrows are scaled in diameter or color, respectively, by the probability of state assignment transition. 72

3.4 The effects of temporal priority and drought stress on the probability of transition of a plot to the Native Perennial state given other previous state assignments. Transition probabilities presented are a function of drought stress (SPEI) and whether native species were included/absent from the seeded species mixture (+/- Priority). Solid lines indicate significant ($P < 0.05$) covariate effects of both SPEI and priority; dashed lines correspond to non-significant effects. 74

A.1 Bivariate relationships between treatments colored by species lifespan. 82

A.2 Bivariate relationships between treatments colored by provenance (introduced / native). 82

B.1 Mantel correlograms demonstrating spatial autocorrelation in plant community composition using pre-treatment data. In both sites, statistically significant ($P < 0.05$) autocorrelation in community composition was detectable to a scale of roughly 2-3 meters. Difference in community composition was calculated using Bray-Curtis dissimilarity and Pearson correlation. Significance tests were perforumed using 999 sample permutations, with P-values adjusted using the Holm correction. 86

B.2 Relative abundances of species in pre-treatment sampling, top 15 most abundant species shown. Values reflect maximum cover observed in three sampling periods to account for variable phenology. 87

B.3 Effect of fertilization on species richness and spatial aggregation as a function of sampling scale in 2017 and 2018, presented as a log response ratio. In subplot a, the solid black line corresponds to mean estimated effects under spatially explicit ("empirical") sample accumulation, while dashed line reflects the median of mean diversity effects under randomized sample accumulation. Shaded areas correspond to Bonferroni-adjusted 95% confidence intervals of mean diversity response across 10,000 random sample accumulation curves. Colored lines denote individual responses of each block. In subplot b, lines correspond to the net effects of spatial aggregation on estimated response, calculated as the observed log-response ratio relative to the median value across bootstrap samples. Shaded areas correspond to Bonferroni-adjusted 95% confidence intervals of aggregation effects on mean diversity response across 10,000 random sample accumulation curves. 88

B.4 NMDS visualizations of variation in species cover data at MCLA summarized at the block level. Points are colored by year, with varying shape according to treatment. Lines link treatment and control plots within each block-year combination. Residualized NMDS was generated by first accounting for effects of block and year variation, then plotting the residual distance matrix. 90

B.5 NMDS visualization of variation in species cover data at SFREC summarized at the block level. Points are colored by year, with varying shape according to treatment. Lines link treatment and control plots within each block-year combination. Residualized NMDS was generated by first accounting for effects of block and year variation, then plotting the residual distance matrix. 91

C.1 Visualization of clustering assignments following K-medoids clustering. Non-metric multidimensional scaling (NMDS) ordination was conducted on all community observations from 2008 – 2018 (n=560). Pairwise community distance was calculated using Bray-Curtis dissimilarity index. Species vectors correspond to taxa that were found to be significantly associated ($p < 0.05$) with state assignments using indicator species analysis. 97

C.2 Relative abundance of species across vegetation state assignments. Values refer to the average abundance of each species (+/- standard error) for observed communities assigned to each state. Species that served as significant ($P < 0.05$) indicators of each state type are highlighted using "*" and colored by representative state. On average, indicator species of each vegetation state accounted for 75% of the cumulative relative abundance of observed communities. 98

C.3 Plot-level shifts in state assignment over time. For each observed community (grid cell), the state assignment of a community is presented as a function of initial seeding treatment (row) and time (column). . 99

Chapter 1

The "Neutral Theory" of Niche Dimensionality

Evan E. Batzer[1*], Siddharth Bharath[2], Elizabeth Borer[2], Stan Harpole[3], Carlos Alberto Arnillas[4], Miguel Bugalho[5], Maria Caldeira[6], Oliver Carroll[7], Mick Crawley[8], Kendi Davies[9], Pedro Daleo[10], Johannes Knops[11], Kimberly Komatsu[12], Andrew MacDougall[7], Rebecca L. McCulley[13], Jason P. Martina[14], Brett Melbourne[9], Timothy Ohlert[15], Sally A. Power[16], Suzanne Prober[17], Christiane Roscher[3,18], Mahesh Sankaran[19,20], Glenda Wardle[21], George Wheeler[22], Peter Wilfhart[2], and Eric Seabloom[2].

1. Department of Plant Sciences, University of California, Davis, USA
2. Department of Ecology, Evolution, and Behavior, University of Minnesota, USA
3. Department for Physiological Diversity, German Centre for Integrative Biodiversity Research (iDiv), Germany
4. University of Toronto at Scarborough, Canada

5. Centre for Applied Ecology (CEABN-InBIO), University of Lisbon, Portugal
6. Forest Research Centre, School of Agriculture, University of Lisbon, Portugal
7. Imperial College London, Silwood Park, UK
8. University of Guelph, Canada
9. Department of Ecology and Evolutionary Biology, University of Colorado, Boulder, USA
10. Instituto de Investigaciones Marinas y Costeras (IIMyC), CONICET – UNMDP, Argentina
11. Department of Health & Environmental Sciences, Xi'an Jiaotong Liverpool University, Suzhou, China
12. Smithsonian Environmental Research Center, Edgewater, USA
13. Department of Plant and Soil Sciences, University of Kentucky, Lexington, USA
14. Deoartment of Biology, Texas State University, USA
15. Department of Biology, University of New Mexico, USA
16. Hawkesbury Institute for the Environment, Western Sydney University, Australia
17. CSIRO Land and Water, Australia
18. UFZ, Helmholtz Centre for Environmental Research, Physiological Diversity, Germany
19. National Centre for Biological Sciences, TIFR, India
20. School of Biology, University of Leeds, UK
21. School of Life and Environmental Sciences, University of Sydney, Australia
22. School of Biological Sciences, University of Nebraska, Lincoln, USA

Abstract

Increases in the availability of limiting soil nutrients are known to produce changes in plant community diversity and composition. Among locally interacting species, this change is tied to competitive trade-offs across gradients of resource availability. Plant responses to fertilization are often thought to be mediated through aboveground competition, where effective competitors are better able to intercept available light. However, plant communities are often subject to simultaneous limitation by multiple nutrients, which may lead to multidimensional trade-offs in the use of individual belowground resources. Depending on the contributions of these two mechanisms to species interactions, treatment effects may vary in their dimensionality – the degree to which community responses to fertilization can be captured across a single axis of change. Using data from a globally replicated nutrient addition experiment, we assessed the dimensionality of community response to fertilization across three different resource addition treatments. Across all studies, species responses to nutrient enrichment were broadly consistent across multiple enrichment treatments, suggesting that fertilization often acts on a one-dimensional trade-off governed by light limitation. However, we also found significant deviations from this general relationship across plant functional groups and local contexts; sites characterized by high pre-treatment productivity and legume abundance exhibited more variation in the direction of community change across treatments. Our findings suggest that while broad functional trade-offs may predominate at a global scale, community responses to fertilization are likely to depend on site-specific variation in coexistence mechanisms.

Introduction

Human alterations of the earth's biogeochemical cycles have produced widespread changes in the availability of key nutrients known to control plant productivity (Vitousek et al. 1997a, Elser et al. 2007). Increased concentrations of soil nutrients are recognized as important drivers of compositional change in plant communities, resulting in altered patterns of abundance and diversity (Tilman 1984, Tilman and Lehman 2001). In turn, these effects on community structure are implicated in changes to key ecosystem properties, including reductions in resilience, resistance, and loss of multifunctionality (Chapin et al. 2000, Hector and Bagchi 2007, Isbell et al. 2015). Nutrient enrichment is thought to control plant community composition through environmental shifts that operate on niche differences among interacting species. Given that photosynthetic organisms compete for a similar set of limiting resources (Hutchinson 1961), plant coexistence is likely mediated by trade-offs in resource use that produce variable fitness across environments. It is through these trade-offs that nutrient enrichment drives changes in plant abundance, favoring species that are better able to exclude their competitors under elevated nutrient conditions (Tilman 1984). To effectively predict compositional shifts following nutrient enrichment, it is thus essential to identify the specific mechanisms that govern plant responses. In many cases, fertilization is linked to a shift between soil nutrients and light as the primary limiting factor for plant growth (Tilman 1984, Dybzinski and Tilman 2007, Hautier et al. 2009, Borer et al. 2014, Clark et al. 2018). The increased abundance of taller species under elevated nutrient inputs suggests a one-dimensional trade-off where plants are differentiated by their ability to acquire belowground resources or intercept available light (Hautier et al. 2009, DeMalach et al. 2017). However, fertilization effects may

not be limited to a single driver. Plants are also known to be limited by (and compete for) multiple belowground resources, even in high productivity contexts (Wilson and Tilman 1991, Fay et al. 2015, Harpole et al. 2016). As a result, biodiversity loss may also stem from multi-dimensional trade-offs in the use and acquisition of individual soil nutrients. In this perspective, plant responses to fertilization are governed by variation in species' ability to utilize specific soil resources, such nitrogen, phosphorous, potassium, or other micronutrients (Harpole and Tilman 2007, Harpole et al. 2016). While trade-offs mediated by light competition or the use of individual soil resources explain declines in species richness following fertilization, there exist few tests of their relative contribution to observed effects (but see DeMalach and Kadmon (2017) and Harpole et al. (2017)). However, these mechanisms present distinct predictions related to the dimensionality of community change across different nutrient enrichment treatments. Under a one-dimensional trade-off mediated by light competition, the addition of any limiting belowground resource will shift species abundances across a single axis. As a result, treatment effects will be directionally equivalent in response to the enrichment of different soil resources. Nutrient-specific trade-offs, however, predict that fertilization effects depend on resource identity, leading to high-dimensional (dissimilar) shifts in composition that vary as a function of the specific soil nutrient added.

Observed patterns of plant niche differentiation offer lines of evidence supporting predictions of both one-dimensional and multi-dimensional patterns of change. At a global scale, conserved patterns of tissue stoichiometry (Ågren 2008) and dominant axes of plant functional variation (Díaz et al. 2016) suggest that one-dimensional trade-offs are likely to predominate – plant growth strategies may be expected to confer increased fitness under elevated nutrient concentrations generally, rather than

varying in response to specific fertilization treatments (Grime 2006). However, outcomes of plant competition are the result of relative differences in resource use among interacting species (Tilman 1982a). Depending on community context, variation in plant nutrient demands and functional strategies may drive resource-specific trade-offs. Critically, performance under variable nutrient concentrations only forms a subset of the possible forms of niche differentiation in plant communities. Correlated patterns of variation in plant functional characteristics and abundance suggest several key ways in which niche differentiation commonly occurs (Grime 2006). Plants are theorized to exhibit trade-offs between competition and colonization (Tilman 1994, Pacala and Rees 1998), herbivore defense and growth (Mattson and Herms 1992), and between leaf longevity and photosynthetic rate (Wright et al. 2004, Reich 2014). Depending on the strength of these other mechanisms, constraints on plant function and physiology may limit the development of nutrient-specific trade-offs; varied responses to different nutrient enrichment treatments may be more common in systems where belowground resource competition acts as an important coexistence mechanism (Passarge et al. 2006, Brauer et al. 2012, Hautier et al. 2018). For example, multi-dimensional trade-offs may be limited in systems characterized by stressful environmental conditions or reduced functional diversity that limit specialization on specific soil resources (Suding et al. 2005, Dwyer and Laughlin 2017). Evaluation of the direction of compositional response to nutrient enrichment, broadly and in site-specific contexts, may identify mechanisms responsible fertilization-driven biodiversity change. Here, we use a globally distributed experiment manipulating the availability of belowground resources to determine if there are tradeoffs in species responses to multiple nutrients. In a geometric approach, we compare observed community response dimensionality to a neutral expectation in which species exhibit

proportionally identical responses to the enrichment of multiple soil nutrients. Deviations from this neutral model provide a metric to quantify the importance of tradeoffs that may drive diversity changes in response to increased nutrient supply rates.

We hypothesize that community responses to fertilization will be less varied (more one-dimensional) in spatially or temporally heterogeneous systems and those of lower productivity, where specialization on individual soil nutrients is unlikely to form an important axis of niche differentiation. In contrast, we expect multi-dimensional tradeoffs in belowground resource use to be more important in in taxonomically diverse, productive, spatially homogenous environments. Quantification of these patterns forms a critical tool to infer how local coexistence mechanisms control community responses to global change and improve predictions of their effects.

Methods

Study Sites

We examined 49 study sites that are part of the Nutrient Network, a cooperative, globally distributed experiment (Borer et al. 2014a). Nutrient Network study sites are constructed in a randomized block design, typically composed of 3 blocks divided into 5m x 5m plots. In each block, we selected four plots to be used in experimental analysis: control plots with no supplemental nutrient enrichment and plots subject to fertilization of either nitrogen (N), phosphorous (P), or potassium with other micronutrients (Kμ), yielding 12 – 20 plots per site.

All nutrient enrichment treatments were applied at a rate of 10 g N, P, or K m-2 year-1 as time-release urea, triple-super-phosphate, and potassium sulfate, respectively. A

micronutrient mix (17% Fe, 12% S , 6% Ca, 3% Mg, 2.5% Mn, 1% Zn, 1% Cu, 0.1% B, and 0.05% Mo) supplied as part of the Kμ treatment occurred only during the first treatment year at a rate of 100g m-2 to avoid accumulation toxicity. Because sites were initialized at different years and observed for different durations, we filtered our dataset to focus on sites with at least 5 years of treatment, a sufficient number of treatment years to have confidence in observed community responses. All sites used in this analysis also included a pre-treatment year (Median = 9.36, Min = 5, Max = 13), which was used to establish baseline community composition metrics used in structural equation modeling. A full list of sites and their characteristics is presented in Appendix Table A.1.

Response Measurements

In each 5m x 5m plot, a 1m x 1m subplot was designated for community observation. Observers evaluated community composition annually, visually estimating areal cover of all species to the nearest 1 percent. Cover for each species was estimated independently, yielding total cover values that often exceeded 100% in vertically stratified communities. We focused our analysis on species with well-characterized responses to nutrient enrichment by including taxa that were observed in all treatments and present in at least 33% of all community observations within a site. Our filtering criteria included species across a range of mean abundance, and in most sites, captured a large proportion of the total observed community cover in control plots (Median = 0.88, Min = 0.36, Max = 0.99). To evaluate relationships between plant life history strategy and fertilization response, species were divided into four functional groups: graminoids (order Poales), legumes (family Fabaceae), woody species, and forbs. At

each site, plants were also characterized by local longevity (annual / biennial / perennial) and provenance (native / introduced).

In most sites, photosynthetically active radiation (PAR) was measured using a ceptometer placed above the grassland canopy and at the soil surface. Light interception was estimated as the fraction of available PAR above the canopy relative to available PAR on the soil surface.

In a separate subplot, aboveground biomass was collected yearly in two 1m x 10cm strips of vegetation, air dried to a constant mass at 60^{o} C, and weighed to the nearest 0.01 g. Biomass harvest locations were moved each year, to avoid effects of the destructive sampling. In the first year of study, 250g of soil was collected to estimate pre-treatment soil nutrient availability. Soil was analyzed for total %C and %N using dry combustion gas chromatography (COSTECH ESC 4010 Element Analyzer) at the University of Nebraska. Assessment of elemental soil phosphorous, potassium, soil pH, and soil texture were performed at A&L Analytical Laboratory in Memphis, TN. For more detail, please visit http://www.nutnet.org/exp_protocol.

Estimation of Treatment Response

Given that species abundances often form lognormal distributions in natural communities, raw species abundances were log¬2-transformed prior to model fitting (Anderson et al. 2006). Transformation yielded stronger adherence to model assumptions while providing a natural scale for model responses, where a coefficient value of 1 corresponds to a doubling in abundance per unit change of a given covariate. To estimate species responses to fertilization treatment, we fit multiple linear regression

models to community composition data from each site:

$$\mathbf{Y} = \mathbf{XB} + \mathbf{E}$$

Where $\mathbf{Y}$ is an $[nxs]$ matrix of abundances of all s species present within a site, $\mathbf{X}$ is an $[n \times p]$ matrix of covariates, $\mathbf{B}$ is a $[p \times s]$ matrix of coefficients, and $\mathbf{E}$ is an $[nxs]$ matrix of residuals. For sites containing three nutrient treatments, i plots, and j years, the coefficient matrix consists of the following terms:

$$\mathbf{B} = [\beta_N, \beta_P, \beta_K, \beta_{Plot_1}, ...\beta_{Plot_i}, \beta_{Year_1}, ...\beta_{Year_j}]$$

where community abundance is estimated as a function of the quantity of fertilizer added in observation (expressed as the number of years of treatment), interannual variation in site-level species abundance (encoded as a factor variable), and plot-level variation in species abundance (encoded as a factor variable). Plot and year terms in this model formula act to de-trend species abundances, providing estimates of responses to nutrient enrichment while accounting for other sources of spatial and temporal variation in community composition.

Significance of model terms was evaluated using permutation-based ANOVA. We ordered model terms in an ANOVA with type "I" sums of squares to account for the spatial and temporal variation in community composition before testing for effects of fertilization treatment.

Response Dimensionality

While multivariate linear modelling approaches may be used to estimate the rate of

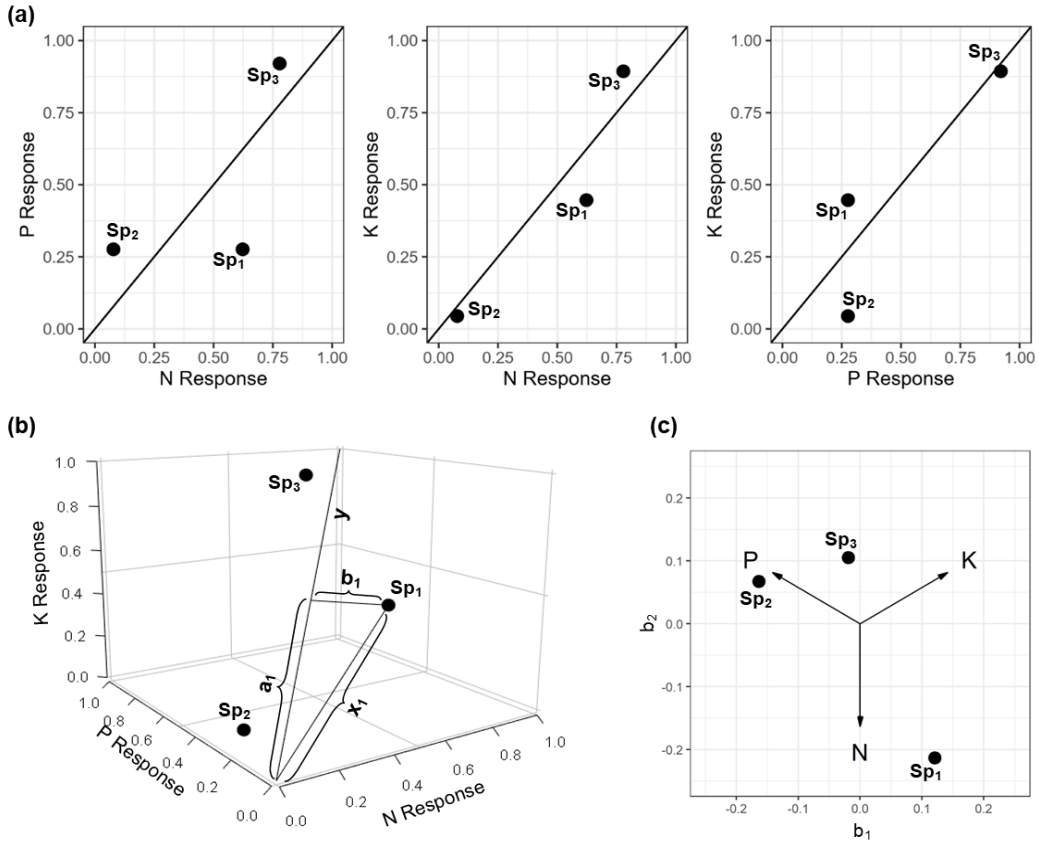

Figure 1.1: Conceptual diagram illustrating the method used to assess dimensionality of community enrichment response.
(a) *Bivariate relationships between responses*: In this hypothetical example, a community of 3 species is subject to enrichment by three different resources. Estimated responses to these nutrients are standardized such that the total magnitude of community response to each nutrient is of unit length.
(b) *Three-dimensional representation of responses*: The responses above are presented as a three-dimensional plot, with the vector y representing the null hypothesis. The vector of responses estimated for each species, x, is projected onto y, producing the projection, a, and rejection, b In this community, strong positive correlation across all three treatment dimensions yielded low overall response dimensionality, D = 0.04.
(c) *Two-dimensional plot of rejection vectors*: Residual elements of the response vector not captured by projection onto y may be visualized in two dimensions, b_1 and b_2.

community change in response to treatment, their output does not provide a quantification of similarity among directions of change. To evaluate correlations among different trajectories of community response – proportional consistency across the responses of individual species that contribute to overall community response – we derive a geometric approach based on work of (Cardinale et al. 2009).

In the context of this study, we evaluate trajectories of community change based on experimental manipulations of three limiting nutrients – N, P, and Kμ. While the following description presents details for this three-dimensional case, our approach may extend to any n-dimensional set of treatments. First, we define $\mathbf{X}$ as a matrix describing the treatment responses (columns) of all S species observed in a community (rows). For simplicity in notation, we define each row vector consisting of the ith species responses to different treatments as x_i; column vectors describing the response of all species within the jth community to a given treatment as $x_{:,j}$.

$$\begin{array}{c|ccc|c} & Sp & Trt_1 & Trt_2 & Trt_3 & \\ \hline & \mathbf{1} & x_{1,1} & x_{1,2} & x_{1,3} & \mathbf{x}_1 \\ \mathbf{X} = & \mathbf{2} & x_{2,1} & x_{2,2} & x_{2,3} & = \mathbf{x}_2 \\ & \vdots & \vdots & \vdots & \vdots & \vdots \\ & \mathbf{S} & x_{S,1} & x_{S,2} & x_{S,3} & \mathbf{x}_S \end{array} = \mathbf{x}_{:,1} \quad \mathbf{x}_{:,2} \quad \mathbf{x}_{:,3}$$

In this study, $\mathbf{X}$ was composed of the three vectors of estimated nutrient response coefficients computed in multiple regression model, B.We captured to total magnitude of compositional change in response to treatments using the Euclidean (L_2) norm of

column (treatment response) vectors, defined as:

$$\|\mathbf{x}_{:,j}\| = \sqrt{\sum_{i=1}^{S} x_{i,j}^2}$$

Where i iterates over the S species present within each community.

To control for differences in magnitudes of change across treatments, column vectors were standardized through dividing by L_2 norm, such that $\|x_{:,j}\| = 1$. After standardization, community responses to treatment are equal in length, allowing for comparison between directions of change.

To compare potential trade-offs among different axes of environmental change, bivariate relationships may be used to illustrate correlated patterns of change between pairs of treatments (Figure 1.1a). To evaluate these bivariate relationships, we fit Semi Major Axis (SMA) regressions to each pairwise combination of treatments, which account for uncertainty in both X and Y variables not captured in Ordinary Least Squares (OLS) regression.

However, bivariate relationships do not provide an aggregate measure of similarity among variables in 3 or more dimensions. Instead, correlation among responses can be evaluated through projection onto a new coordinate basis. Conceptually, our approach is similar to dimensionality reduction through Principal Component Analysis (PCA). Rather than defining the first Principle Component through eigenvalue decomposition, axes are pre-specified under a null hypothesis. We define this null model as a "neutral" expectation where the effects of nutrient enrichment are one-dimensional, resulting in trajectories of community change that are directionally equivalent. While the total magnitude of effect may vary, our null model assumes

that species exhibit proportionally equal responses to multiple nutrient enrichment treatments.

First, we define a vector of 1's, $\mathbf{y}$, to form an estimate of species responses under our "neutral" null hypothesis. Under this neutral expectation, proportionally equal responses to treatment will be perfectly captured by variation along this 1:1:1 vector (Figure 1.1b).

To evaluate the degree to which this null hypothesis captures the responses of species i, we define a vector, a, as the projection of observed responses onto the 1:1:1 vector, $\mathbf{y}$:

$$\mathbf{a}_i = \frac{\mathbf{y} \cdot \mathbf{x}_i}{\|\mathbf{y}\|}$$

The orthogonal compliment of the projection, $\mathbf{b}$, defines the elements of $\mathbf{x}$ not captured by projection onto $\mathbf{y}$:

$$\mathbf{b}_i = \mathbf{x}_i - \mathbf{a}_i$$

The fraction of variance in species response that is captured by this projection is thus defined as the ratio of squared norms (sums of squares) of $\mathbf{a}$ and $\mathbf{x}$:

$$D = 1 - \frac{\|\mathbf{a}_i\|^2}{\|\mathbf{x}_i\|^2}$$

Under our null hypothesis, the set of responses observed for species i, $\mathbf{x}_i$, will be of equal magnitude to the projection, $\mathbf{a}_i$,. The proportional magnitude of these vectors thus serves as a measure of response dimensionality for a given species, i.

Extending this method to all S observed species gives an aggregate measure of com-

munity dimensionality, bounded between 0 and 1:

$$D = 1 - \frac{\sum_{i=1}^{S} \|\mathbf{a}_i\|^2}{\sum_{i=1}^{S} \|\mathbf{x}_i\|^2}$$

Where dimensionality (D) is equal to one minus the ratio of summed magnitudes of change when projected on y over their observed magnitudes. When trajectories of community change are directionally identical (low dimensional), response vectors will be perfectly captured by this projection ($D = 0$). Orthogonal responses (high dimensional), where community responses to treatment are uncorrelated, will be poorly captured by this projection ($D = 1$). When possible, elements of the rejection, $\mathbf{b}$, may be used to visualize deviations from this 1:1:1 line (Figure 1.1c). In this study, we project this rejection component to two other dimensions orthogonal to $\mathbf{y}$, constituting a change of basis. Thus, the overall projection onto y and residual coordinates may be expressed as $XP^\top$, with projection matrix:

$$\mathbf{P} = \begin{array}{ccc} y & b_1 & b_2 \\ \hline 0.577 & 0 & -0.816 \\ 0.577 & -0.707 & 0.4082 \\ 0.577 & 0.707 & 0.4082 \end{array}$$

Where column vectors above are standardized to unit length.

Structural Equation Modeling

To capture variation in site-level community properties and abiotic characteristics, we generated a series of derived variables to supplement observations made during

sampling. Climate characteristics were obtained from each site using BioClim, a publicly available dataset of global climate layers. Following prior analyses of the Nutrient Network dataset (Grace et al. 2016), we chose to represent climatic effects on plant growth through site mean temperature at the wettest quarter of year (BIO8) and site mean precipitation during the warmest quarter of the year (BIO18).

Community properties were generated from compositional data collected during pre-treatment sampling. To estimate community spatial heterogeneity ("Species Turnover"), we calculated beta diversity using the ratio of site-level species richness to mean plot-level species richness ($\beta = \frac{\gamma}{\alpha}$). Pre-treatment community composition was also used to calculate the relative abundance of plant functional groups present within each site (e.g. "Legume Abundance"), defined as the mean proportion of total cover across all plots. Estimates of the total site species pool ("Species Pool') were calculated by the total number of unique species observed in the first 5 years of sampling, to account for varying durations of observation across sites.

From sites with complete data (n = 35), we used structural equation modeling (SEM) to evaluate hypothesized links between environmental characteristics, community properties, and the dimensionality of community response to fertilization ("Response Dimensionality"). In our initial model, we specified pathways capturing site resource limitation and community characteristics. We incorporated pathways between composite variables describing soil nutrient availability ("Soil Resources") and climatic conditions ("Climate") on response dimensionality, also mediated through intermediate connections between community biomass ("Community Biomass") and light availability ("Light Availability"). These same variables were also combined in pathways to estimate effects mediated by species turnover and the abundance of species

in the legume functional group. After fitting this initial model, we evaluated model fit and pruned non-significant pathways to reduce model complexity.

Statistical Software

All statistical analyses were performed in R version 4.0.2. Multivariate linear model fitting was conducted using RRPP (Collyer and Adams 2018). Semi-Major Axis (SMA) regression was performed using "smatr" (Warton et al. 2012). Linear mixed effects modeling was conducted using "lme4" and "lmerTest" packages (Bates et al. 2015, Kuznetsova et al. 2017). SEM analyses were conducted using "lavaan" (Rosseel 2012).

Results

Community Responses to Nutrient Enrichment

Of the 49 sites included in analysis, 37 showed significant ($P < 0.05$) community responses to nutrient addition treatments (Figure 1.2a). While a majority of sites (30) exhibited significant effects of N enrichment, significant impacts of P (20) and Kμ (17 sites) addition were also common. Community rate of change per year of treatment was greatest in response to N enrichment (Figure 1.2b). Once accounting for site-level variation in average effect, estimated mean magnitude of community change (in net Euclidean distance per year) was significantly greater following N fertilization than either P or Kμ ($F_{2,96} = 4.8$, $P < 0.05$).

Correlation Among Species Responses

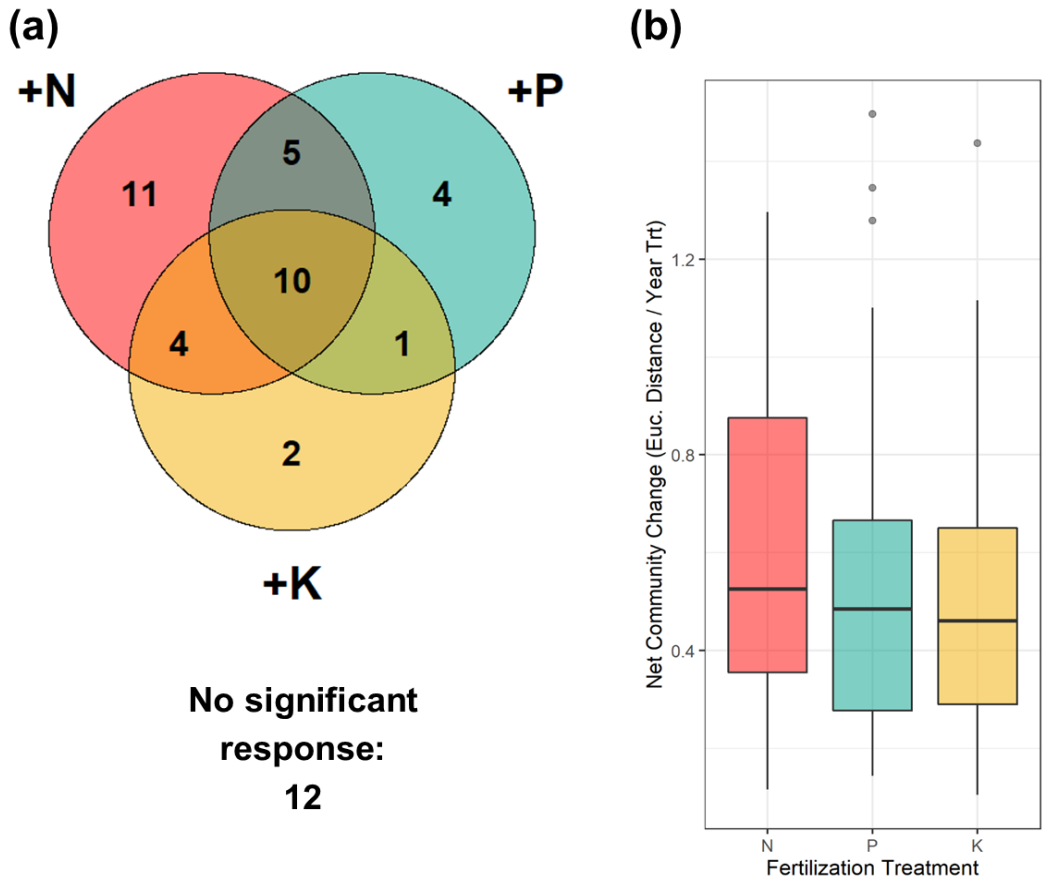

Figure 1.2:
(a) Frequency of sites exhibiting significant ($P < 0.05$) effects of nutrient (N, P, or Kμ) fertilization on plant community composition. Of 49 total sites, 37 showed significant compositional changes to at least one of three fertilization treatments, while 12 sites showed non-significant compositional responses to all nutrient manipulations.
(b) Rate of estimated fertilization-driven change in species composition, prior to standardization of response coefficients. The rate of total compositional change was calculated as the magnitude of the vector of estimated species response coefficients, as net Euclidean change in log_2_-transformed community cover per year of treatment. Higher values indicate greater overall rate of compositional change.

After standardizing overall community trajectories to unit length within each site, semi major axis (SMA) regression was used to evaluate correlations among responses to treatments at the species level. Pairwise comparisons between nutrient addition treatments (N-P, N-Kμ, P-Kμ) revealed positively correlated responses among all treatments, generally (Figure 1.3, Table 1.1). However, these relationships varied as a function of plant functional group. Small intercept terms and slope coefficients nearly equal to 1 indicate that Forb, Graminoid and Woody species exhibited relatively equal responses across all treatment comparisons. For these functional groups, SMA models captured a statistically significant portion of total response variance. High R2 values of Woody species, in particular, suggest that this group exhibit a more consistent trend than others, though this result should be interpreted with caution given their limited occurrence in our dataset (n = 18, Table 1.1). In contrast, SMA regression fits to Legume species yielded slope coefficients and intercept terms that suggest stronger responses to P and Kμ treatments than would otherwise be predicted by response to N: positive intercept terms and slope coefficients greater than 1 produced when comparing responses to N and P treatments, for example, demonstrate the legumes exhibit more positive responses to P enrichment than N, which skew more strongly to P as total response magnitude increases (Figure 1.3, Table 1.1). Repeated SMA regression with respect to plant dominance or longevity showed no consistent deviations from general positive correlation in response coefficients (Appendix Figures A.1, A.2).

Global Scale Response Dimensionality

Across all sites and species, we found strong evidence that plant responses to

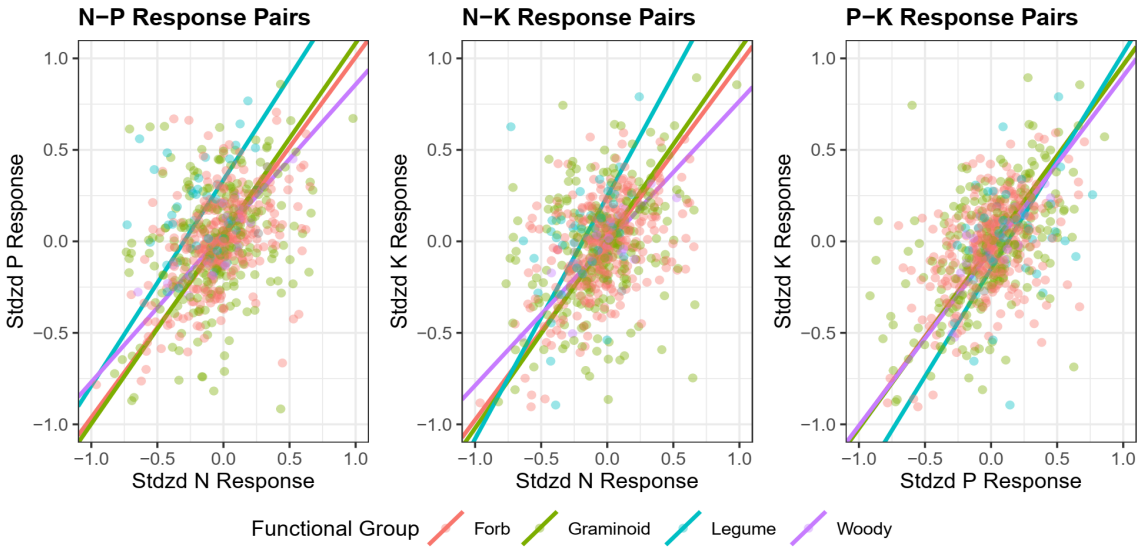

Figure 1.3: Visualization of pairwise relationships between plant responses to nutrient addition treatments. Each point refers to a unique site x species combination, colored by functional group. Lines correspond to results of semi major axis (SMA) regression applied to each functional group.

fertilization treatments are characterized by a largely one-dimensional relationship. (Figure 1.4a). Projection of responses onto the y vector (assuming proportionally equal responses to treatment) captured 60.68% of the total observed variance across all species; overall species response dimensionality, D, was equal to 0.29. This proportion is nearly identical to the fraction of variance captured by the first component in Principal Component Analysis (PCA) of our data, 60.77%. Given that PCA attempts to transform data into a new coordinate basis that maximizes the fraction of variance present in the first component, projection onto the y vector under our null hypothesis achieves an equivalent fit to the best one-dimensional description of species responses to fertilization. In line with observations made in pairwise comparisons, plant functional groups exhibited consistent patterns of deviation from the null hypothesis of proportionally consistent responses to treatment

Functional Group	Pair	n	Slope	Intercept	R^2
Forb	N-P	307	0.99	0.02	0.20
Graminoid	N-P	241	1.04	0.04	0.11
Legume	N-P	46	1.13	0.34	0.032^{ns}
Woody	N-P	18	0.81	0.04	0.76
Forb	N-K	307	0.97	0.00	0.21
Graminoid	N-K	241	1.03	0.01	0.11
Legume	N-K	46	1.33	0.25	0.10
Woody	N-K	18	0.78	-0.01	0.63
Forb	P-K	307	0.99	-0.03	0.21
Graminoid	P-K	241	0.99	-0.03	0.27
Legume	P-K	46	1.18	-0.15	0.09
Woody	P-K	18	0.96	-0.05	0.67

Table 1.1: Summary of semi major axis (SMA) regression model fits to each of 3 pairwise comparisons of response to fertilization treatment. A majority of models captured significantly more variation ($P < 0.05$) in response than models assuming no correlation between treatment responses; models with non-significant fits are denoted by superscript "ns".

(Figure 1.4b, Table 1.2). While mean coordinates of plant functional groups did not differ significantly on either y or b1 dimensions, the mean coordinate position of Legume species on the second rejection dimension, b2, was significantly larger than the means of all other functional groups. Given the loadings specified in our projection, P, larger average coordinate values in this second rejection dimension are correlated with proportionally more positive responses to P or Kμ treatments than N enrichment.

	$\bar{y}$	$\bar{b_1}$	$\bar{b_2}$
Forb	-0.0331^1	-0.0181^1	0.0081^1
Graminoid	-0.0561^1	-0.0211^1	0.0021^1
Legume	-0.0051^1	-0.0871^1	0.2062^2
Woody	-0.0581^1	-0.0371^1	0.0221^1

Table 1.2: Mean coordinate position of functional groups along 1:1:1 vector ($\bar{y}$) and residual components ($\bar{b_1}$,$\bar{b_2}$). Superscripts correspond to significant ($P < 0.05$) contrasts between functional group means in each dimension.

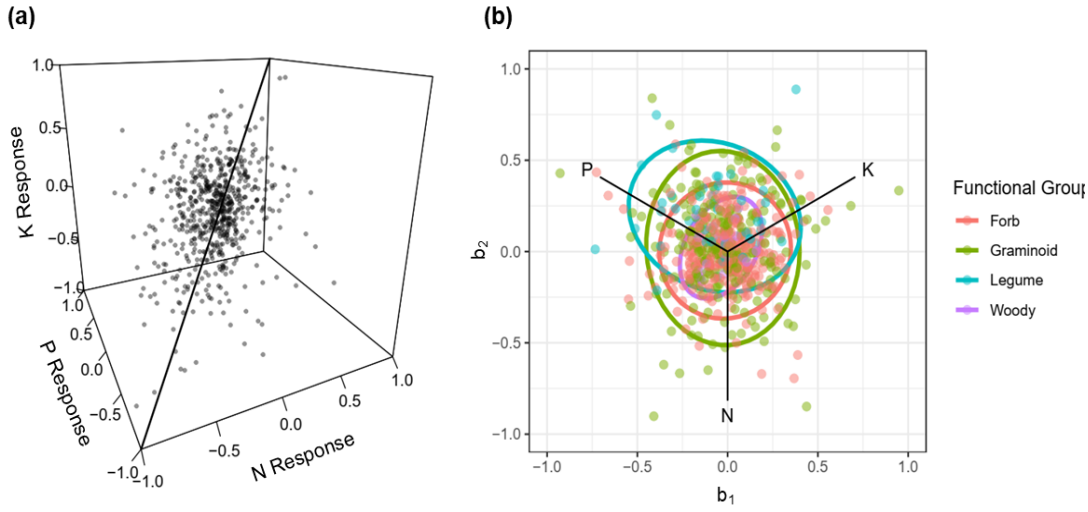

Figure 1.4:
(a) Three-dimensional visualization of species responses to nutrient enrichment across all sites, with line corresponding to 1:1:1 vector (y) assuming proportionally equal responses.
(b) Residual deviation from 1:1:1 vector displayed in two dimensions (b1, b2) orthogonal to y. Points are colored by functional group with 95% confidence ellipses centered on group means.

Site Variation in Response Dimensionality

To evaluate the environmental and community determinants of response dimensionality, we subdivided data by sites to calculate community response dimensionality, D, that captures variation in fertilization response across all observed species. Estimates D ranged between 0.08 and 0.73 (Mean = 0.39; Appendix Table A.2). Consistent with our hypotheses, SEM analysis identified significant relationships between soil resource availability, climatic characteristics, and response dimensionality (Figure 1.5). While increasing precipitation and lower growing season temperatures produced a positive, direct effect on response dimensionality, the effects of resource availability were primarily mediated through changes in average biomass and canopy light interception – experiments performed in more productive environments characterized by stronger competition for available light were significantly correlated with greater variation in trajectories of community change across our three fertilization treatments. Site species richness, soil resources, and climate also had effects on response dimensionality through changes in pre-treatment spatial turnover in species diversity (Figure 1.5). Less species turnover, estimated as spatial beta diversity of communities prior to treatment, and pre-treatment abundance of legumes combined to have negative effects on the dimensionality of community response to treatment. Community responses to fertilization treatment appear directionally varied in systems where N-fixing functional strategies are common and species diversity is likely to rely less on spatial coexistence mechanisms.

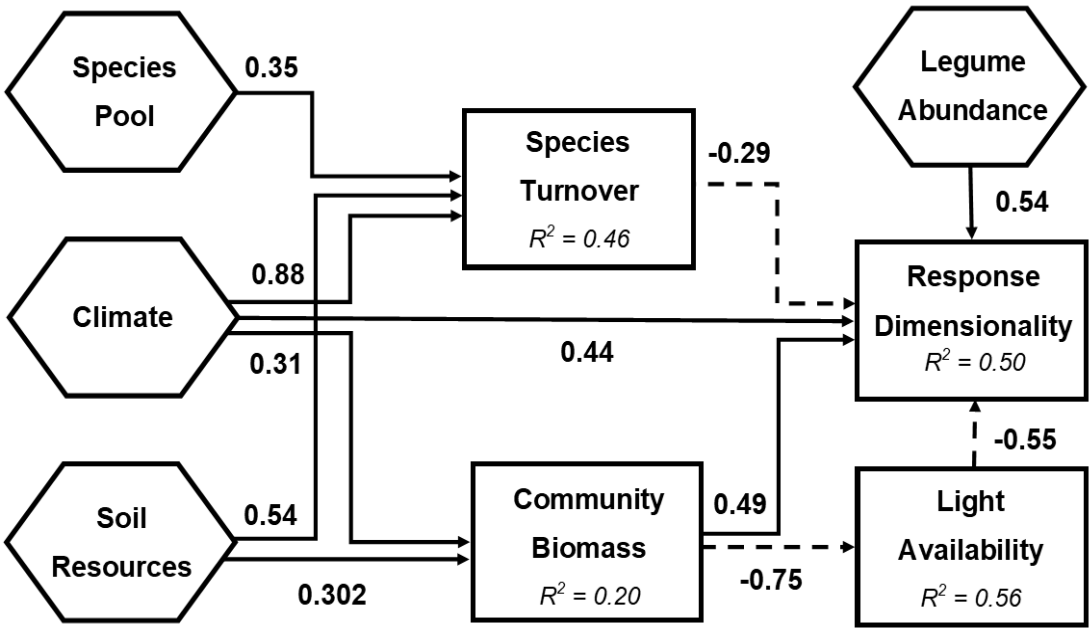

Figure 1.5: Visual representation of structural equation model (SEM) used to evaluate pre-treatment site factors that explain variation in community response dimensionality (D) following multiple nutrient enrichment. All statistically significant ($P < 0.05$) pathways are presented. Solid lines correspond to positive effects, while dashed lines correspond to negative effects. Chi-square test statistic = 23.408 on 20 degrees of freedom indicates close model-data fit ($P = 0.269$; Comparative Fit Index = 0.943).

Discussion

In terrestrial plant communities, trade-offs among multiple niche axes are theorized to govern the coexistence of diverse, interacting species. Using data from a globally replicated experiment in grassland systems, we find support for the simultaneous contribution of two mechanisms – a shift from belowground to aboveground resource limitation and multi-dimensional belowground tradeoffs – that vary in their relative importance across sites. Consistent with other studies of nutrient limitation in grassland systems, including those using data from the Nutrient Network experiment, we found that nitrogen enrichment produced greater average effects on composition than either phosphorous or potassium and micronutrient fertilization (Crawley et al. 2005, Fay et al. 2015, Harpole et al. 2016, Soons et al. 2017).

Given constraints on nitrogen fixation in many terrestrial systems (Vitousek and Howarth 1991), these results suggest that nitrogen availability may often act as a dominant niche axis of belowground resource availability. However, these findings may also be skewed by the disproportionate representation of Nutrient Network sites in temperate North America and Europe (Appendix Table A.1). In arid environments and those composed of more weathered soils, plant demands for phosphorous and other micronutrients may exceed those of nitrogen (Handreck 1997, Vitousek et al. 2010); experimental sites in Australia, for example, often exhibited the strongest community responses to phosphorous enrichment, on average (Appendix Table A.1). Surprisingly, 24 percent (12 of 49) sites did not respond significantly to any of the three resource enrichment treatments, despite addition at a rate much greater than natural fluxes (Vitousek et al. (1997b); Vitousek et al. (2010); Appendix Table A.1).

This finding may be linked to other sources of resource limitation; qualitatively, sites with low precipitation (and likely higher interannual community turnover) appear more likely to exhibit non-significant responses to treatment. However, this may also be the result of our conservative analytical approach that first accounts for spatial and temporal variation in site community composition before testing for fertilization effects. After controlling for differences in the total magnitude of compositional change, directional comparison found support for a strongly one-dimensional pattern of variation at a global scale. The dominance of a single axis of variation implies the presence of a general trade-off between plant performance in low or high nutrient conditions, likely driven by asymmetric competition for light (Dybzinski and Tilman 2007, DeMalach et al. 2017). This result supports other findings that identify light limitation as a primary mechanism of fertilization-driven compositional change (Borer et al. 2014, Hautier et al. 2018).

More broadly, our results likely reflect differentiation across a "fast-slow" economic spectrum of adaptation (Reich 2014). Absent other drivers, such as disturbance, herbivores, or pathogens, we find evidence that plant growth strategies increase performance under high soil nutrient conditions, generally, as opposed to nutrient-specific trade-offs (Grime 2006, 1974). Physiological requirements of primary producers are known to be largely consistent in stoichiometry (Ågren 2004, 2008), and as a result, interacting species are more likely to vary in total resource demand, rather than affinity for specific soil nutrients. The development of resource-specific trade-offs appears an unlikely coexistence strategy in many grassland systems. In response to other environmental changes, functional strategies that promote growth across multiple niche dimensions appear common – grassland plant responses to elevated fertility and herbivore exclosure are generally correlated (Lind et al. 2013), and exhibit similar shifts

in abundance across treatments removing different herbivore groups (Seabloom et al. 2018). Despite the strength of a one-dimensional relationship across all species, we also found key deviations from this pattern based on plant functional strategies and site-specific contexts. In all sites, species in the Legume functional group responded more positively to potassium and phosphorous addition than nitrogen enrichment. While we still observed generally correlated patterns of change among these species, our findings suggest that nitrogen fixation may provide an additional advantage to effective competitors when other resources are supplied (Bobbink (1991);Suding et al. (2005), Tognetti et al. *in review*) . Enzymatic costs of nitrogen fixation, which result in steeper requirements for phosphorous, potassium, sulfate, and other micronutrients relative to other plant functional types, may also contribute to this response (McKey 1994).

In turn, pre-treatment legume abundance served as an important predictor of site-level response dimensionality. It appears likely that greater diversity in plant functional strategy at the species level contributes to more directionally varied responses within a community to fertilization by different nutrients (Díaz and Cabido 2001). However, distinctions between legumes and non-legume species are relatively coarse, and likely do not capture other key sources of plant functional variation and their relationship with fertilization. Further exploration of the links between plant nutrient response and other key trait dimensions, such as the leaf economic spectrum (Wright et al. 2004), tissue stoichiometry (Güsewell 2004), and root physiology (Kramer-Walter et al. 2016) may better distinguish species groups at a global level, as well as their relationship to site-specific effects.

At the site scale, we also found that community responses to fertilization treatments

were strongly contingent on site-specific characteristics. Community variation in treatment response – response dimensionality – was positively correlated with a series of covariates related to pre-treatment patterns of resource limitation and community interactions. We found increased response dimensionality in sites with low light interception, high productivity, and low spatial community turnover. This suggests that trade-offs in the belowground nutrient use are more common in systems where coexistence is maintained through local competition. While not presenting a direct mechanistic link to plant resource use strategies, these findings are supported by reports that functional trade-offs are often more constrained in stressful environments (Dwyer and Laughlin 2017). In grasslands, disturbance and climatic stress frequently act as strong habitat filters, and their fluctuations are known to serve as important mechanisms of species coexistence (Chesson 2000, Adler et al. 2006). Under conditions where growing season precipitation strongly controls plant growth and fitness, for example, viable functional strategies are primarily distributed along a single axis related to relative growth rate and stress tolerance (Angert et al. 2009).

Like all studies exploring plant responses at the community, our results are subject to the properties of unique community assemblages occurring at each site. While able to infer some of these properties based on aggregate community attributes, such as biomass and functional group abundance, our results do not provide a link to species-level responses. Moreover, by limiting our analysis to species with well-characterized abundance shifts following fertilization, we necessarily exclude transient ones. These species can have important roles governing community response to nutrient enrichment and may exhibit functional strategies that are distinct from more persistent taxa (Wilfhart et al. *in review*).

Together, our findings present evidence for a generally one-dimensional axis of variation in plant response to fertilization, yet underscore the importance of site-specific constraints. Outcomes of plant competition for limiting soil nutrients are best predicted by relative differences in resource use (Tilman 1982b), and represent a subset of many potential axes of niche differentiation (Kraft et al. 2015). As a result, the relative contribution of trade-offs mediated by light competition or competition for individual belowground resources will depend on the unique set of factors structuring community interactions in each context.

Just as functional diversity and environmental characteristics are known to control ecosystem sensitivity global change, this study suggests that these same factors likely influence what mechanisms govern plant community response. Consideration of the direction of community change across multiple stressors thus forms an important complement to differences in their magnitude. Given that many ecosystems are subject to many global changes simultaneously, nuanced understand of their effects depends on identifying the trade-offs on which they operate. Stressors applied in tandem often have additive or super-additive effects on plant diversity and community composition (Zavaleta et al. 2003, Harpole et al. 2016, Komatsu et al. 2019), though effect sizes alone do not indicate whether communities shift along one dimension or several. While plant responses to nutrient enrichment may be captured along a single axis in general, broad assumptions of community dynamics are unlikely to apply in all contexts. Instead, we emphasize that cross-site comparisons and deep consideration of the unique factors shaping compositional responses to global change are essential to effective management and conservation of ecosystem diversity and function.

Chapter 2

Nitrogen enrichment has scale-dependent effects on plant diversity in California grasslands.

Evan E. Batzer[1*] and Valerie T. Eviner[1]

1. Department of Plant Sciences, University of California, Davis, USA

Abstract

The increased availability of nitrogen is implicated in widespread loss of plant community biodiversity in terrestrial systems. However, this diversity change is commonly evaluated in small plots, which translate poorly to effects at larger scales of conservation or management interest. Cross-scale studies may better capture the effects of N addition, and frequently report variation in the loss of species richness as a function

of sampling scale. While the mechanisms responsible for this scale-dependence are not well understood, attempts to link biodiversity scaling to shifts in species richness, relative abundance, and spatial distribution offer more detailed interpretation of observed effects.

In this study, we evaluated scale-dependent patterns of plant diversity change following experimental N fertilization in two California grassland sites. At both sites, we found that N enrichment significantly decreased plant diversity in small subplots yet failed to produce richness declines at larger scales. In contrast, effects on community evenness were consistent across scales, indicating that scale-dependent patterns were primarily driven by the increased abundance of dominant species without any large-scale loss of species. While N addition may have limited effects on large-scale persistence mechanisms, we observed greater intraspecific aggregation in fertilized plots that may make them more vulnerable to extirpation in the long term. Together, our findings underscore the need to supplement cross-scale comparisons of species richness with those of other factors, such as abundance and spatial distribution, to better understand community responses to N enrichment.

Introduction

Human effects on regional and global nutrient cycles have caused shifts in the availability of resources that control plant productivity, more than doubling the total amount of plant-available nitrogen in terrestrial systems (Vitousek et al. 1997b, Canfield et al. 2010). Increased concentrations of soil nitrogen are theorized to be a major contributor to widespread plant diversity loss; nitrogen loading is known to produce

shifts in the abundance of dominant species, increases in invasive plant cover, and species extirpation (Tilman and Lehman 2001, Butchart et al. 2010, Harpole et al. 2016). This diversity loss, in turn, is implicated in declines of ecosystem resilience, resistance, and the provision of key services (Chapin et al. 2000, Loreau et al. 2001, Hector and Bagchi 2007).

However, there exists a key discrepancy in the scale of global and regional biodiversity changes and experimental approaches that often take place over much smaller areas. Empirical studies are critical to understanding the drivers of biodiversity loss; yet attempts to link richness changes at small scales to those at larger ones often produce estimates that significantly over- or under-predict effects (e.g.; He and Hubbell (2011); Sax and Gaines (2003); Vellend and Baeten (2013)). A central challenge to this translation between experimental and observed contexts stems from the nature of species diversity as a scale-dependent measure – by definition, measures of biodiversity increase non-linearly as a function of sampling effort (Scheiner 2003, Chase et al. 2018). Accounting for this scale-dependence is essential to predict at what scales biodiversity may be most affected by nitrogen enrichment, or the scale at which it is conserved most effectively.

The scale-dependence of biodiversity in plant systems emerges, in large part, from a suite of coexistence mechanisms that operate across different areas or timeframes. Depending on the extent or duration of sampling, dominant coexistence mechanisms at a given scale will vary (Hart et al. 2017). In local neighborhoods of interaction, for example, species richness is often thought to be driven by resource partitioning and stochastic community assembly (Tilman 1982b). Coexistence at larger scales, in contrast, may be more dependent on other mechanisms, such as storage effects,

environmental filtering, dispersal limitation, and competition-colonization trade-offs (Chesson 2000, Leibold et al. 2004). Based on how different mechanisms are affected by nitrogen enrichment, biodiversity change at small scales may not reflect shifts at larger ones. While this topic has yet to be examined extensively, cross-scale studies often report differences in the magnitude or direction of effects between the smallest and largest area sampled (Chase et al. 2018).

To better understand this scale-dependence, treatment effects are often evaluated at the sample level (α diversity), study extent (γ diversity), and at intermediate scales using species accumulation curves (Gotelli and Colwell 2001, Scheiner 2003). However, characterization of richness change across multiple sampling areas is insufficient to capture drivers of scale-dependent effects. Scale-dependent relationships are known to depend on a set of independent components – including species pool size, relative abundance, and spatial distribution – that present markedly different interpretation of biological phenomena (Chase et al. 2018, McGlinn et al. 2019). While several studies have compared scale-dependent richness change following nitrogen addition in grassland systems, few have captured its relationship with these components (but see Lan et al. (2015)).

N enrichment in California grasslands is known to reduce species richness at local scales (Zavaleta et al. 2003, Harpole and Tilman 2007), yet its effects on large-scale coexistence are less understood. An annual-dominated system characterized by high species diversity, heterogenous soils, and variable climatic conditions, California grasslands are known to exhibit organization across multiple scales (Germain et al. 2017). Species diversity in this system is maintained by many mechanisms, including resource competition, temporal and spatial storage effects, disturbance, and environ-

mental variation (Seabloom et al. 2005, Hobbs et al. 2007, Elmendorf and Harrison 2009).

Scale-dependent relationships of N addition in California grasslands may be characterized by many potential outcomes, each with associated links between drivers of change and coexistence mechanisms. In the simplest case, N enrichment may have consistent effects on both local and regional (γ) scale diversity through species extirpation across the extent of observation (Lan et al. 2015). Alternatively, N additions can result in intermediately abundant species less frequently occupying a sampling unit, thus decreasing community evenness without changing species richness. This also results in the decreases in richness seen at smaller scales being diminished at larger scales (Tjørve et al. 2008). This pattern may also emerge from changes in environmental suitability that increase the dominance of a few species yet fail to affect larger-scale mechanisms such as spatial or temporal storage effects (Chesson 2000, Adler et al. 2006). Finally, changes in intraspecific aggregation can also result in scale-dependent effects, independent of changes in total richness or relative abundance. N enrichment may reduce aggregation through environmental homogenization, affecting γ diversity, or increase aggregation through reduced dispersal or concentration of individuals in spatial refugia, disproportionately reducing α diversity (Eskelinen and Harrison 2015).

Here, we expand upon prior studies by relating scale-dependent diversity loss to three key components – species richness, community evenness, and spatial distribution – to generate a more complete understanding of the effects of nitrogen enrichment in California grasslands.

Methods

Study Design

This study was conducted at two sites in the foothills of California's Sierra and Coast Ranges, roughly 600m in elevation: The Donald and Sylvia McLaughlin Natural Reserve (MCLA) and Sierra Foothill Research and Extension Center (SFREC; Figure 2.1). Both sites experience a Mediterranean climate defined by dry, hot summers and cool wet winters. Average temperatures in each site ranged between 15° C (MCLA) and 16.7° C (SFREC); mean total annual precipitation ranged between 698mm yr^{-1} (MCLA) and 818mm yr^{-1} (SFREC).

To capture changes in core mechanisms underlying scale-dependent relationships, we selected communities that were likely sensitive to multiple elements of change – in both sites, sampled grasslands were species-rich (often >10 spp. m^{-2}), exhibited relatively even species abundance distributions, and spatial structure detectable to a range of 2-3m (Appendix Figure B.1). During peak growth, the most abundant species in our chosen sites consisted of annual grasses (Elymus caput-medusae, Bromus hordeaceous), with a subcanopy of forbs (Agoseris heterophylla), legumes (Lupinus bicolor) and grasses (Festuca myuros; Appendix Figure B.2, Appendix Table B.1). Late-season communities were primarily composed of late blooming forb species (Lagophylla ramosissima, Holocarpha virgata).

In the spring of 2016, we selected 4 locations in each site classified as the California Annual Grassland type (Keeler-Wolf et al. 2007). At each location, we established a randomized block design consisting of two $100m^2$ plots (8 blocks / 16 plots total). In each plot, we designated the interior 8x8m portion for community sampling, leav-

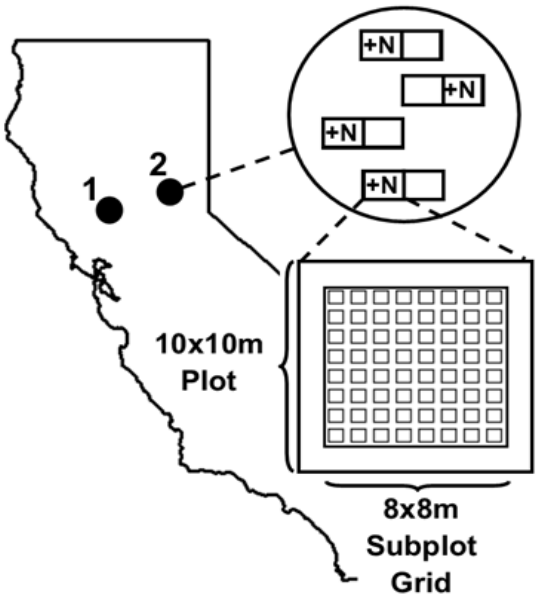

Figure 2.1: Study site locations and sampling design. Site 1: McLaughlin Natural Reserve (MCLA). Site 2: Sierra Foothill Research and Extension Center (SFREC). In each site, we established 4 blocks consisting of 10x10m paired plots randomly subject to nitrogen enrichment (+N). Within each plot, we constructed a grid of sixty-four 0.5x0.5m subplots with a 1m boundary to plot edges.

ing a 1m buffer on all edges to limit edge effects caused by fertilization treatments. Within this interior core, we established sixty-four 0.5x0.5m subplots centered on 1m intervals to be used in community sampling (Figure 2.1). Plots within blocks were randomly assigned either an N enrichment treatment (10g N m^{-2} yr^{-1}, delivered as 44-0-0 time-release urea) or control treatment (no manipulation). Between 2017 and 2019, fertilization was applied in late January or early February, coinciding with peak plant nutrient demands as spring temperatures begin to rise (Eviner and Firestone 2007).

Prior to initiation of the experiment, we conducted more limited pilot sampling at each location in the spring of 2015 to characterize site spatial structure and assess potential

sources of bias in our sampling design (Appendix Figure B.1). Using a similar study design replicated in 2 blocks in each site, we found scale-dependent patterns of species diversity but no significant differences in subplot or plot-level species richness within blocks. Together with a lack of observed treatment effect on diversity in our first treatment year, it is unlikely that inherent differences of treatment vs control plots within blocks significantly affected any observed results.

Response Measurements

Starting in 2017, we assessed the total areal cover of all species present in each subplot using a modified Daubenmire method with the following binned cover classes: 0-1%, 1-5%, 5-25%, 25-50%, 50-75%, 75-95%, 95-100%. Cover was estimated visually for each species, often yielding total plot cover values greater than 100% in dense communities. To account for variable species phenology, we repeated cover estimates at three time points – mid- to late-April (peak cover of species with early to mid-season phenology), mid-May (peak cover of late-spring species), and late June (including cover of summer species) – depending on precipitation and temperature patterns in each year. Percent cover of each species was calculated as the highest observed cover value across the three observation periods.

To assess changes in community biomass and light availability driven by fertilization, we sampled total aboveground biomass and light interception during peak biomass (mid-May) in each year. As not to disturb subplots used in community sampling, we collected all aboveground plant material along ten 1m x 10cm strips placed in the margins of sampling grids in each plot. Strips were rotated each year to prevent the same location from being sampled twice. After collection, biomass samples were

dried to a constant mass at 60° C and weighed.

Light availability was measured as photosynthetically active radiation (PAR) using a Decagon Ceptometer. Ten locations in each plot were randomly distributed but fixed across years. At each of these locations, PAR was measured above the tallest vegetation and in two locations placed at the soil surface. The proportion of available light reaching the soil surface was calculated as the ratio of canopy PAR relative to the mean of the two surface-level measurements.

Statistical Analysis

Effects of fertilization on community biomass and light availability were analyzed using linear mixed effects models to account for a repeated-measures design. For biomass, where sampling was randomly distributed in each year, we included random effects of site, block, and plot. For light availability, which was measured in the same locations across multiple years, we included random effects of site, block, plot, and sampling location.

To explore effects of N enrichment on community diversity, we used a modified analytical framework developed by McGlinn et al. (2019) through capture of the specific contributions of changes in species richness, relative abundances, and spatial distribution at different scales.

First, to test for effects on scaling relationships driven by shifts in species pool size and abundance distribution, we tested for changes in community diversity at the subplot and plot scales. Using a multiplicative diversity partition, we constructed estimates of community diversity at α (0.25m^2), γ (cumulative across 64 subplots), and β scales, where $\beta = \gamma/\bar{\alpha}$. To capture effects on community richness and evenness, we calcu-

lated community diversity using Hill numbers, linearized diversity metrics with variable weighting of species abundances, allowing for cross-scale diversity comparisons (Hill 1973, Jost 2006, 2007). We calculated Hill diversity at two different abundance weights: zeroth order (Q = 0) diversity, which is based on species presence-absence, equivalent to total species richness; and second order (Q = 2) diversity, which weights species proportional to their squared abundances, equivalent to the inverse Simpson diversity index.

For comparisons made across multiplicative diversity metrics, we calculated a log response-ratio of diversity in treatment relative to control plot, e.g. $log(\alpha_{treatment}/\alpha_{control})$ = $log(\alpha_{treatment}) - log(\alpha_{control})$. For α diversity, response ratios were constructed using the mean observed α in each plot. Significance of log-response ratios was calculated using confidence intervals generated using 10,000 bootstrap samples, stratified by block, site, and year. Confidence intervals were adjusted using a Bonferroni correction to account for pairwise comparisons in each diversity metric between treatments across three years. For β and γ diversity, bootstrap estimates were constructed using resampling of subplot-level samples which were then aggregated into larger-scale metrics.

While diversity partitioning between the smallest and largest scale of sampling captures changes in the richness and evenness of plant communities, it does not evaluate changes in plant spatial aggregation that operate on richness observed at intermediate scales. To visualize observed effect size across scales and test for the effects of changing spatial aggregation in response to treatment, we constructed species accumulative curves composed of all subplots within each plot ("Type IIIA" accumulation curves; Scheiner 2003). Using a null model approach, we compared effects on species rich-

ness between accumulative curves assembled using spatial and non-spatial rarefaction orders. In the former, mean richness is calculated across all 64 possible starting positions when samples are accumulated in order of observed spatial proximity, while in the latter, sample positions are randomized prior to spatial accumulation. We tested for the effects of aggregation by comparing observed log response ratios of species richness to a distribution composed of 10,000 randomized accumulation orders. Significant effects of spatial aggregation were detected by deviations from the quantiles of this null distribution using Bonferroni-corrected 95% confidence intervals.

While effects on spatial aggregation at intermediate scales may be detected using this method, like many biodiversity analyses, they are subject to arbitrary decisions regarding spatial grain and extent. As a result, comparison between spatial and nonspatial rarefaction methods are unable to detect changes in spatial aggregation occurring at the smallest scale (concentration of species in individual subplots). To better understand these small-scale shifts in spatial distribution, we supplemented our null-model approach by evaluating changes in the relationship between species presence-absence and relative abundance; under increasing aggregation, species will occupy a smaller proportion of subplots relative to their total cover. Using generalized linear mixed effects models, we compared the proportion of subplots occupied by species in a plot as a function of their average cover across plots, including random effects of species identity, site, and block. Tests for significance of model terms were conducted using Wald (Z-score) tests.

Statistical Software

All analyses were conducted using R version 4.0.2 (R Core Team 2020). Generalized

and linear mixed-effects modeling was conducted using 'lme4' and 'lmerTest' (Bates et al. 2015, Kuznetsova et al. 2017). Rarefaction was performed using 'mobr' (McGlinn et al. 2019).

Results

Biomass and light availability

Experimental N enrichment resulted in increases in both total aboveground biomass and percent light interception (Figure 2.2; table2_1). Biomass effects magnified over time, resulting in statistically significant differences only after 3 years of treatment. In contrast, changes in light availability were pronounced after a single year of treatment, and varied between years (Figure 2.2b), with no effect of fertilization after three years of treatment (Figure 2.2a). *Diversity across scales*

Source	Sum Sq	Mean Sq	Num Df	Den Df	F	P
Year	14893.50	7446.70	2.00	408.55	45.82	< 0.01*
Treatment	2628.80	2628.80	1.00	406.02	16.17	< 0.01*
Year x Treatment	2186.20	1093.10	2.00	406.02	6.73	< 0.01*

Table 2.1: ANOVA of linear mixed-effects models used to estimate changes in total aboveground biomass in response to fertilization treatment. Degrees of freedom were calculated using Satterthwaite Approximation, often yielding non-integer denominator degrees of freedom. Coefficients with statistically significant effects ($P < 0.05$) are highlighted with "*".

Construction of species-accumulation curves relating observed species richness to cumulative sample number suggested scale-dependent effects of fertilization treatment (Figure 2.3). Both control and treatment plots accumulated a similar number of species, on average, indicating diminished effects as scale expands. However, treat-

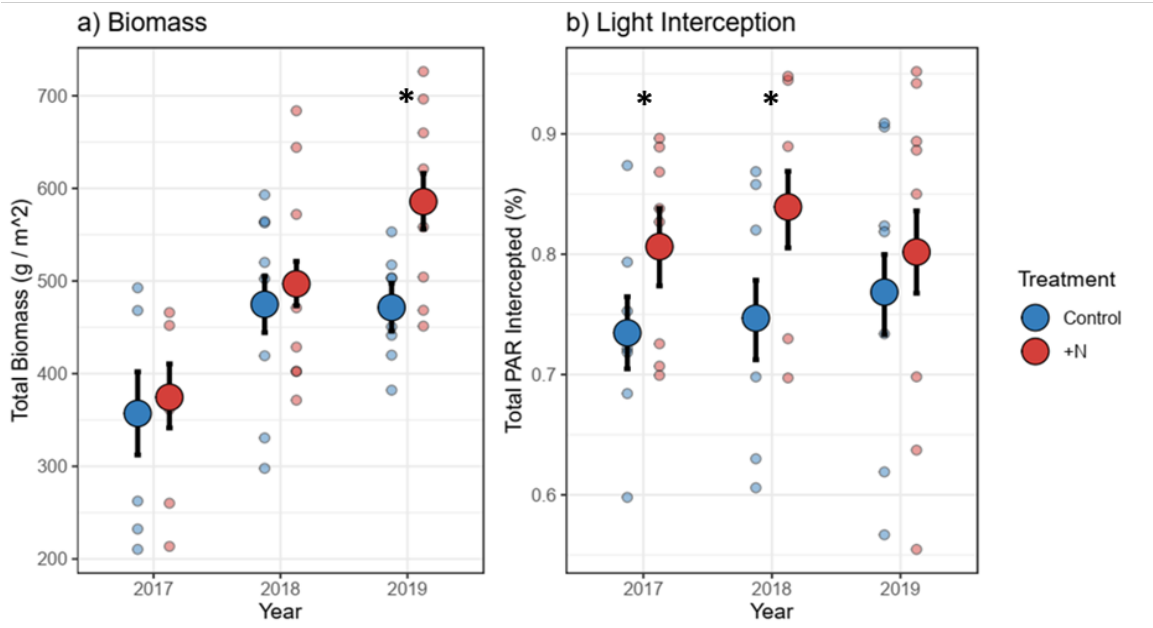

Figure 2.2: Effects of fertilization on (a) total aboveground biomass and (b) canopy light interception, colored by treatment. Large points correspond to mean values across all plots with associated Bonferroni-adjusted 95% confidence intervals. Small points reflect plot-level means. Statistically significant differences in means ($P < 0.05$) are highlighted with "*".

Source	Sum Sq	Mean Sq	Num Df	Den Df	F	P
Year	0.04	0.02	2.00	467.00	1.01	0.37
Treatment	0.52	0.52	1.00	467.00	24.99	< 0.01*
Year x Treatment	0.07	0.04	2.00	467.00	1.73	0.18

Table 2.2: ANOVA of linear mixed-effects models used to estimate changes in light interception in response to fertilization treatment. Degrees of freedom were calculated using Satterthwaite Approximation, often yielding non-integer denominator degrees of freedom. Coefficients with statistically significant effects ($P < 0.05$) are highlighted with "*".

ment effects decreased species richness at smaller sampling scales, most apparent on the log scale (Figure 2.3b).

Effects on richness and evenness

By decomposing the endpoints of each accumulation curve into $\alpha/\beta/\gamma$ diversity partition, we found that scale-dependent effects on species diversity were primarily a function of richness, but not evenness (Figure 2.4). When focused on species richness, our results confirmed the patterns observed in species-accumulation curves: fertilization significantly reduced the average species richness observed at the subplot scale in the second and third year of treatment (α), with no significant change in plot richness (γ), resulting in an increase in turnover or accumulation rate (β; Figure 2.4a).

In contrast, for abundance-weighted diversity, in which fertilization in years two and three reduced community evenness at both the subplot scale (α; Figure 2.4b) and at the plot scale (γ). Consistent effects at small and large scales yielded no change to abundance-weighted turnover (β).

Compositional analysis of community response to treatment indicated that nitrogen fertilization generally increased the abundance of species that were dominant in control plots (Appendix Tables B.4, B.5). While treatment responses were not consistent

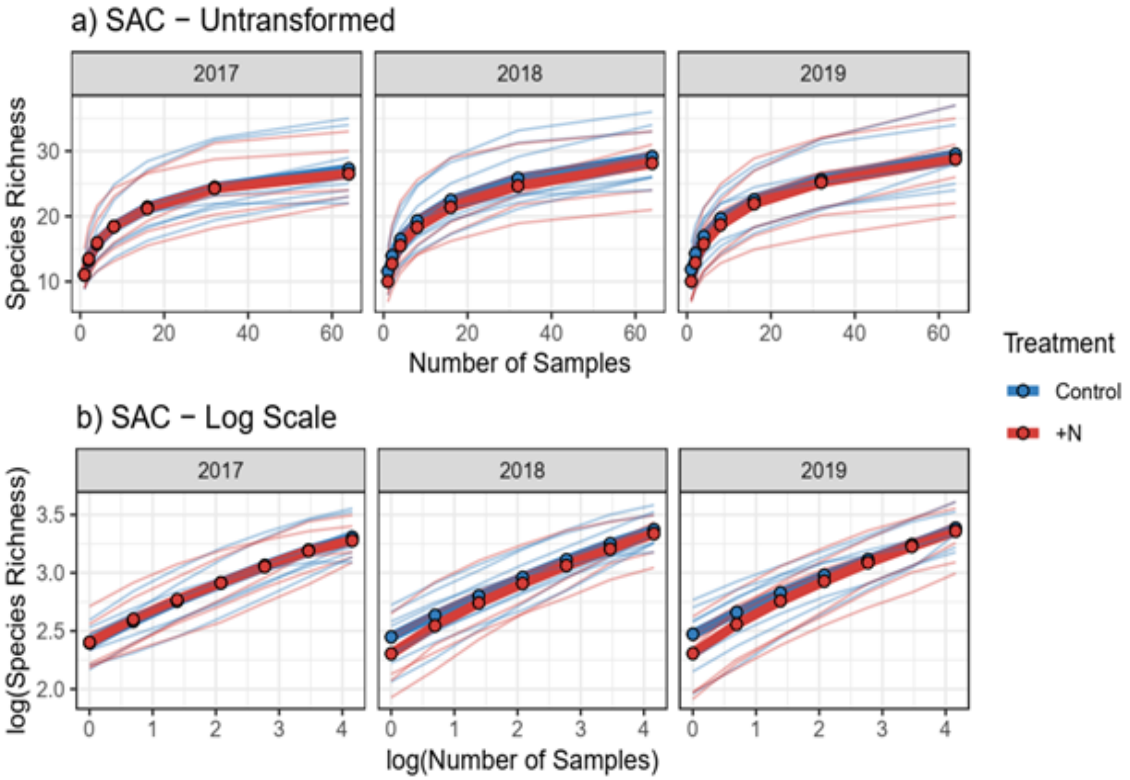

Figure 2.3: Species accumulation curves (SACs) depicting the cumulative number of observed species as a function of sampling effort, presented on untransformed (a) and log scales (b). Accumulation curves presented were generated through spatially explicit sample accumulation ("empirical" SACs), where samples are accumulated in order of proximity to the starting sample. Bolded lines represent the mean SAC across all treatment and control plots in each year; standard lines correspond to individual plots across all sites in each year.

across plant functional groups or species origin, individual species often responded in similar fashion across blocks. In both sites, spatial (block) and temporal (year) variation accounted for significant ($P < 0.05$) fractions of total compositional variance (Appendix Figures B.3, B.4; Appendix Tables B.2, B.3).

Effects on sample occupancy

N enrichment produced a significant effect on spatial aggregation at the subplot-scale (Figure 2.5). For a given amount of recorded cover, species in fertilized plots were found to occupy a smaller fraction of subplots in the second and third year of treatment. This reduction in occupancy indicates that infrequent species between 1-10 percent of average cover (intermediate values on the log scale) exhibited the greatest concentration of individuals into a smaller number of sampling units; species with an average cover of 5 percent (1.6 when log-transformed), for example, were estimated to decrease in percent occupancy from 63 to 57 percent of subplots, on average.

Effects on aggregation

Comparison of species accumulation curves constructed using spatial and random rarefaction orders demonstrated no clear effects on intraspecific aggregation across multiple subplots (Figure 2.6, Appendix Figure C.6). Across all years, the average response ratio constructed using spatial rarefaction curves rarely deviated from a random distribution generated using 10,000 random permutations of community spatial arrangements. While data from the third year of treatment suggest minor changes in aggregation occurring at intermediate scales, these results were not consistent in direction between years (Appendix Figure C.6).

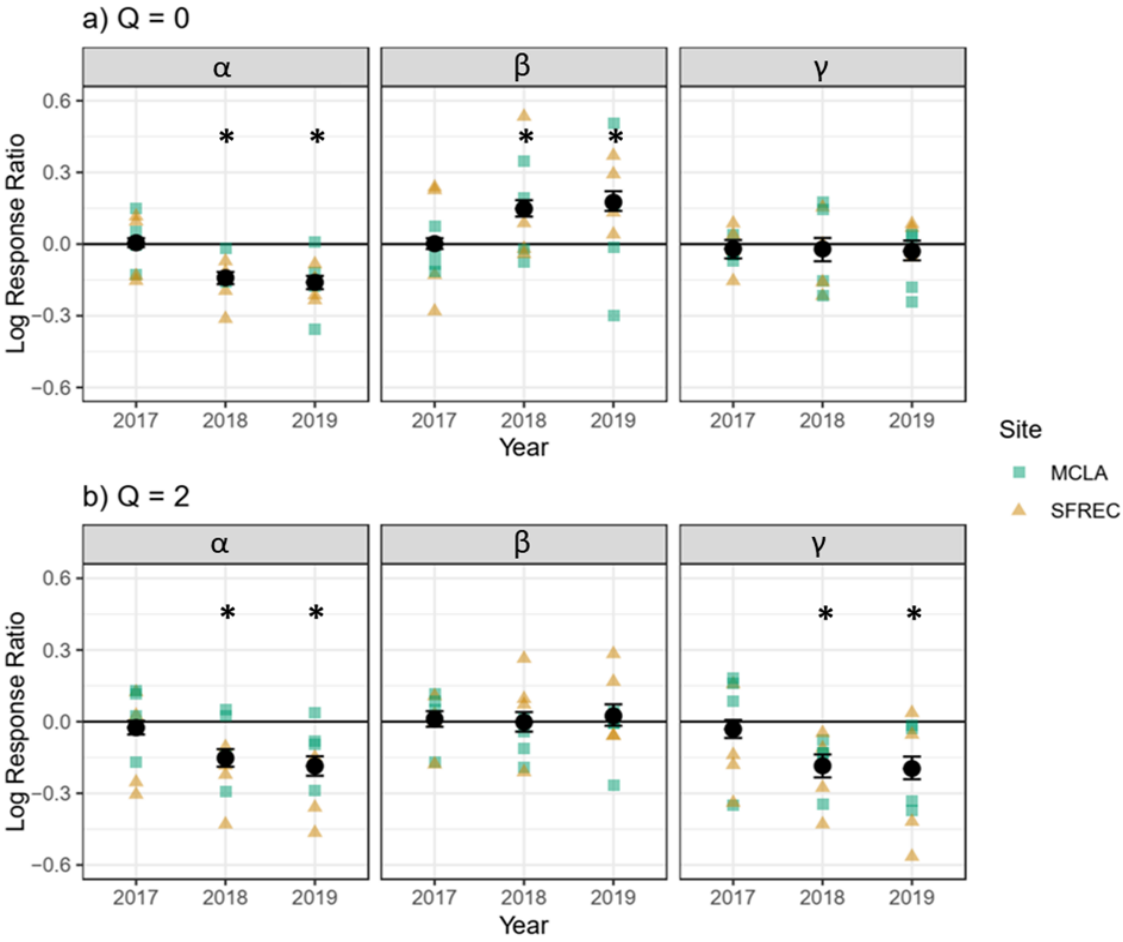

Figure 2.4: Changes in community diversity at α (subplot), β, and γ (plot) scales using multiplicative diversity partitioning using Hill diversity indices. Diversity was calculated as function of species richness (Q = 0) and abundance-weighted diversity (Q = 2). Effects are presented as log response ratios of each diversity metric within blocks. Black points correspond to mean effect across all blocks, with Bonferroni-corrected 95% confidence intervals generated using 10,000 bootstrap samples. Colored points correspond to estimated effects within each block. Statistically significant effects are highlighted, "*", when 95% confidence intervals do not overlap 0.

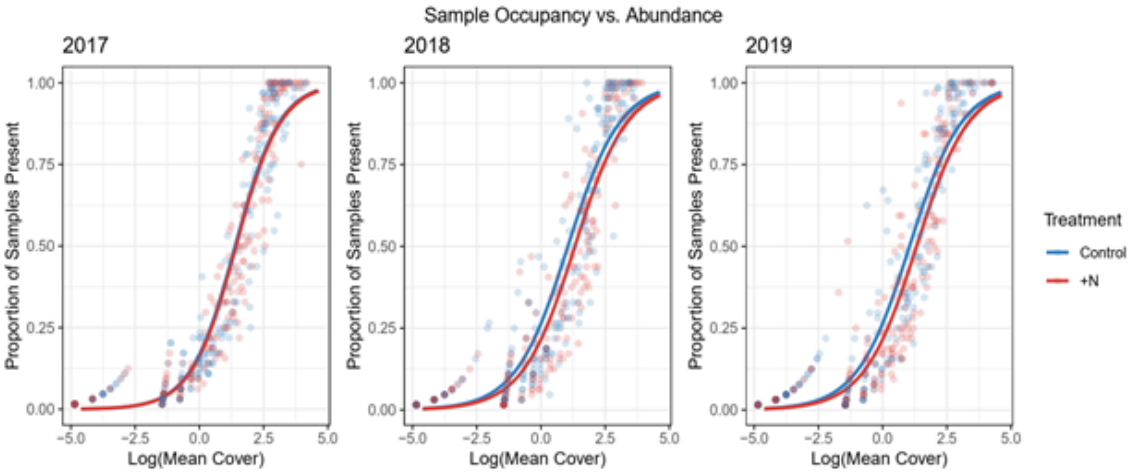

Figure 2.5: Effect of fertilization on the proportion of subplots occupied by species, relative to average subplot cover. Lines correspond to mean relationship reported by mixed-effects logistic regression, after accounting for random variance across species and blocks within sites (2018 data not shown). Treatment effects indicate significant decreases in occupancy relative to cover in the second and third year of treatment (2018: Z = -0.274, P $<$ 0.001; 2019: Z = -0.288, P $<$ 0.001). Effects on occupancy were not significant in the first year of treatment (2017: Z = -0.008, P = 0.803).

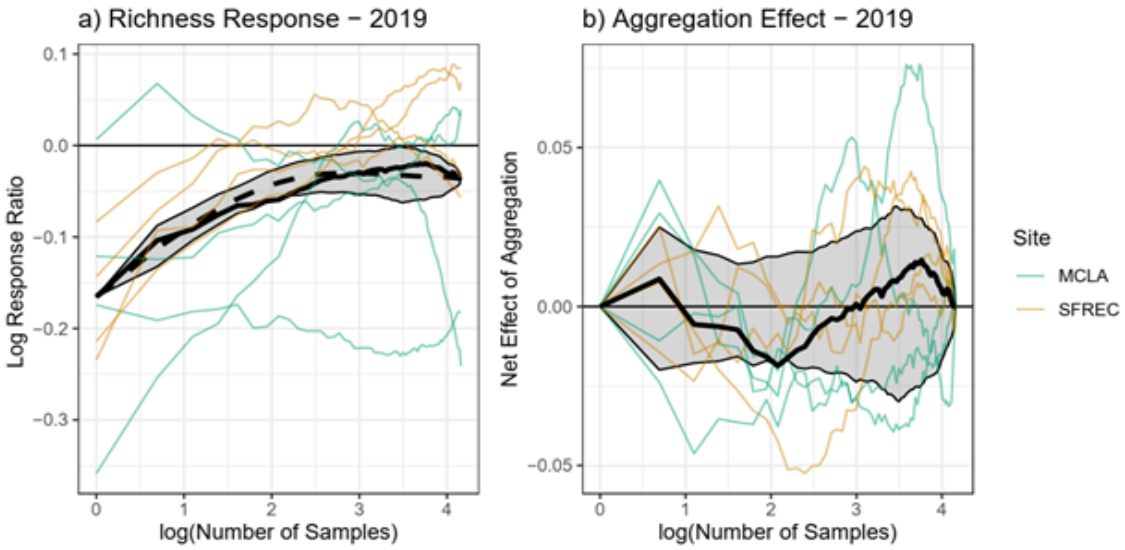

Figure 2.6: Effect of fertilization on species richness and spatial aggregation as a function of sampling scale in 2019, presented as a log response ratio. In subplot 5a, the solid black line corresponds to mean estimated effects under spatially explicit ("empirical") sample accumulation, while dashed line reflects the median value of mean diversity effects under randomized sample accumulation. Shaded areas correspond to Bonferroni-adjusted 95% confidence intervals of mean diversity response across 10,000 random sample accumulation curves. Colored lines denote individual responses of each block. In subplot 5b, lines correspond to the net effects of spatial aggregation on estimated response, calculated as the observed log-response ratio relative to the median value across bootstrap samples. The shaded area depicts Bonferroni-adjusted 95% confidence intervals of aggregation effects on mean diversity response across 10,000 random sample accumulation curves.

Discussion

The increased availability of soil nitrogen is widely considered to be an important driver of loss of biodiversity in plant systems (Bobbink et al. 2010). However, many experimental N enrichment studies assess changes to community diversity at a single spatial scale. Cross-scale studies may generalize more effectively to areas of conservation or management interest, and management approaches will be improved by understanding the many drivers that produce scale-dependent effects. Here, we demonstrate that scale-dependent community responses to nitrogen addition are not captured by focusing on species richness alone, but also require an assessment of changes to community evenness and spatial distribution

As reported in many experimental manipulations in nitrogen-limited systems, we found that N addition resulted in reduced community diversity at a scale typical of other studies ($1m^2$). Also consistent with these other findings, N fertilization in our experiment resulted in increased biomass and light limitation that likely acted to decrease subplot species richness. At these local scales, competitive interactions are known to be an important driver of community diversity (Tilman 1982b, 1987). Loss of average richness across subplots, therefore, is likely to be driven by shifts in the identity of limiting nutrients from soil resources to light that produces competitive exclusion (Hautier et al. 2009, Borer et al. 2014, DeMalach et al. 2017).

While fertilization produced significant changes to light interception in the first year of treatment, delayed effects on biomass and richness suggest our results depended on both the accumulating nature of our treatments and seasonal dynamics of California grasslands (Eviner and Firestone 2007). In annual grasslands, seedling dynamics

during winter months are known to exert considerable control over the composition of plant communities at peak biomass (Bartolome 1979, Harrison and LaForgia 2019); our treatments, applied several months after germination, may not significantly affect species diversity or composition within the year. Instead, successive years of nitrogen addition may spur growth and reproduction of effective competitors that generate positive feedbacks over time.

Similar dynamics may explain changes in aboveground biomass, in which fertilization produced positive effects that were not statistically significant until the third year of our experiment. Multiple years of treatment may be needed to promote substantial litter accumulation. Development of thatch layers is observed to be an important mechanism of compositional change in this system (Amatangelo et al. 2008); litter suppression is often linked to the spread of certain introduced species that responded positively to treatment in our experiment, such as E. caput-medusae, that often suppresses the growth of smaller-statured forbs (DiTomaso et al. 2008).

Despite strong effects observed at local scales of interaction, we found that nitrogen enrichment produced no significant change in plot-level species richness across all three years of study. Comparison across multiple diversity metrics, however, demonstrates that this scale-dependence in richness change should not be interpreted as a lack of effect on community structure at large scales (Chase and Knight 2013, Chase et al. 2018). Instead, the increased abundance of dominant species (at the expense of intermediately abundant ones) appears to act as the main driver of this scale-dependence; richness loss at small scales occurs not through extirpation, but the decreased probability of observing intermediately-abundant and rare species in small samples of highly uneven communities (Tjørve et al. 2008).

Understanding scaling relationships will likely depend on integrating the effects of multiple coexistence mechanisms (Chase et al. 2018, Demalach et al. 2019). While we are unable to identify changes to specific mechanisms in our study, our observed patterns suggest that large-scale persistence is not strongly affected by N enrichment. In California grasslands, spatial and temporal environmental variation is known to be an important driver of storage effects in less competitive species, which rely on soil seedbanks to maintain persistence (Hobbs et al. 2007, LaForgia et al. 2018, Hallett et al. 2019). Even in plots receiving fertilization, considerable variation in space and time suggests these communities are still subject to the influence of these environmental drivers.

As in our study, diminished effect sizes of diversity loss at larger scales are often observed in experiments manipulating fertility or disturbance in grassland environments (Sandel and Dangremond 2012, Lepš 2014, Lan et al. 2015), but are not a uniform finding (Seabloom et al. *Personal Communication*). While cross-site syntheses of scale-dependent diversity change are limited, evidence suggests that site productivity is likely to control effects. For example, Chalcraft et al. (2008) found that declines in -diversity were strongest in highly productive systems but were unable to identify a particular mechanism responsible for this pattern.

We caution that these results do not indicate that N enrichment will fail to result in species extirpation in this system. While our results are limited to an area smaller than most considered in conservation or management, changes in plant spatial distributions highlight potential drivers of diversity loss that may occur at larger scales, particularly over time. The concentration of individuals into a smaller number of favorable locations may elevate risks of stochastic extirpation and reduce dispersal

(Tilman and Lehman 2001, Kuussaari et al. 2009). If these patterns hold, this system may be subject to extinction debt in the long-term, as populations are unable to effectively capitalize on favorable conditions to replenish seedbanks or colonize potential sites (Jackson and Sax 2010, Gilbert and Levine 2013, Hylander and Ehrlén 2013). Shifts in spatial distribution may also interact with other global change factors, such as plant invasion and climate change, to amplify diversity loss caused by increasingly frequent drought events or dampen recovery (Harrison et al. 2015a, 2018).These results underscore the need to supplement incidence-based monitoring with other metrics, as richness trends alone are unlikely to provide a sufficiently detailed picture of biodiversity change (Hillebrand et al. 2018).

Our findings do not exclude changes to plant size as a potential mechanism of scale-dependence, given the impracticalities of estimating density in a system that regularly exceeds 8,000 mature individuals per square meter (Heady 1958). Fertilization may produce biodiversity loss independent of any shifts in spatial distribution or species abundance through decreased numbers of individuals that manifest as sampling effects (Goldberg and Miller 1990, Stevens and Carson 1999). While changes in density may drive scale-dependent responses to other global change factors (Powell et al. 2013, Schuler et al. 2015), there is little evidence that this phenomenon acts as an important mechanism in grassland systems (Lan et al. 2015).

Global biodiversity loss remains a primary environmental concern in the 21st century (Butchart et al. 2010). Experimental manipulations of global changes serve as a critical tool to assess the drivers and consequences of this diversity change, though are often limited by choices in sampling area or duration. Biodiversity is inherently a scale-dependent phenomenon (Chase et al. 2018); failure to account for mechanisms

that operate beyond a focal sampling unit will likely generate conclusions which fail to capture the complexity of the community response (Englund and Cooper 2003). Instead, we emphasize that deliberate capture of biodiversity change across multiple scales can improve our understanding of how communities change, which will improve our ability to both predict and manage change. Together, assessment of scale-dependent patterns of biodiversity change and related metrics, including community distribution and evenness, form an essential tool to better understand and manage human impacts on natural ecosystems.

Chapter 3

Climate drives transitions between vegetation states in California grasslands.

Evan E. Batzer[1*], Carolyn Malmstrom[2], and Valerie T. Eviner[1]

1. Department of Plant Sciences, University of California, Davis, USA
2. Department of Plant Biology, Michigan State University, East Lansing, MI, USA

Abstract

Climate change is forecast to influence plant community composition through shifts in climate variability and increased frequency of extreme events. In arid- and semi-arid

grassland systems, community turnover is known to depend on both climate conditions and historical contingency, where prior community configurations affect future dynamics. These contingencies are likely to act as an important driver of vegetation responses to climate events; their capture may enhance forecasts of community change and identify targets for active management. In this study, we planted various California grassland plant community types and observed changes in their composition during a ten-year period that included a drought of historic magnitude, followed by one of the wettest years on record. Using algorithmic partitioning methods and multistate modeling, we evaluated both the number of discrete vegetation types that best captured community turnover and the probability of transition between them. We found that compositional variance was best partitioned in 4 discrete groups, distinguishing between two sets of annual grasses often considered as one species group in expert models. Moreover, vegetation states differed in their persistence under variable climate conditions, and often exhibited directional patterns of transition. Certain vegetation states, such as communities dominated by native perennial grasses, demonstrated strong persistence across a range of climatic conditions; persistence of others, including invasive annual grasses, exhibited linear relationships with precipitation. These findings indicate that ecosystem resilience may be enhanced by certain vegetation states, while eradication efforts are likely to be most effective when climate conditions are favorable. Quantification of the unique properties of community states may greatly improve models of community dynamics under a changing climate in grassland systems.

Introduction

Across ecosystems, climate change forecasts emphasize the increasing frequency of extreme events, in addition to changes in average climatic conditions (IPCC 2014). Changing climatic extremes are important drivers of compositional dynamics, responsible for shifts in species distributions, invasion events, and biodiversity loss (Smith 2011, Felton and Smith 2017)

As ecological communities are increasingly subject to climate patterns outside historical bounds of variation, capturing the effects of unprecedented climatic extremes will be critical to generating new paradigms for conservation and management (Hobbs et al. 2009). However, given the complexity of many factors that control species abundances, these changes are often difficult to predict.

A central challenge to predicting climate-driven shifts in plant community composition is the influence of local biotic conditions that constrain species responses to environmental change. While species may exhibit varied tolerances to conditions imposed by heatwaves, droughts, and extreme cold, local interactions are also known to moderate the effects of these stressors (Tylianakis et al. 2008, Fukami 2015). Compensatory responses to climate change, for example, may be limited by competitors that inhibit growth and colonization (Alexander et al. 2015). At the community scale, such local interactions depend on key emergent properties that vary as a function of community attributes, including species richness, functional diversity, or dominant taxa (Chapin et al. 1997, Emery and Gross 2007). As a result, short-term compositional changes are likely to be historically contingent, where community responses to climate events vary in magnitude or direction depending on their prior composition

(Fukami 2015).

While it is understood that climate change will result in greater frequency of extreme events, it is often unclear to what degree ecosystem responses to these events will be contingent on community assembly. As "no-analog" conditions are increasingly encountered in many systems (Williams and Jackson 2007, Hobbs et al. 2009), contemporary observation of climatic extremes presents an opportunity to evaluate the interaction of environmental change and biotic context. In arid- and semi-arid grasslands, conceptual models of ecosystem dynamics (*sensu* Galatowitsch 2012, Ogden et al. 2005) provide a natural framework to examine complex relationships between climatic drivers and species assemblages. Applied ecologists in these systems often make management recommendations on "state-transition models" that identify the properties of different species groups ("states") and their likely direction of change under various contexts ("transitions"; Bestelmeyer et al. 2003). In response to climate events, these state-transition models can predict which communities are likely to persist in their current figuration and which are expected to transition to other state types.

In contrast to traditional development of state-transition models, which are often based on qualitative observation by experts, data-driven approaches are better predisposed to capture effects of climate and historical contingency [Allen-Diaz and Bartolome (1998); Bartolome et al. (2008). Though still limited by available observations, these computational methods may better capture potential mechanisms of change and rapidly update predictions as new information becomes available. In grassland systems, clustering algorithms have shown promise in tests of expert models and in the tracking of community responses to variable grazing regimes and species

invasions (e.g.; Jackson and Bartolome 2002, Stein et al. 2016, Stringham et al. 2003). While there are few tests of their application to vegetation dynamics under climate change, quantitative state-transition models may provide a rigorous assessment of both the key community configurations that structure plant communities in a system, and their associated interactions with extreme events.

In California, climate change is predicted to produce a 50% increase in the frequency of extreme events by the end of the 21st century (Yoon et al. 2015). California grasslands are particularly sensitive to climatic extremes, given compositional dynamics defined by a predominantly annual life history, climate sensitivity (Hobbs et al. 2007), non-hierarchical competitive relationships (Uricchio et al. 2019), and strong priority effects (Young et al. 2014). In this system, state-transition models often decompose compositional turnover into variation between three species groups defined by shared life history strategy and history of colonization: (1) naturalized exotic annual grasses and forbs, (2) native perennial grasses and forbs, and (3) recently invasive exotic annual grasses.

Compositional shifts in California grasslands are thought to be governed by differences in fecundity, phenology, and plant-soil feedbacks that characterize these species groups (Corbin et al. 2007). While this functional variation may govern responses to interannual climate variation (Pitt and Heady 1978, LaForgia et al. 2018), communities composed of different dominant species may also exhibit emergent properties that constrain subsequent compositional change. Invasive annual grasses, for example, produce thick litter layers that suppress competitor growth (DiTomaso et al. 2008, LaForgia et al. 2020). These litter feedbacks may enhance invasive grass persistence when future climatic conditions favor other species groups, particularly those that

may exhibit limited recruitment capacity, such as native perennial grasses (Seabloom et al. 2003a).

While warming average temperatures in California are forecast to produce increases in the distribution and abundance of annual grasses across the state (Sandel and Dangremond 2012), the effects of changing climate variance are less understood. Recent extreme climatic events, however, may provide insight into future vegetation dynamics. A drought from 2011-2015, which included the driest period in recorded history, was observed to produce significant changes in the composition and diversity of many grassland communities (Harrison et al. 2015b, Prugh et al. 2018). This event provides a unique opportunity to test conceptual models of California grassland community dynamics through monitoring of species abundance changes across different vegetation types.

In turn, the capture of these contingencies may actively inform ecosystem management. Often focused on the establishment of native species and reduction in invasive species abundances, management of California's grasslands under novel climatic conditions is likely to benefit from the application of modern computational tools to characterize vegetation change. Quantitative description of community transitions between dominant species groups may supplement largely qualitative models generated during climatic norms. Are certain desirable species groups more resistant to variable climatic conditions than others? Can extreme climatic events provide opportunities for targeted management action?

Here, we assess interactions between community assembly and climatic variation on vegetation composition in California annual grasslands across a 10-year period encompassing extreme drought. Using data from experimental plantings of three key

grassland species groups – naturalized annual, native perennial, and invasive annual grasses — we test key assumptions of grassland community dynamics under extreme drought stress.

Specifically, we ask:

1. What species groups best capture the key community configurations under varying climate conditions?

2. How does prior community configuration constrain vegetation responses to climate shifts, including extreme drought?

Methods

Study site and Experimental Methods

Plantings were conducted in research fields at the University of California, Davis (38.545751, -121.784780). Previously used in crop production, these fields were left fallow from 1985 to the start of experimental plantings in 2007. 75% of the experiment was set on Reiff series soil (coarse-loamy, mixed, superactive, nonacid, thermic Mollic Xerofluvents), with the rest on Brentwood soil series (fine, smectitic, thermic Typic Haploxerepts) with a 0-2% slope (USDA Web Soil Survey). The site has a Mediterranean climate, experiencing a mean annual rainfall of 457mm and mean daily temperature of 15.5 deg C between 1983-2018.

In order to minimize the previously established seedbank, soil was disked, irrigated to stimulate germination, and sprayed with a broad-spectrum herbicide (glyphosate). Irrigation and herbicide treatments occurred twice in the early fall of 2007.

Seeds were planted to establish vegetation treatments representing commonly used species groups in California's grasslands — native perennial grasses and forbs ("native"), naturalized annual grasses and forbs ("naturalized"), and invasive annual grasses ("invasive"; Table 3.1). Species chosen for planting are commonly found in annual grasslands near our study site, and reflect distinctions often made in management applications. "Native" species, for example, include a mixture of perennial grasses and native forbs commonly used in local restoration efforts that contrast with "invasive" grasses that are highly undesirable for both conservation and range management.

Each group was planted alone, in all possible 2-group combinations, and all together in a 3-group combination. Plots were 1.5m x 1.5m (2.25 m^2), with 1m buffer between plots, and 8 replicates per treatment (56 plots total) laid out in a randomized block design. In each plot, a total of 139 grams of seed was added, reflecting an average of 8,000 plants/m^2 - a typical mature plant density in this system (Heady 1958). For each monotypic community (e.g. native vs. invasive vs. naturalized), an equal proportion of seeds of each species were added. For community mixtures, an equal proportion of community type seed was added (e.g. in invasive + naturalized, 50% invasive, 50% naturalized seed), with equal proportion of individual species within each community type.

From 2008 - 2018, total areal cover of all species was estimated to the nearest 10%. Cover observations for each species were performed in early and late spring to capture maximum percent cover for each species when varying in phenology. The highest percent cover value in each year for each species was used in analysis.

Native	Naturalized	Invasive
Acmispon americanus	Avena fatua	Aegilops triuncialis
Bromus carinatus	Bromus hordeacous	Elymus caput-medusae
Elymus glaucus	Festuca perennis var. multiflorum	
Elymus triticoides	Trifolium subterraneum	
Festuca microstachys		
Lupinus bicolor		
Poa secunda		
Stipa pulchra		

Table 3.1: Species mixtures used in initial plot seeding. Distinctions between "Native", "Naturalized", and "Invasive" species groups reflect species origins in California grasslands.

State Classification

Prior to vegetation group classification, plant community observations were filtered to include only those species present within initial seeding mixtures and *Bromus diandrus*, a locally abundant annual grass that self-recruited into the experiment and is an important component of the California grassland type. Despite regular weeding, a number of agricultural weeds (largely *Convolvulus arvensis*) occasionally recruited into plots from the seedbank and nearby fields and roadways over the course of our experiment. Due to the effects of weeding and generally low abundance, these species were removed from community analysis. The resulting dataset captured 93% of the total vegetation abundance observed over the course of the experiment.

Algorithmic partitioning was used to determine core species groups that correlated in abundance over the course of our study. It is important to note that partitioning is limited to the suite of observations made between 2008 - 2018, capturing n = 560 plot:year combinations. This period includes a historic drought (2011-2015) and significantly wet year (2017). Statistical clustering of compositional variation was therefore a function of both the range of climatic conditions observed during our

experiment, in addition to starting conditions imposed in experimental design.

Partitioning was performed using an unsupervised clustering algorithm, K-medoids clustering. The K-medoids algorithm clusters data into k unique groups by identifying k medoid samples that best partition the total distance-based inertia of all observations. Distance between observations was calculated using Bray-Curtis dissimilarity.

Because the number of relevant clusters in our study was not pre-defined, we applied K-medoids clustering across values of k from 2-10, yielding a number of clustering solutions. We then compared the output of each of these clustering solutions using numerous tests—Hartigan, CH, Beale, KL, Cindex, DB, Silhouette, and Duda indices (Malika et al. 2014). The value of k with the best performance across all tests was chosen as the number of clusters that best represented vegetation partitions within this dataset.

Following the partitioning of states, we then conducted indicator species analysis to establish which species are associated with each state. Indicator species analysis was performed using 9999 random permutations of state assignments to quantify statistical significance. Clustering and diagnostics were generated using "cluster" (Maechler et al. 2019) and "nbclust" (Malika et al. 2014). Community analyses were performed using "vegan" (Oksanen et al. 2016).

Weather data

To contextualize drought stress observed during our experiment, we quantified precipitation and evapotranspiration using data provided by a local California Irrigation Management Information System (CIMIS) monitoring station in Davis, CA (38.535694, -121.777636). CIMIS automated dataloggers collect weather

data on a minute-by-minute basis, including air temperature, soil temperature, precipitation, solar radiation, vapor pressure, and wind speed. We aggregated these data into monthly intervals, where we calculated Standardized Precipitation-Evapotranspiration Index (SPEI). This metric can be used to quantify the magnitude of drought stress relative to historic norms (Vicente-Serrano et al. 2010, Slette et al. 2019).

SPEI defines drought stress (D) at a given timepoint, i:

$$D_i = P_i - ETo_i$$

Where represents observed precipitation and ETo_i represents estimated evapotransporation. ETo was calculated using the Penman-Monteith equation, defined as:

$$ETo = \frac{\Delta(R_n - G) + \rho_a c_p \frac{e_s - e_a}{r_a}}{\Delta + \gamma(1 + \frac{r_s}{r_a})}$$

Here, Rn is net radiation, G is soil heat flux, $(e_s - e_a)$ is the vapor pressure deficit of air, ρ_a is the mean air density at constant pressure, cp is the specific heat of air, Δ is the slope of the saturation vapor pressure temperature relationship, γ is the psychometric constant, and r_s and r_a are the surface and aerodynamic resistances (Vicente-Serrano et al. 2010).

To contextualize observed climate patterns relative to long-term variation, we calculated SPEI for a 35-year span between 2018 and 1983 (the first year that sufficient climate data was collected by the CIMIS system). To account for potential temporal lag in the effects of climate variation on grassland species abundance (Sala et al. 2012, Dudney et al. 2017), we created drought indices across several cumulative

water year durations. For each year of available data, we calculated SPEI for a single water year (October – May; 8 months), two consecutive water years (20 months), and three consecutive water years (32 months). We then standardized these values by fitting the drought index series to a log-logistic distribution. Resulting values of SPEI were centered at the mean drought stress across overall observations ($D = 0$), and individual years range between extreme droughts ($D < -2$) and significant water surplus ($D > +2$).

SPEI calculations were performed with the "SPEI" package (Beguería et al. 2014).

Construction of Multistate Models

To quantify the probability of vegetation transitions, we fit a multistate model (syn. Markov model) to community state assignments over time. In this model, the probability that a given plot transitions from one vegetation state to another is estimated by a transition matrix, whose terms may also interact with different covariates.

We fit 8 candidate multi-state models to our data, beginning with a baseline model consisting of a transition matrix without influence of any covariates. This base model was then further modified through inclusion of additional terms reflecting the influence of drought stress calculated over 1-, 2-, and 3-year intervals (SPEI) in a given year, t, that modified the probability of transition from a state observed in a previous year, $t-1$. We also included covariates related to the influence of seeded species mixtures, which were assumed to have constant effects on transition probability across all years. Seeding effects (temporal priority) were defined as a binary (1/0) variable describing whether indicator species of a given state were a component of the seeded species mixture. We fit models consisting of only drought effects as covariates, seeding

as a covariate, and models containing both drought and seeding as additive effects.

AIC scores were used to compare the relative fit of all potential candidate models. We selected the model with the lowest AIC score as our best fit model. A table consisting of model descriptions and AIC scores is presented in Appendix Table C.4. Multistate model fitting and model selection was performed using the "msm" package. (Jackson 2011)

All analyses were conducted in R version 3.06 (R Development Core Team).

Results

Seeding treatment effects on community composition

In the first year of observation (2008), plant communities were highly segregated as a function of seeded species mixture (PERMANOVA, pseudo-$F_{6,49} = 32.815, P < 0.001$; Appendix Figure C.1, Appendix Table C.1). Pairwise contrasts of community dissimilarity indicate clear distinctions in vegetation group establishment following seeding – all planting mixtures containing the "naturalized annuals" group were similar in their species composition, as were mixtures composed of "invasive grasses" and "invasive grasses + native species". The single group "native species" treatment composition was also compositionally segregated from others.

Partitioning vegetation into discrete states

Community composition observed in 2008 - 2018 was highly dynamic. On average, plant communities in the same plot compared in two consecutive years were observed

to share roughly 50% of their total relative species cover (mean Bray-Curtis dissimilarity = 0.52 +/- 0.01 standard error). Clustering captured a substantial proportion of total compositional variation (Pseudo-R^2 = 0.39; Figure 3.1). However, residual variation suggests that fluctuations in cover within clusters were still common. This indicates that our method best captured broad changes in the dominance of correlated groups of species, rather than the varying abundance of individual species.

Partitioning of community variance into vegetation states was best characterized by 4 discrete clusters (Appendix C, Appendix Table C.2). Indicator species analysis of these assignments demonstrated that 2 of 4 vegetation states largely followed established conceptions of vegetation types within this system (Table 3.2). State 1 (hereafter, Native Perennials) was characterized by a group of native perennial grasses, while State 3 (Invasive Annuals) was composed of the two planted invasive annual species. However, State 2 (B. hordeaceus-Festuca Annuals) and State 4 (Avena-B. diandrus Annuals) reflected the partitioning of the "Naturalized Annual" group into two separate types. Cluster assignments reflected a 75% cumulative relative abundance of associated indicator species, on average. Less than one tenth of observations had cumulative indicator species relative abundances of less than 40% (Appendix Figure C.2).

Frequency of state assignments over time

The climatic conditions we observed included a period of normal to above-average water availability (2008 – 2011), followed by drought (2012 – 2016), and substantial water surplus (2017; Figure 3.2a). During this period, community transitions between vegetation states were common in all plots (mean number of total transitions observed

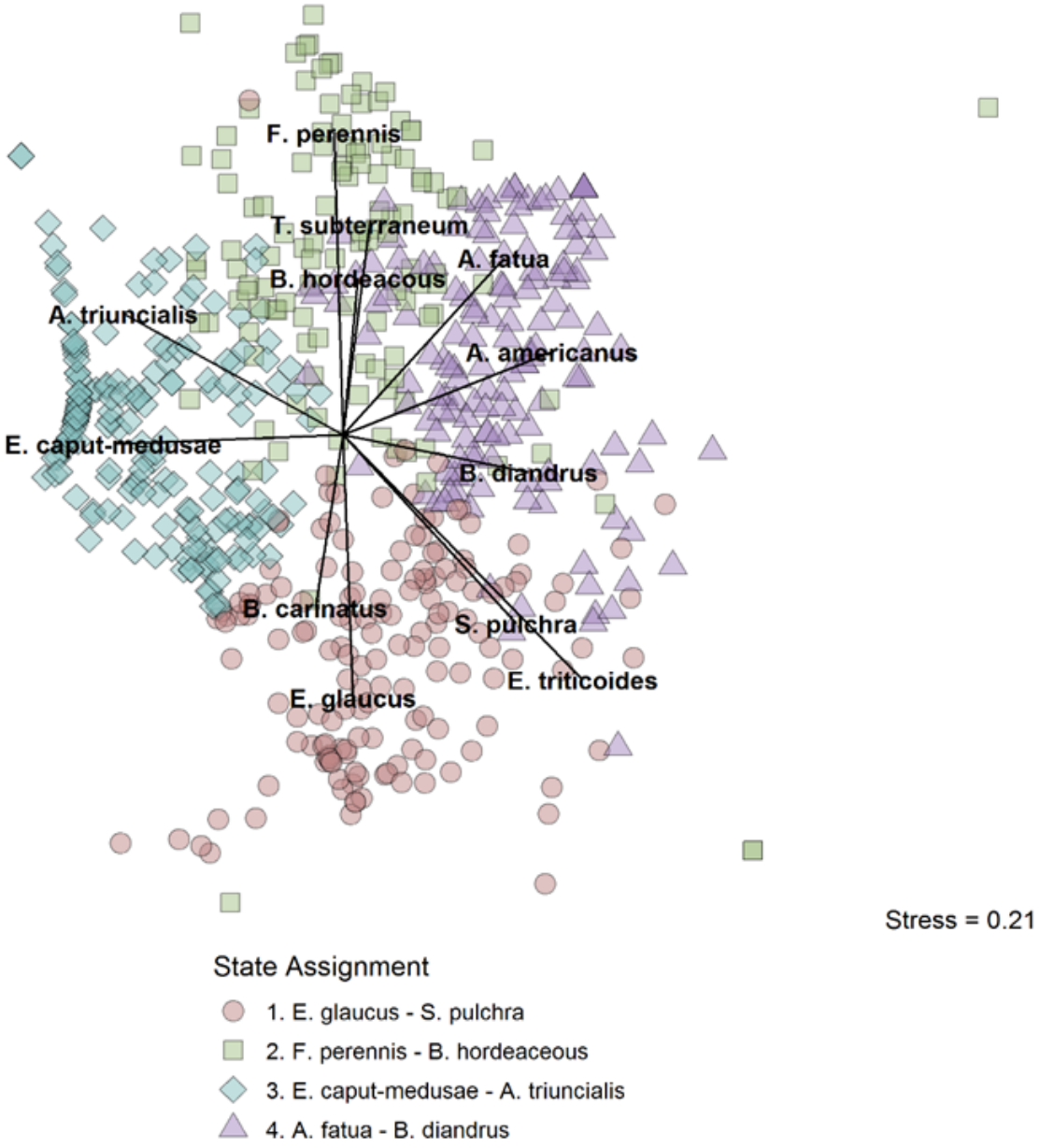

Figure 3.1: Visualization of clustering assignments following K-medoids clustering. Non-metric multidimensional scaling (NMDS) ordination was conducted on all community observations from 2008 – 2018 (n=560). Pairwise community distance was calculated using Bray-Curtis dissimilarity index. Species vectors correspond to taxa that were found to be significantly associated ($P < 0.05$) with state assignments using indicator species analysis.

State	Species	Statistic	P-value
1	E. glaucus	0.801	0.001
1	S. pulchra	0.574	0.001
1	B. carinatus	0.548	0.001
1	F. microstachys	0.284	0.001
2	F. perennis	0.825	0.001
2	B. hordeaceus	0.723	0.001
2	T. subterraneum	0.607	0.001
3	E. caput-medusae	0.871	0.001
3	A. triuncialis	0.741	0.001
4	A. fatua	0.819	0.001
4	B. diandrus	0.553	0.001
4	E. triticoides	0.303	0.036
4	A. americanus	0.274	0.011

Table 3.2: Results of indicator species analysis following K-medoids clustering. High values of the indicator species statistic reflect strong associations between a taxon and a given state assignment. P-values calculated using 1,000 permutations.

per plot = 3.73 +/- 0.16 SE). The frequency of these transition events – summarized in a contingency table (Appendix Table C.3) – were highly non-random, varying as a function of a plot's state assignment in a previous year, in addition to current climatic conditions (plot-level state assignments presented in Appendix Figure C.3).

Following seeding, a majority of communities were characterized by a single state assignment, as each of the 32 plots that received naturalized annual seed (including Avena fatua and Trifolium subterraneum) assumed the Festuca-B. hordeaceus state (Figure 3.2b). The predominance of this community configuration was short-lived, however, and subsequent community dynamics were largely driven by a series of sequential, unidirectional transitions. Invasive Annual communities increased in frequency during the years following seeding, peaking in 2012 after two successive years of above-average precipitation (Figure 3.2). While these transitions were largely

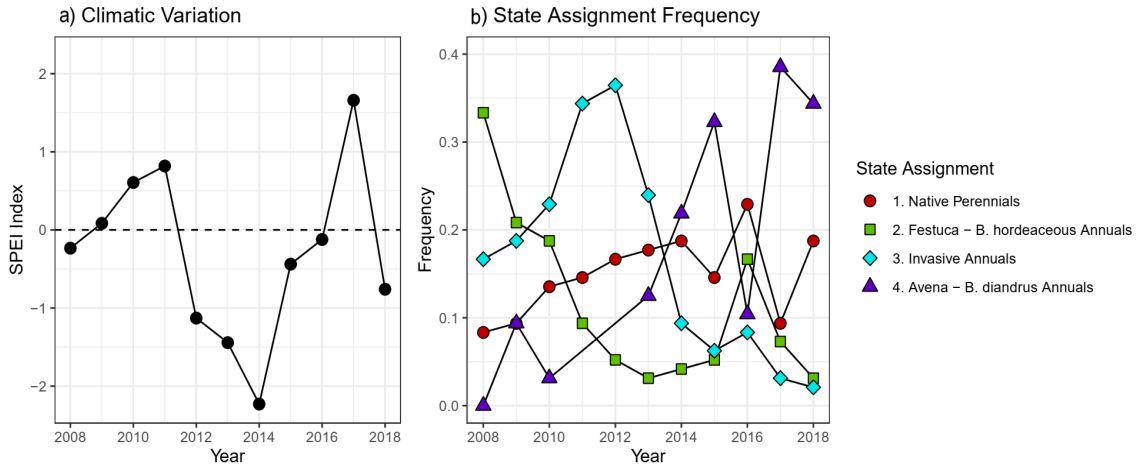

Figure 3.2: Variation in total water year drought severity (A) and frequencies of state assignments (B) from 2008-2018. Average drought stress (SPEI = 0) between 1983-2008 is presented as a dotted line in panel A. Drought in California from 2012-2016 included several years of substantially below-average water availability, including a single year with recorded drought stress greater than two standard deviations beyond historic norms (SPEI < -2).

driven by dominance of Invasive Annual species in plots previously characterized by the Festuca-B. hordeaceus state, the onset of drought in 2012 did not prompt a reversal back to this prior configuration. Instead, many Invasive Annual communities experienced a transition to the Avena-B. diandrus state type between 2013-2015, a change which persisted in many plots until the end of monitoring in 2018.

Curiously, the frequency of Native Perennial communities increased slowly, yet steadily over the course of our experiment (Figure 3.2B). Closer inspection of plot-level state assignments demonstrated that conversion of any vegetation type to the Native Perennial state was rare in cases where native perennial grasses were not included in seeding mixtures (Appendix Table C.3). Once established, however, these communities were quite resistant to state transition, often maintaining their assignment for multiple years under variable climatic conditions.

Model Selection

We fit multi-state models to observed state assignment data to quantify likely pathways of vegetation transition across different state types, treatment combinations, and environmental contexts. From model comparison, we found that that best fit models included both the influence of initial seeding composition and climate variation (Appendix Table C.4). While both 1-year and 3-year cumulative drought stress models provided comparable fits, here we present results from the former due to lower AIC score and greater parsimony. Chi-squared goodness of fit test of observed and expected state frequencies showed no significant deviations from model assumptions $\chi^2_9 = 12; P > 0.20$.

State Transitions

Multi-state modeling attributed our observed variation in state frequencies to several mechanisms of community turnover that differed significantly between species groups (Figure 3.3, Table 3.3). State resistance, the probability of a community changing its state assignment in a subsequent year, varied significantly across the four vegetation types. Baseline transition matrix values in our model, which assume drought stress equivalent to the long-term average (i.e. SPEI = 0) and no effects of seeding, estimated that the Festuca-B.hordeaceus state was more likely to undergo transition than any of the other state types (Figure 3.3, Table 3.3). Whether driven by competitive differences or interannual feedbacks, the short-term predominance of this community type may be the result of an inherent lack of resistance to colonization by other species groups.

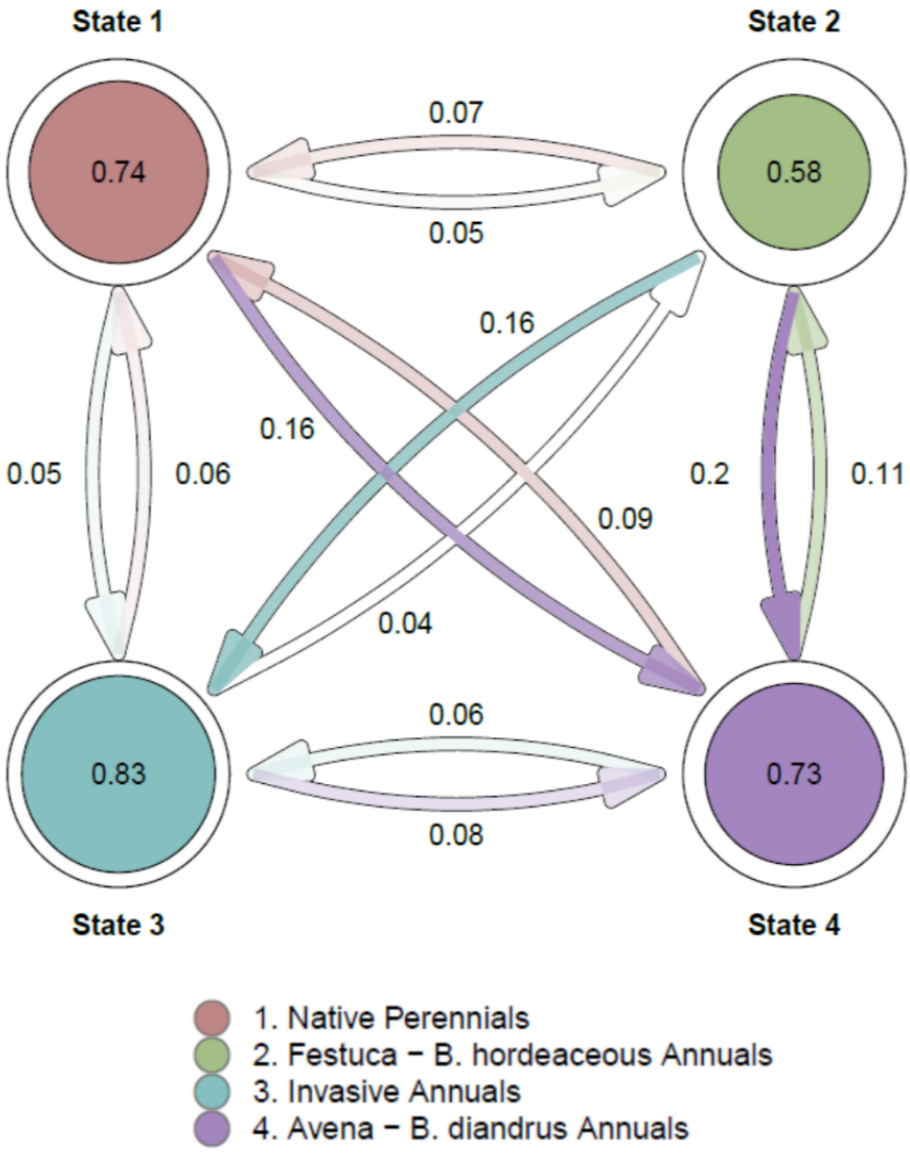

Figure 3.3: State-transition representation of fitted multi-state model coefficients at baseline, assuming no effects of seeding composition and average drought stress (SPEI = 0). Labels refer to the probability a plot transitions between 2 different state assignments (arrows) or the probability a plot retains its assignment (circles) in consecutive years. Circles and arrows are scaled in diameter or color, respectively, by the probability of state assignment transition.

Invasive Annual and Avena-B. diandrus vegetation states that characterized most plant communities exhibited contrasting relationships with drought stress (SPEI; Table 3.3). Estimated transition probabilities from the Invasive Annual state were negatively correlated with drought stress (SPEI hazard ratio < 1), indicating increased state stability when precipitation is above average. Avena-B. diandrus communities, on the other hand, were estimated to arise more frequently from the Invasive Annual state and maintain this configuration with greater probability under drought (SPEI hazard ratio > 1). In contrast to states which exhibited linearly correlated responses

Assignment	Transition	Probability	Priority	Drought Stress (SPEI)
State 1	State 1	0.74 (0.65,0.8)	-	-
State 1	State 2	0.05 (0.03,0.08)	4.77’	0.8
State 1	State 3	0.05 (0.03,0.1)	2.96	0.95
State 1	State 4	0.16 (0.11,0.23)	1.53	0.86
State 2	State 1	0.07 (0.04,0.11)	3.31’	0.83
State 2	State 2	0.58 (0.48,0.65)	-	-
State 2	State 3	0.16 (0.11,0.23)	1.71	1.41
State 2	State 4	0.2 (0.14,0.27)	0.54	0.71
State 3	State 1	0.06 (0.03,0.11)	12.74**	0.56*
State 3	State 2	0.04 (0.02,0.07)	0.55	0.55’
State 3	State 3	0.83 (0.75,0.88)	-	-
State 3	State 4	0.08 (0.05,0.12)	3.26*	0.56*
State 4	State 1	0.09 (0.06,0.15)	2.53*	1.43*
State 4	State 2	0.11 (0.08,0.17)	0.77	1.02
State 4	State 3	0.06 (0.04,0.11)	1.93	0.98
State 4	State 4	0.73 (0.65,0.79)	-	-

Table 3.3: Parameter estimates of the best fit multi-state model (Model 6). For each state assignment, potential state assignments in subsequent years (Transitions) and their associated probabilities (with 95 percent confidence intervals) are reported. Covariate effects reported as hazard ratios, where superscripts correspond to statistical significance: ’ $= P < 0.1$; $* = P < 0.05$; $** = P < 0.01$.

to drought stress, plots characterized by the Native Perennial state displayed complex interactions between effects of drought stress and initial planting composition (Figure

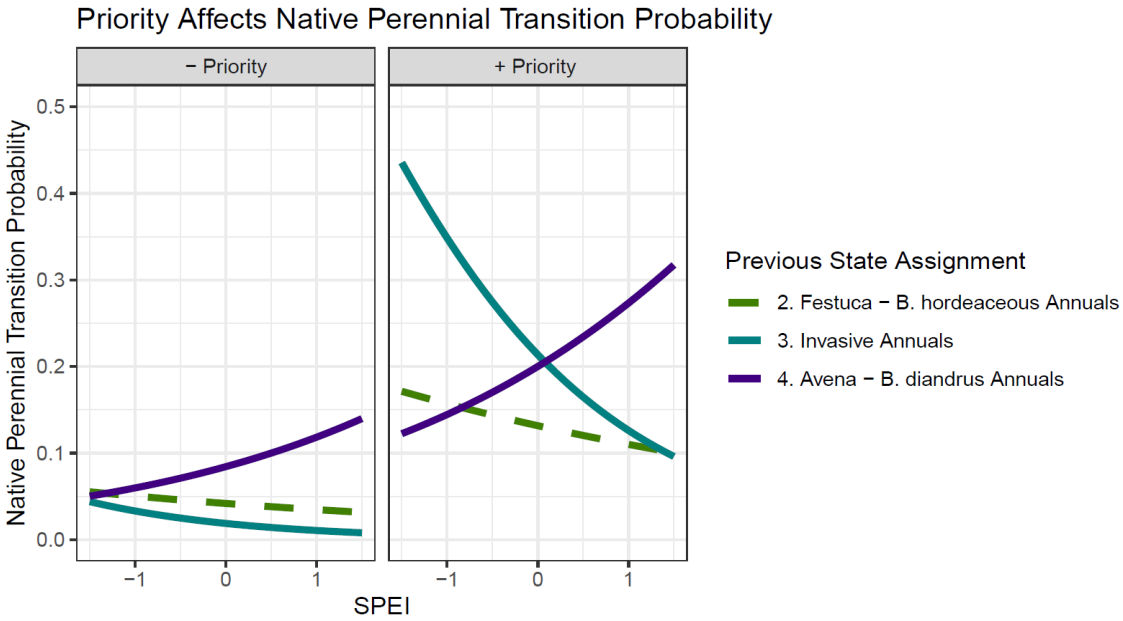

Figure 3.4: The effects of temporal priority and drought stress on the probability of transition of a plot to the Native Perennial state given other previous state assignments. Transition probabilities presented are a function of drought stress (SPEI) and whether native species were included/absent from the seeded species mixture (+/- Priority). Solid lines indicate significant ($P < 0.05$) covariate effects of both SPEI and priority; dashed lines correspond to non-significant effects.

3.4, Table 3.3). The probability of community transition to the Native Perennial state significantly increased under both positive and negative values of SPEI, depending on prior configuration; Invasive Annual communities were more likely to transition to a Native Perennial state under drought, while Avena-B. diandrus communities were more likely to do so with increased water availability. Critically, these transitions were strongly affected by seeding treatments, where plots seeded with native perennial grasses were significantly more likely to transition (Temporal Priority hazard ratios > 1; Table 3.3).

Discussion

Species response groups under climate extremes

The emergence of unique community assemblages under climate change is expected to pose a major challenge to the study and management of natural systems in the near future (Hobbs et al. 2009). California, like many Mediterranean systems, is projected to experience increasing temperatures and fewer, more extreme rainfall events (Yoon et al. 2015). Unprecedented climatic extremes will likely produce unintuitive patterns of community assembly that are poorly predicted by prior observations (Williams and Jackson 2007); however, contemporary observation of extreme events can shed light onto future dynamics.

In this study, we found evidence that core community assemblages under extreme drought differed from historic norms. Classic conceptual models that describe vegetation through three discrete state types failed to capture community turnover as effectively as a four-state model that partitioned the traditional "Naturalized Annual Grasses" state into two separate groups defined by B. hordeaceous and F. perennis, or A. fatua and B. diandrus. This result is particularly striking given the structure imposed by our initial planting composition.

Despite similar life history strategies and observed climate responses (Sandel and Dangremond 2012), short-term persistence of the B. hordeaceous-F.perennis state and subsequent increases in the A. fatua-B. diandrus state suggest that the unique conditions imposed by extreme drought may have crossed previously unobserved thresholds to separate "winners" and "losers" within functional groups (Prugh et al. 2018). The mechanism of this partitioning is unclear, but it appears likely that extreme events

may operate on secondary divisions within the "Naturalized Annual Grass" group. B. diandrus, for example, is a more common dominant in Southern California grasslands (Barbour et al. 2007), and may exhibit adaptations that provide a competitive advantage under lower water availability. In contrast, F. perennis tends to be active later into the dry season, and likely fares poorly in drought.

Our partitioning results highlight the potential difficulty in extending species-environment relationships to unobserved conditions (Nippert et al. 2006). In semi-arid systems, predictions of ecosystem responses to extreme drought are likely to perform poorly when extrapolated from less extreme events. Drought severity is defined by a suite of characteristics related to event size, frequency, and soil water content, whose combined effect on vegetation may not scale linearly with an aggregate measure of drought stress (Fay et al. 2008). In addition, drought responses of locally interacting species are further controlled by factors such as resource competition, mutualism, and herbivory (Tylianakis et al. 2008, Suttle et al. 2007). In some cases, these complex interactions under novel climate conditions may produce nonlinear relationships or unintuitive mechanisms of change (Stuble et al. 2017). Warmer temperatures and decreased rainfall has been observed to favor cold-adapted species in the Chihuahuan desert (Kimball et al. 2010), for example, while species abundances following an extreme drought in Switzerland were best predicted by seed production in a system formerly governed by competitive outcomes (Stampfli and Zeiter 2004).

As these results collectively demonstrate, refinement of conceptual ecosystem models following extreme events may increase their utility under future climate conditions. Our findings underscore the need for analytical approaches able to critically evaluate

these conceptual tools. Particularly in rangeland systems, which decompose community dynamics into fluctuations between species groups, clustering approaches may effectively capture the novel, site-specific community assemblages that are likely to arise under climate change.

Contingency in vegetation dynamics

In this study, we found that species turnover in California grasslands is contingent on both climatic variation and prior patterns of community assembly. Early abundance of the Festuca-B. hordeaceous state gave rise to communities dominated by Invasive Annual species under above-average precipitation. Under drought, however, many of these communities failed to return to this initial state type, instead transitioning to the Avena-B. diandrus state. Transitions to a fourth state, Native Perennials, increased under both drought and water surplus, but depended strongly on a community's prior state type and experimental seed addition.

These state-specific patterns of change are likely driven by variation in the dominant species which characterize each state. Dominant species are often observed to be primary determinants of key community attributes in grassland systems, such as productivity (Smith and Knapp 2003), drought tolerance (Hoover et al. 2014), and resistance to invasion (Smith et al. 2004). And like other studies of California grassland dynamics in a state-transition perspective (Jackson and Bartolome 2002, Stein et al. 2016), the species that define our vegetation states may be linked to a number of potential mechanisms that influence community turnover.

Across the four vegetation groups we identified, known species characteristics related to competitor inhibition and recruitment appear correlated with observed persistence

and transition probabilities, respectively. Invasive annual grasses, A. triuncialis and E. caput-medusae, facilitate their persistence through deposition of dense thatch layers that inhibit germination and growth of competitors (Eviner and Hawkes 2012). While native perennial grasses are effective competitors once mature, increased transition probabilities following experiment seeding likely reflects recruitment limitation that is thought to limit colonization [Seabloom et al. (2003b); Seabloom2003b]. This contrasts with many naturalized annual grasses, whose large investment into seed production may facilitate rapid colonization and contribute to positive nutrient cycling feedbacks (Eviner and Hawkes 2012, Hillerislambers et al. 2010).

While climate variation may favor certain species groups in isolation, the pathways of community change we observed suggest that climatic effects interact strongly with other state properties – rather than exhibiting a consistent relationship with precipitation, state frequencies in a given year depended on both climate conditions and state frequencies in years prior. Though limited to short-term recovery, our findings indicate that state persistence and variable susceptibility to community change may help explain lagged recovery or a failure to return to previous ecosystem states following drought (Smith et al. 2015). Compositional changes following climate events can produce long-lasting effects on successional trajectories, where post-drought species assemblages exhibit strong persistence or altered pathways of community change (Kreyling et al. 2011). Other studies of drought effects in California grasslands show similar trends, in which community recovery lags behind climate trends (Harrison et al. 2018); or exhibits selective pathways of change, where return to only a subset of initial state types is possible (Larios et al. 2013).

Implications for Restoration and Management

While drought is often linked to a number of negative ecosystem changes, such as reduced biodiversity and invasive species spread, the novel conditions imposed by extreme climatic events may also facilitate management efforts (Hobbs et al. 2006, 2009, Seastedt et al. 2008). By quantifying the persistence of species assemblages under various contexts, our results provide a foundation to better predict windows of opportunity and design effective interventions. The establishment of native perennial grasses is a common restoration target in California annual grasslands, though success is limited and highly contingent on year-to-year variation (Stromberg et al. 2007, Young et al. 2014). Many restoration efforts in this system utilize temporal or spatial priority to manipulate competitive relationships during planting, in the hope that early establishment delays or prevents encroachment by less desirable species (Wainwright et al. 2012, Fry et al. 2017, Young et al. 2017). For native perennial grasses in California annual grasslands, we found strong evidence that priority seeding can assist in establishing and maintaining a desired community that remains relatively persistent after planting or provide the basis for subsequent dominance when conditions are favorable (Porensky et al. 2012).

In contrast, our study suggests that eradication of invasive annual grasses may be facilitated by targeted management during drought. Common interventions–grazing, herbicide application, and targeted burning–may be more effective when conditions naturally disadvantage E. caput-medusae and A. triucialis (DiTomaso et al. 2008). However, given that vegetation states may vary in persistence, managers must take care to ensure that colonizing vegetation is robust to re-invasion. Growth of ruderal weeds appears common following management in California grasslands, which often

do little to resist colonization of invasive grasses (Young 1992, DiTomaso et al. 2008).

Generally, our findings underscore the potential value of maintaining functional and taxonomic diversity in restoration and management (Funk et al. 2008) . Particularly in highly dynamic systems where environmental fluctuations drive turnover, long-term ecosystem health may depend on turnover among desirable community types–the maintenance of multiple potential vegetation states can maintain favorable pathways of compositional change following disturbance that may otherwise favor spread of undesirable species (Hoover et al. 2014, Griffin-Nolan et al. 2019, Wilcox et al. 2020).

Future Directions

This study highlights the need to employ analytical approaches capable of distinguishing novel assemblages as they arise. Reliance on long-standing divisions between species groups to characterize system responses to climate change may fail to capture emergent complexity. However, while we were able to capture the immediate effects of a historic drought on grassland plant communities, the scope of our study is focused on a relatively narrow time period that may be insufficient to capture long-term changes to vegetation dynamics. Continued observation, particularly over a broader range of climatic conditions, may further refine partitions between core species groups and better capture ecosystem recovery to extreme events.

Appendix A

Chapter 1 Supporting Information

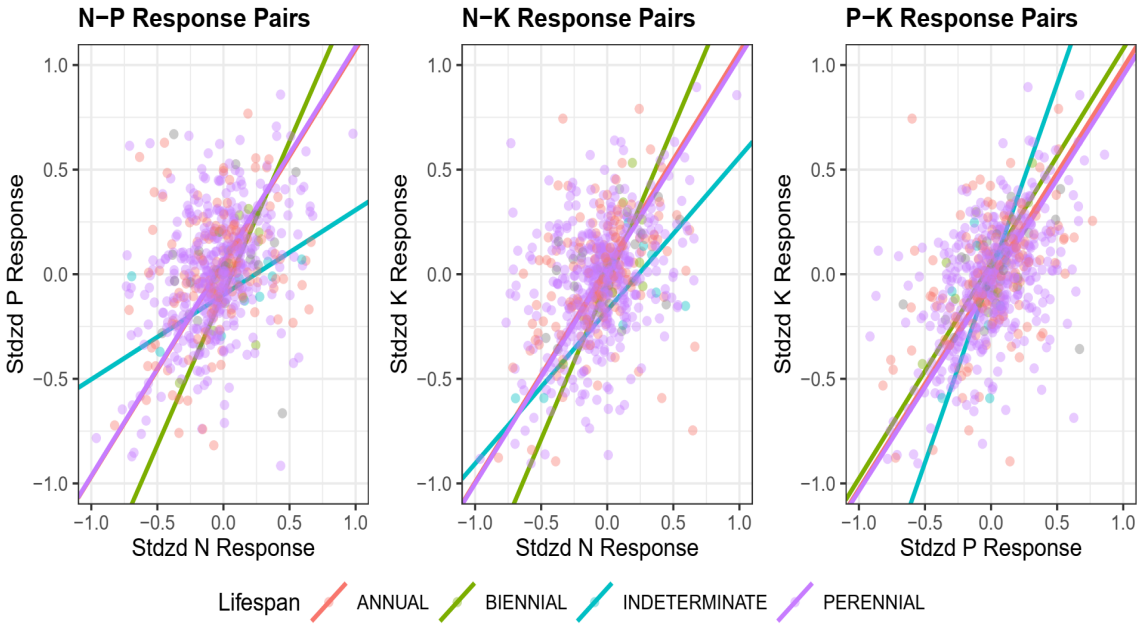

Figure A.1: Bivariate relationships between treatments colored by species lifespan.

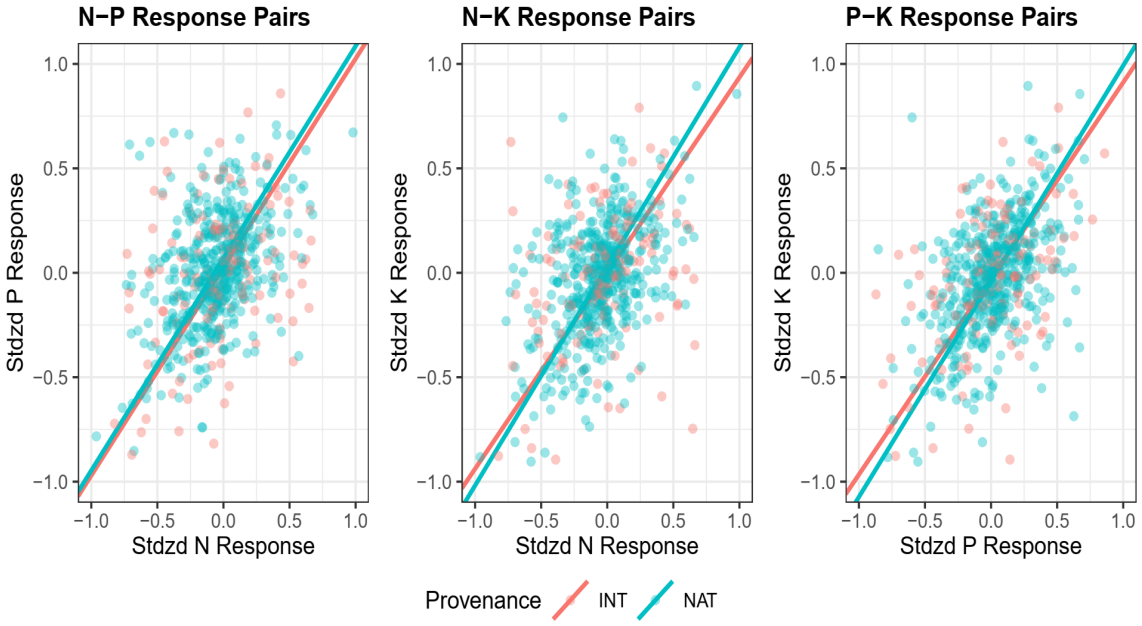

Figure A.2: Bivariate relationships between treatments colored by provenance (introduced / native).

Site Name	Continent	Country	Habitat	First Year	Last Year	Total Years	MAP	MAT	Taxa
Azi	Asia	CN	alpine grassland	2007	2012	5	711	1.36	43
Bogong	Australia	AU	alpine grassland	2009	2019	11	1678	5.98	19
Boulder South Campus	North America	US	shortgrass prairie	2008	2016	9	487	9.9	9
Bunchgrass (Andrews LTER)	North America	US	montane grassland	2007	2018	12	1618	6.77	10
Burrawan	Australia	AU	semiarid grassland	2008	2019	12	643	18.22	10
Cedar Creek LTER	North America	US	tallgrass prairie	2007	2018	12	740	6.34	8
Cedar Point Biological Station	North America	US	shortgrass prairie	2007	2019	13	456	9.64	12
CEREEP - Ecotron IDF	Europe	FR	old field	2012	2018	7	632	10.82	16
Chichaqua Bottoms	North America	US	tallgrass prairie	2009	2019	11	871	9.26	6
Companhia das Lezirias	Europe	PT	annual grassland	2012	2019	8	564	16.58	26
Cowichan	North America	CA	old field	2007	2018	12	762	10.45	5
Elliott Chaparral	North America	US	annual grassland	2008	2019	11	344	17.71	6
Ethabuka (Main Camp)	Australia	AU	desert grassland	2013	2019	7	192	24.06	4
Ethabuka (South Site)	Australia	AU	desert grassland	2013	2019	7	203	23.95	3
Fruebuel	Europe	CH	pasture	2008	2015	8	1546	6.96	15
Hall's Prairie	North America	US	tallgrass prairie	2007	2014	8	1289	13.83	4
Hart Mountain	North America	US	shrub steppe	2007	2012	6	259	7.75	11
Heronsbrook (Silwood Park)	Europe	UK	mesic grassland	2007	2013	7	668	10.17	19
Hopland REC	North America	US	annual grassland	2007	2019	13	1065	13.24	19
Jena	Europe	DE	grassland	2013	2018	6	654	8.57	18
Kibber (Spiti)	Asia	IN	alpine grassland	2011	2018	8	400	-1.45	7
Kilpisjärvi	Europe	FI	tundra grassland	2013	2018	6	569	-3.25	24
Kinypanial	Australia	AU	semiarid grassland	2007	2018	11	408	15.59	8
Koffler Scientific Reserve	North America	CA	pasture	2010	2019	10	853	6.28	10
Konza LTER	North America	US	tallgrass prairie	2007	2019	13	889	12.08	17
Lancaster	Europe	UK	mesic grassland	2008	2017	10	1522	8.01	10
Las Chilcas	South America	AR	mesic grassland	2013	2019	7	955	15.09	8
Lookout (Andrews LTER)	North America	US	montane grassland	2007	2018	12	1877	6.9	8
Mar Chiquita	South America	AR	grassland	2011	2018	8	907	14.32	14
Mclaughlin UCNRS	North America	US	annual grassland	2007	2019	13	936	13.97	8
Mt. Caroline	Australia	AU	savanna	2008	2018	11	324	17.75	15
Pingelly Paddock	Australia	AU	old field	2013	2018	6	456	16.28	10
Pinjarra Hills	Australia	AU	pasture	2013	2018	5	1085	19.99	5
Rookery (Silwood Park)	Europe	UK	mesic grassland	2007	2013	7	685	10.13	12
Saana	Europe	FI	montane grassland	2014	2019	6	521	-2.6	25
Sagehen Creek UCNRS	North America	US	montane grassland	2007	2013	7	831	5.83	16
Savannah River	North America	US	savanna	2007	2012	6	1184	17.43	12
Sedgwick Reserve UCNRS	North America	US	annual grassland	2007	2017	11	478	15.58	4
Sevilleta LTER	North America	US	desert grassland	2007	2018	12	252	13.06	5
Sheep Experimental Station	North America	US	shrub steppe	2007	2016	10	246	5.32	18
Shortgrass Steppe LTER	North America	US	shortgrass prairie	2007	2018	12	369	8.95	6
Sierra Foothills REC	North America	US	annual grassland	2007	2019	13	936	16.31	7
Smith Prairie	North America	US	mesic grassland	2007	2016	10	605	10.18	25
Spindletop	North America	US	pasture	2007	2019	13	1152	12.48	9
Temple	North America	US	tallgrass prairie	2007	2016	10	877	19.4	15
Trelease	North America	US	tallgrass prairie	2008	2017	10	992	11.07	5
Ukulinga	Africa	ZA	mesic grassland	2009	2018	10	832	17.65	17
Val Mustair	Europe	CH	alpine grassland	2008	2019	11	681	0.13	30
Yarramundi	Australia	AU	mesic grassland	2014	2019	6	844	17.32	5

Table A.1: Table of sites included in analysis.

Site Name	ρ(N-P)	ρ(N-K)	ρ(P-K)	ΔN	ΔP	ΔK	D
Azi	0.4	0.68	0.47	1.3	1.35	1.44	0.32
Bogong	0.28	0.59	0.57	0.44*	0.42*	0.38*	0.35
Boulder South Campus	-0.06	0.05	0.67	0.44	0.56*	0.44	0.52
Bunchgrass (Andrews LTER)	0.22	0.67	0.52	0.25	0.46*	0.43*	0.35
Burrawan	0.26	0.32	-0.03	0.17	0.2	0.17	0.54
Cedar Creek LTER	0.43	0.14	0.57	0.53*	0.18	0.22	0.41
Cedar Point Biological Station	0.2	0.18	0.43	0.36*	0.23*	0.27*	0.49
CEREEP - Ecotron IDF	0.13	0.15	0.61	1.12*	0.91	1.12*	0.47
Chichaqua Bottoms	0.48	0.57	0.6	0.30*	0.25	0.27*	0.3
Companhia das Lezirias	0.44	0.2	0.38	1.15*	1.10*	0.75	0.44
Cowichan	-0.3	0.66	-0.01	0.12	0.27*	0.17	0.59
Elliott Chaparral	0.5	-0.12	0.66	0.22	0.26	0.27	0.44
Ethabuka (Main Camp)	-0.08	0.57	0.28	0.28	0.83*	0.43	0.5
Ethabuka (South Site)	0.77	0.88	0.92	0.59*	0.32	0.52	0.09
Fruebuel	0.58	0.15	0.49	1.05*	0.99*	0.83*	0.4
Hall's Prairie	0.56	0.58	0.04	1.13*	0.66*	0.68*	0.4
Hart Mountain	0.91	0.46	0.5	0.96*	0.73	0.57	0.25
Heronsbrook (Silwood Park)	0.21	0.6	0.28	1.03*	0.67	0.66	0.42
Hopland REC	0.33	0.75	0.58	1.01*	0.49	0.68*	0.3
Jena	-0.25	0.06	0.2	0.97*	0.62	0.64	0.67
Kibber (Spiti)	0.3	0.48	0.74	0.25	0.26	0.27	0.33
KilpisjÃ¤rvi	0.4	0.22	0.8	1.03*	0.78	0.46	0.35
Kinypanial	-0.08	0.23	0.84	0.16	0.32	0.26	0.45
Koffler Scientific Reserve at Joker's Hill	0.32	0.6	0.53	0.88*	0.65*	0.54*	0.34
Konza LTER	0.29	0.23	0.55	0.43*	0.28	0.37	0.43
Lancaster	0.55	0.57	0.57	0.44	0.38	0.38	0.29
Las Chilcas	0.71	0.55	0.83	0.78*	0.52	0.84*	0.2
Lookout (Andrews LTER)	0.66	0.88	0.86	0.38*	0.39*	0.50*	0.13
Mar Chiquita	0.75	0.54	0.6	0.62	0.58	0.6	0.25
Mclaughlin UCNRS	0.51	0.24	0.24	0.41	0.33	0.38	0.45
Mt. Caroline	0.67	0.71	0.6	0.67*	0.62*	0.52*	0.23
Pingelly Paddock	0.46	-0.08	-0.29	0.74	1.28*	0.61	0.65
Pinjarra Hills	0.55	0.25	0.81	0.78	1.06	0.77	0.31
Rookery (Silwood Park)	0.8	0.74	0.8	0.99*	1.50*	0.73	0.15
Saana	0.61	0.56	0.62	1.25*	0.98*	1.09*	0.27
Sagehen Creek UCNRS	0.12	0.49	0.17	0.63	0.49	0.45	0.49
Savannah River	0.42	0.12	0.38	0.76	0.99	0.55	0.46
Sedgwick Reserve UCNRS	0.61	0.84	0.94	0.38*	0.39*	0.36*	0.14
Sevilleta LTER	0.8	0.92	0.94	0.36*	0.14	0.14	0.08
Sheep Experimental Station	-0.11	0.53	-0.12	0.28*	0.17	0.21	0.6
Shortgrass Steppe LTER	-0.01	0.36	0.53	0.43*	0.26*	0.1	0.47
Sierra Foothills REC	-0.38	0.23	0.59	0.34	0.24	0.29	0.57
Smith Prairie	0.15	0.15	0.06	0.53*	0.47*	0.35	0.59
Spindletop	0.66	0.14	0.2	0.24	0.25	0.60*	0.44
Temple	0.28	0.24	0.5	0.41	0.61*	0.55	0.44
Trelease	-0.27	-0.51	0.48	0.55*	0.28	0.23	0.73
Ukulinga	0.17	-0.06	0.51	0.58*	0.51*	0.75*	0.53
Val Mustair	0.56	0.4	0.45	0.45*	0.57*	0.3	0.35
Yarramundi	0.75	0.65	0.2	0.36	0.36	0.65*	0.31

Table A.2: Table of sites, pairwise correlations between community responses to different treatments (ρ), rate of community change in response to treatment (Δ), and estimated response dimensionality (D). Significant ($P < 0.05$) magnitudes of community response are labelled with *.

Appendix B

Chapter 2 Supporting Information

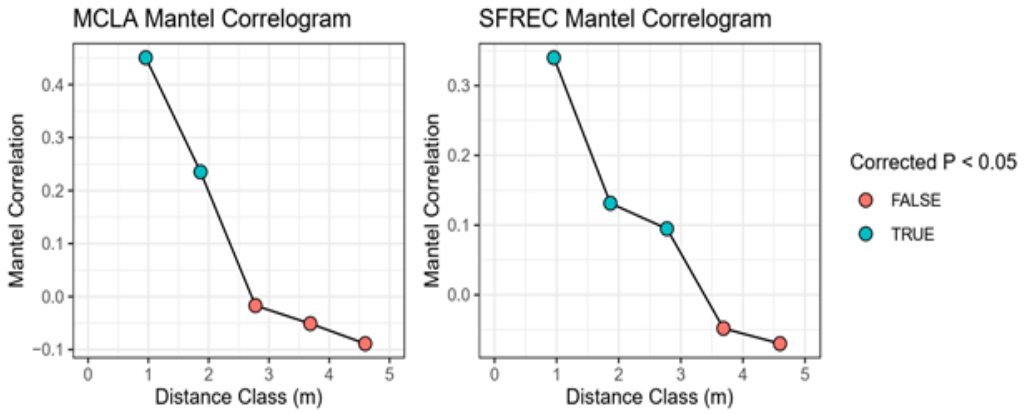

Figure B.1: Mantel correlograms demonstrating spatial autocorrelation in plant community composition using pre-treatment data. In both sites, statistically significant ($P < 0.05$) autocorrelation in community composition was detectable to a scale of roughly 2-3 meters. Difference in community composition was calculated using Bray-Curtis dissimilarity and Pearson correlation. Significance tests were performumed using 999 sample permutations, with P-values adjusted using the Holm correction.

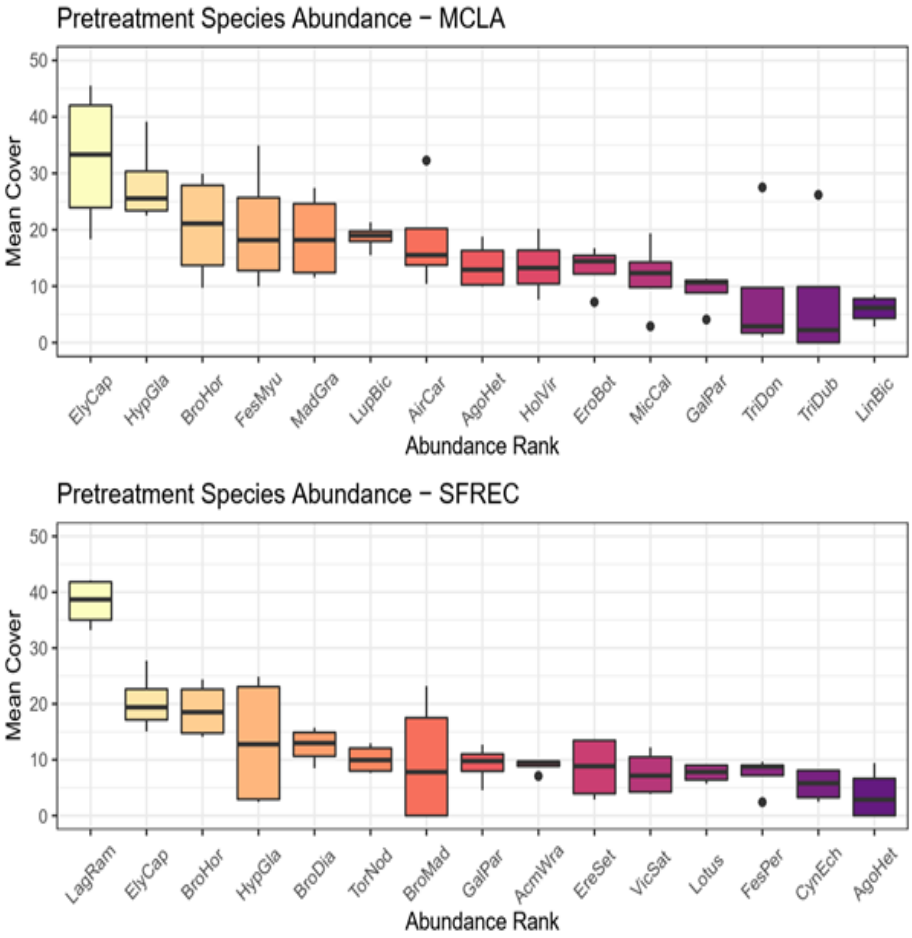

Figure B.2: Relative abundances of species in pre-treatment sampling, top 15 most abundant species shown. Values reflect maximum cover observed in three sampling periods to account for variable phenology.

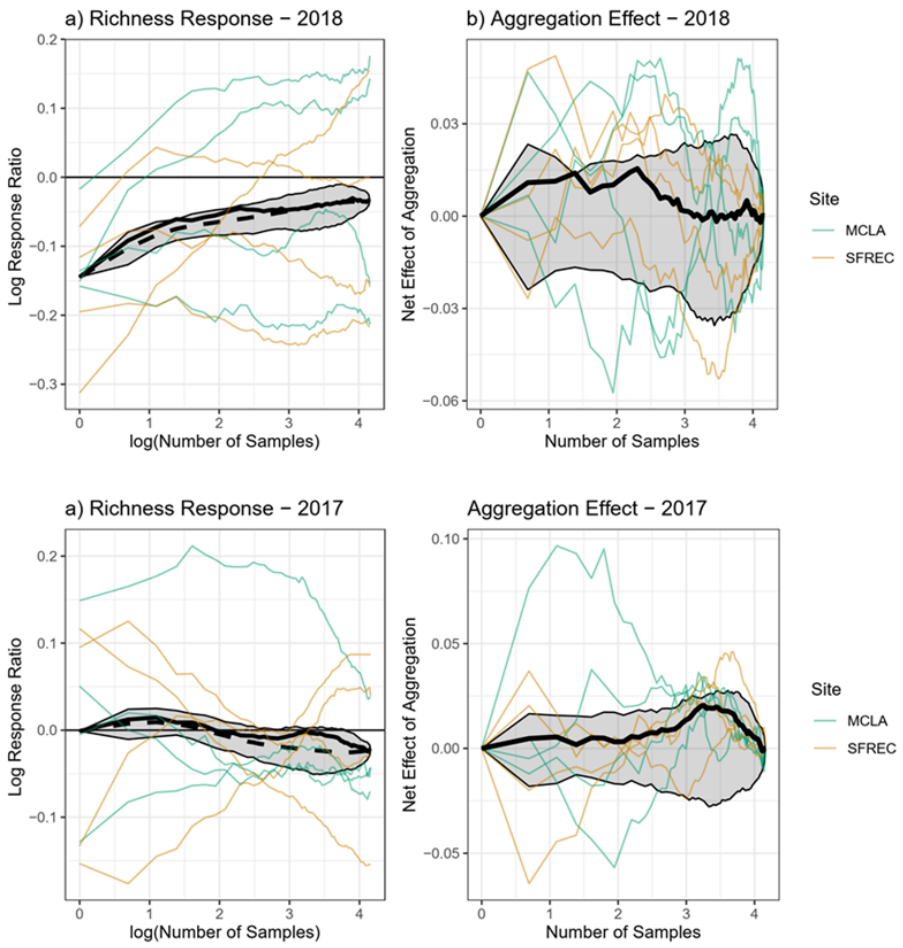

Figure B.3: Effect of fertilization on species richness and spatial aggregation as a function of sampling scale in 2017 and 2018, presented as a log response ratio. In subplot a, the solid black line corresponds to mean estimated effects under spatially explicit ("empirical") sample accumulation, while dashed line reflects the median of mean diversity effects under randomized sample accumulation. Shaded areas correspond to Bonferroni-adjusted 95% confidence intervals of mean diversity response across 10,000 random sample accumulation curves. Colored lines denote individual responses of each block. In subplot b, lines correspond to the net effects of spatial aggregation on estimated response, calculated as the observed log-response ratio relative to the median value across bootstrap samples. Shaded areas correspond to Bonferroni-adjusted 95% confidence intervals of aggregation effects on mean diversity response across 10,000 random sample accumulation curves.

Abbreviation	Taxon	Functional Type
AcmPar	Acmispon parviflorus	Legume
AgoHet	Agoseris heterophylla	Forb
AirCar	Aira caryophyllaea	Grass
BroDia	Bromus diandrus	Grass
BroHor	Bromus hordeaceous	Grass
BroMad	Bromus madritensis	Grass
ElyCap	Elymus caput-medusae	Grass
EreSet	Eremocarpus setigerus	Forb
EroBot	Erodium botrys	Forb
FesMyu	Festuca myuros	Grass
FesPer	Festuca perennis	Grass
GalPar	Galium parisiense	Forb
HolVir	Holocarpha virgata	Forb
HypGla	Hypochaeris glabra	Forb
LagRam	Lagophylla ramosissima	Forb
LinBic	Linanthus bicolor	Forb
LupBic	Lupinus bicolor	Legume
MadGra	Madia gracilis	Forb
MicCal	Micropus californica	Forb
TorNod	Torilis nodosa	Forb
TriDon	Trifolium microdon	Legume
TriDub	Trifolium dubium	Legume
VicSat	Vicia sativa	Legume

Table B.1: Taxon abbreviations and functional types in pre-treatment sampling

Source	DF	SS	R2	F	P
Block	3	0.90722	0.30593	11.4242	0.001***
Year	2	1.29772	0.43761	24.5124	0.001***
Treatment	3	0.16033	0.05407	2.019	0.038*
Block x Treatment	9	0.44136	0.14883	1.8526	0.012*
Residual	6	0.15882	0.05356		
Total	23	2.96545	1		

Table B.2: PERMANOVA of Compositional Variation – MCLA

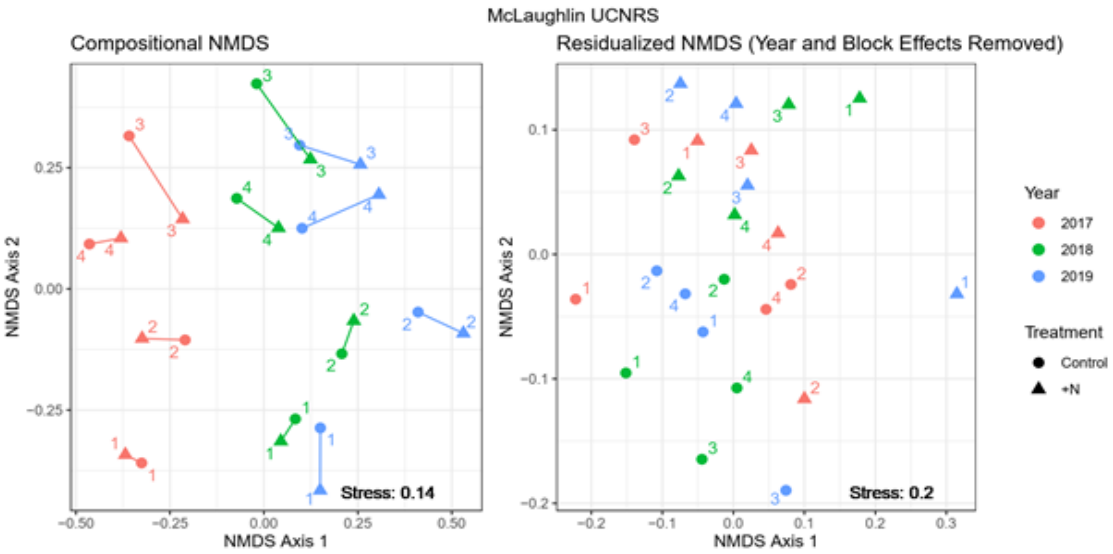

Figure B.4: NMDS visualizations of variation in species cover data at MCLA summarized at the block level. Points are colored by year, with varying shape according to treatment. Lines link treatment and control plots within each block-year combination. Residualized NMDS was generated by first accounting for effects of block and year variation, then plotting the residual distance matrix.

Source	DF	SS	R2	F	P
Block	3	1.53996	0.5931	21.9146	0.001***
Year	2	0.22878	0.08811	4.8836	0.002**
Treatment	3	0.17522	0.06749	2.4935	0.012*
Block x Treatment	9	0.51194	0.19717	2.4284	0.003**
Residual	6	0.14054	0.05413		
Total	23	2.59644	1		

Table B.3: PERMANOVA of Compositional Variation – SFREC

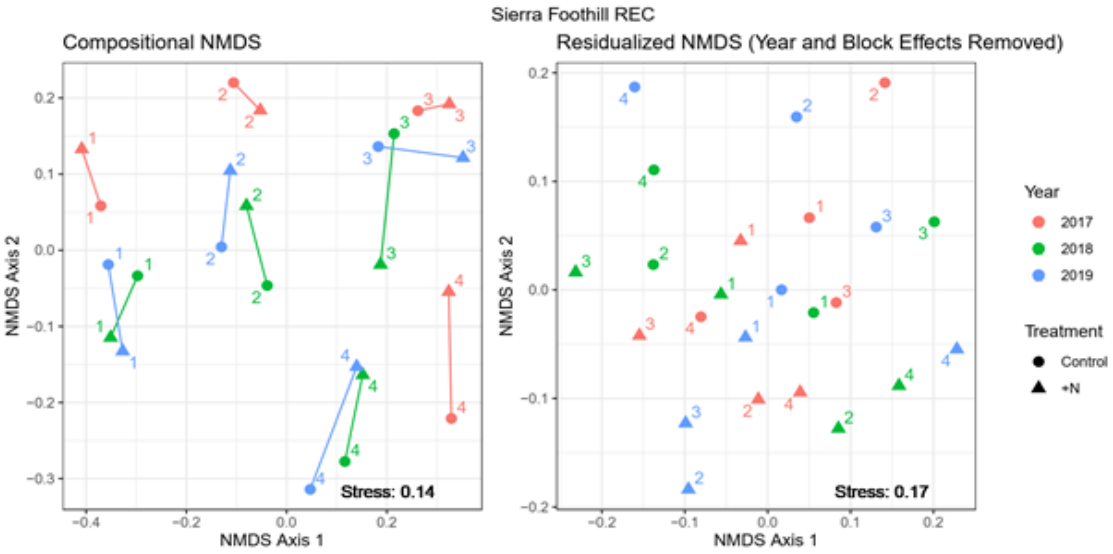

Figure B.5: NMDS visualization of variation in species cover data at SFREC summarized at the block level. Points are colored by year, with varying shape according to treatment. Lines link treatment and control plots within each block-year combination. Residualized NMDS was generated by first accounting for effects of block and year variation, then plotting the residual distance matrix.

Site	Genus	Species	Group	Origin	Cover 2017	Effect 2017	Cover 2018	Effect 2018	Cover 2019	Effect 2019
SFREC	Lagophylla	ramosissma	Forb	Nat	9.57	-0.61	8.27	-1.05	13.34	2.28
SFREC	Agoseris	heterophylla	Forb	Int	16.39	6.02	9.14	6.32	10.59	7.96
SFREC	Bromus	hordeaceous	Grass	Int	7.44	2.27	7.93	3.54	10.41	-2.73
SFREC	Bromus	madritensis	Grass	Int	6.62	-2.15	5.59	0.03	9.04	-4.65
SFREC	Elymus	caput-medusae	Grass	Int	4.47	2.67	7.72	2.92	6.22	1.78
SFREC	Bromus	diandrus	Grass	Int	7.45	-1.62	9.51	-3.35	6.02	-3.05
SFREC	Trifolium	dubium	Legume	Int	8.21	-3.60	7.60	-3.89	4.66	-2.84
SFREC	Torilis	nodosa	Forb	Nat	4.97	-1.92	4.56	-0.30	4.59	-1.81
SFREC	Vicia	sativa	Legume	Int	5.81	-1.99	6.88	0.35	4.49	-1.26
SFREC	Geranium	dissectum	Forb	Int	4.37	0.10	6.14	-2.32	4.10	-0.06
SFREC	Clarkia	Purpurea	Forb	Nat	2.07	-1.28	1.85	-0.89	2.44	-1.29
SFREC	Acmispon	purshianus	Legume	Nat	2.47	-1.79	3.85	-2.61	2.42	-0.93
SFREC	Aira	caryophyllaea	Grass	Int	2.88	0.92	2.30	-0.35	2.32	1.71
SFREC	Bromus	sterilis	Grass	Int	1.00	1.59	0.90	-0.07	2.25	-0.85
SFREC	Cynosurus	echinatus	Grass	Int	0.80	1.10	2.38	0.29	2.15	0.42
SFREC	Galium	parisiense	Forb	Int	0.00	-0.00	2.09	-0.00	2.05	-0.45
SFREC	Vulpia	myuros	Grass	Int	0.66	0.37	1.26	0.95	1.65	1.87
SFREC	Dichlostemma	capitatum	Forb	Nat	0.06	-0.06	0.00	-0.00	1.44	0.40
SFREC	Crucianella	angustilfolia	Forb	Int	0.00	0.00	1.39	-1.03	1.40	-0.73
SFREC	Briza	minima	Grass	Int	1.55	0.29	1.25	0.70	1.31	0.16
SFREC	Carduus	pachnocephalus	Forb	Int	0.96	0.64	1.65	0.22	1.26	0.37
SFREC	Trifolium	hirtum	Legume	Int	2.23	0.35	1.41	-0.94	1.05	-0.37
SFREC	Acmispon	parviflorus	Legume	Nat	0.35	-0.02	0.00	0.00	0.77	-0.72
SFREC	Elymus	glaucus	Grass	Nat	0.85	-0.31	1.02	-0.17	0.74	-0.20
SFREC	Euphorbia	spathulata	Forb	Int	0.14	0.44	0.84	-0.17	0.64	0.56
SFREC	Centaurea	melitensis	Forb	Int	0.00	0.00	0.38	-0.23	0.51	0.11
SFREC	Avena	barbata	Grass	Int	1.42	-0.38	1.06	1.29	0.44	1.73
SFREC	Navarretia	pubescens	Forb	Nat	0.19	0.27	0.35	0.31	0.39	0.77
SFREC	Madia	gracilis	Forb	Nat	0.03	0.17	0.21	0.02	0.31	0.11
SFREC	Daucus	pusillus	Forb	Int	0.21	-0.21	0.04	0.09	0.18	-0.04
SFREC	Petrorhagia	dubia	Forb	Int	1.60	-0.54	0.54	-0.38	0.14	0.25
SFREC	Bromus	carinatus	Grass	Nat	0.00	0.00	0.24	-0.24	0.12	-0.12
SFREC	Festuca	perennis	Grass	Int	0.04	0.26	0.00	1.07	0.10	-0.10
SFREC	Cerastium	glomeratum	Forb	Int	0.24	-0.09	0.04	0.16	0.08	0.08
SFREC	Tritileia	hyacinthina	Forb	Nat	0.62	0.47	0.26	-0.13	0.07	0.09
SFREC	Tritileia	hyacinthina	Forb	Nat	0.62	0.47	0.26	-0.13	0.07	0.09
SFREC	Lomatium	californicum	Forb	Nat	0.03	-0.03	0.03	-0.03	0.07	-0.07
SFREC	Hypochaeris	glabra	Forb	Int	0.00	0.00	0.00	0.00	0.06	0.14
SFREC	Clatonia	perfoliata	Forb	Nat	0.00	0.11	0.00	0.00	0.03	0.04
SFREC	Eremocarpus	setigerus	Forb	Nat	0.01	0.02	0.10	-0.09	0.02	0.06
SFREC	Tritileia	laxa	Forb	Nat	0.03	-0.03	0.04	-0.03	0.01	-0.00
SFREC	Anagallis	arvensis	Forb	Int	0.12	0.06	0.17	-0.17	0.01	0.12
SFREC	Erodium	botrys	Forb	Int	0.58	0.13	0.18	0.20	0.01	0.17
SFREC	Athysanus	pusillus	Forb	Nat	0.06	0.13	0.00	0.00	0.01	0.03
SFREC	Linanthus	bicolor	Forb	Nat	0.12	0.30	0.09	-0.09	0.01	0.30
SFREC	Cardamine	oligosperma	Forb	Nat	0.00	0.08	0.04	0.10	0.00	-0.00
SFREC	Githopsis	specularioides	Forb	Nat	0.00	0.00	0.00	0.00	0.00	0.12
SFREC	Lactuca	serriola	Forb	Int	2.46	-2.22	0.15	-0.15	0.00	-0.00
SFREC	Sherardia	arvensis	Forb	Int	0.26	0.12	0.01	0.03	0.00	0.04
SFREC	Dichlostemma	multiflorum	Forb	Nat	0.00	0.00	0.03	-0.03	0.00	-0.00
SFREC	Centaurea	solstitialis	Forb	Int	0.20	-0.20	0.37	-0.37	0.00	0.00
SFREC	Epilobium	brachycarpum	Forb	Nat	0.00	0.00	0.00	0.00	0.00	0.00
SFREC	Filago	gallica	Forb	Int	0.12	-0.05	0.00	0.00	0.00	0.00
SFREC	Linanthus	parviflora	Forb	Nat	0.00	-0.00	0.00	0.06	0.00	0.00
SFREC	Odontostomum	hartwegii	Forb	Nat	0.00	0.44	0.00	0.47	0.00	0.50
SFREC	Githopsis	specularioides	Forb	Nat	0.00	0.00	0.00	0.00	0.00	0.00
SFREC	Sanicula	bipinnatifida	Forb	Nat	0.00	0.00	0.03	-0.03	0.00	0.00
SFREC	Thysanocarpus	curvipes	Forb	Nat	0.00	0.00	0.04	0.00	0.00	0.00
SFREC	Trifolium	microcephalum	Legume	Nat	0.00	0.00	0.00	0.00	0.00	0.00
MCLA	Trifolium	microdon	Legume	Nat	0.02	-0.02	0.00	0.00	0.00	0.00
MCLA	Trifolium	wildenovii	Legume	Nat	0.00	0.05	0.00	0.00	0.00	0.00
MCLA	Vicia	sativa	Legume	Int	0.00	0.00	2.34	1.54	0.00	0.00
MCLA	Navarretia	pubescens	Forb	Nat	0.15	0.09	0.00	0.00	0.00	0.00

Table B.4: Summary of identified species, functional group, origin (native/introduced) mean cover in control plots, and average net change in treatment (+N) plot at MCLA. Sorted by mean relative cover in control plots in 2019 sampling.

Site	Genus	Species	Group	Origin	Cover 2017	Effect 2017	Cover 2018	Effect 2018	Cover 2019	Effect 2019
SFREC	Lagophylla	ramosissma	Forb	Nat	9.57	-0.61	8.27	-1.05	13.34	2.28
SFREC	Agoseris	heterophylla	Forb	Int	16.39	6.02	9.14	6.32	10.59	7.96
SFREC	Bromus	hordeaceous	Grass	Int	7.44	2.27	7.93	3.54	10.41	-2.73
SFREC	Bromus	madritensis	Grass	Int	6.62	-2.15	5.59	0.03	9.04	-4.65
SFREC	Elymus	caput-medusae	Grass	Int	4.47	2.67	7.72	2.92	6.22	1.78
SFREC	Bromus	diandrus	Grass	Int	7.45	-1.62	9.51	-3.35	6.02	-3.05
SFREC	Trifolium	dubium	Legume	Int	8.21	-3.60	7.60	-3.89	4.66	-2.84
SFREC	Torilis	nodosa	Forb	Nat	4.97	-1.92	4.56	-0.30	4.59	-1.81
SFREC	Vicia	sativa	Legume	Int	5.81	-1.99	6.88	0.35	4.49	-1.26
SFREC	Geranium	dissectum	Forb	Int	4.37	0.10	6.14	-2.32	4.10	-0.06
SFREC	Clarkia	Purpurea	Forb	Nat	2.07	-1.28	1.85	-0.89	2.44	-1.29
SFREC	Acmispon	purshianus	Legume	Nat	2.47	-1.79	3.85	-2.61	2.42	-0.93
SFREC	Aira	caryophyllaea	Grass	Int	2.88	0.92	2.30	-0.35	2.32	1.71
SFREC	Bromus	sterilis	Grass	Int	1.00	1.59	0.90	-0.07	2.25	-0.85
SFREC	Cynosurus	echinatus	Grass	Int	0.80	1.10	2.38	0.29	2.15	0.42
SFREC	Galium	parisiense	Forb	Int	0.00	-0.00	2.09	-0.00	2.05	-0.45
SFREC	Vulpia	myuros	Grass	Int	0.66	0.37	1.26	0.95	1.65	1.87
SFREC	Dichlostemma	capitatum	Forb	Nat	0.06	-0.06	0.00	-0.00	1.44	0.40
SFREC	Crucianella	angustilfolia	Forb	Int	0.00	0.00	1.39	-1.03	1.40	-0.73
SFREC	Briza	minima	Grass	Int	1.55	0.29	1.25	0.70	1.31	0.16
SFREC	Carduus	pachnocephalus	Forb	Int	0.96	0.64	1.65	0.22	1.26	0.37
SFREC	Trifolium	hirtum	Legume	Int	2.23	0.35	1.41	-0.94	1.05	-0.37
SFREC	Acmispon	parviflorus	Legume	Nat	0.35	-0.02	0.00	0.00	0.77	-0.72
SFREC	Elymus	glaucus	Grass	Nat	0.85	-0.31	1.02	-0.17	0.74	-0.20
SFREC	Euphorbia	spathulata	Forb	Int	0.14	0.44	0.84	-0.17	0.64	0.56
SFREC	Centaurea	melitensis	Forb	Int	0.00	0.00	0.38	-0.23	0.51	0.11
SFREC	Avena	barbata	Grass	Int	1.42	-0.38	1.06	1.29	0.44	1.73
SFREC	Navarretia	pubescens	Forb	Nat	0.19	0.27	0.35	0.31	0.39	0.77
SFREC	Madia	gracilis	Forb	Nat	0.03	0.17	0.21	0.02	0.31	0.11
SFREC	Daucus	pusillus	Forb	Int	0.21	-0.21	0.04	0.09	0.18	-0.04
SFREC	Petrorhagia	dubia	Forb	Int	1.60	-0.54	0.54	-0.38	0.14	0.25
SFREC	Bromus	carinatus	Grass	Nat	0.00	0.00	0.24	-0.24	0.12	-0.12
SFREC	Festuca	perennis	Grass	Int	0.04	0.26	0.00	1.07	0.10	-0.10
SFREC	Cerastium	glomeratum	Forb	Int	0.24	-0.09	0.04	0.16	0.08	0.08
SFREC	Tritileia	hyacinthina	Forb	Nat	0.62	0.47	0.26	-0.13	0.07	0.09
SFREC	Tritileia	hyacinthina	Forb	Nat	0.62	0.47	0.26	-0.13	0.07	0.09
SFREC	Lomatium	californicum	Forb	Nat	0.03	-0.03	0.03	-0.03	0.07	-0.07
SFREC	Hypochaeris	glabra	Forb	Int	0.00	0.00	0.00	0.00	0.06	0.14
SFREC	Clatonia	perfoliata	Forb	Nat	0.00	0.11	0.00	0.00	0.03	0.04
SFREC	Eremocarpus	setigerus	Forb	Nat	0.01	0.02	0.10	-0.09	0.02	0.06
SFREC	Tritileia	laxa	Forb	Nat	0.03	-0.03	0.04	-0.03	0.01	-0.00
SFREC	Anagallis	arvensis	Forb	Int	0.12	0.06	0.17	-0.17	0.01	0.12
SFREC	Erodium	botrys	Forb	Int	0.58	0.13	0.18	0.20	0.01	0.17
SFREC	Athysanus	pusillus	Forb	Nat	0.06	0.13	0.00	0.00	0.01	0.03
SFREC	Linanthus	bicolor	Forb	Nat	0.12	0.30	0.09	-0.09	0.01	0.30
SFREC	Cardamine	oligosperma	Forb	Nat	0.00	0.08	0.04	0.10	0.00	-0.00
SFREC	Githopsis	specularioides	Forb	Nat	0.00	0.00	0.00	0.00	0.00	0.12
SFREC	Lactuca	serriola	Forb	Int	2.46	-2.22	0.15	-0.15	0.00	-0.00
SFREC	Sherardia	arvensis	Forb	Int	0.26	0.12	0.01	0.03	0.00	0.04
SFREC	Dichlostemma	multiflorum	Forb	Nat	0.00	0.00	0.03	-0.03	0.00	-0.00
SFREC	Centaurea	solstitialis	Forb	Int	0.20	-0.20	0.37	-0.37	0.00	0.00
SFREC	Epilobium	brachycarpum	Forb	Nat	0.00	0.00	0.00	0.00	0.00	0.00
SFREC	Filago	gallica	Forb	Int	0.12	-0.05	0.00	0.00	0.00	0.00
SFREC	Linanthus	parviflora	Forb	Nat	0.00	-0.00	0.00	0.06	0.00	0.00
SFREC	Odontostomum	hartwegii	Forb	Nat	0.00	0.44	0.00	0.47	0.00	0.50
SFREC	Githopsis	specularioides	Forb	Nat	0.00	0.00	0.00	0.00	0.00	0.00
SFREC	Sanicula	bipinnatifida	Forb	Nat	0.00	0.00	0.03	-0.03	0.00	0.00
SFREC	Thysanocarpus	curvipes	Forb	Nat	0.00	0.00	0.04	0.00	0.00	0.00
SFREC	Trifolium	microcephalum	Legume	Nat	0.00	0.00	0.00	0.00	0.00	0.00

Table B.5: Summary of identified species, functional group, origin (native/introduced) mean cover in control plots, and average net change in treatment (+N) plot at SFREC. Sorted by mean relative cover in control plots in 2019 sampling.

Appendix C

Chapter 3 Supporting Information

Source	DF	SS	MS	F	R-squared	P
Seeding composition	6	12.0487	2.0081	32.815	0.8	0.001
Residual	49	2.9986	0.19928			
Total	55	15.0473	1			

Table C.1: Permutational ANOVA (PERMANOVA) output of variance in plot community composition in the first year of sampling.

K	Hartigan	Rk	CH	Rk	Beale	Rk	KL	Rk	Cindex	Rk	DB	Rk	Sil.	Rk	Duda	Rk
2	133.88	9	163.1	3	2.7	8	1.22	5	0.5	9	1.69	9	0.21	9	0.82	9
3	128.56	5	166.15	2	1.96	7	1.12	6	0.45	8	1.59	8	0.23	8	0.86	7
4	52.25	1	176.75	1	-2.02	1	3.09	2	0.42	7	1.49	6	0.26	7	1.19	1
5	70	7	156.78	5	5.41	9	0.7	8	0.4	6	1.42	3	0.27	6	0.7	8
6	84.36	6	153.65	6	-2.03	2	0.87	7	0.36	4	1.48	5	0.3	2	1.2	3
7	28.88	2	159.7	4	1.12	6	3.83	1	0.36	5	1.4	1	0.3	1	0.92	6
8	63.54	8	147.31	9	-3.12	3	0.39	9	0.31	1	1.5	7	0.27	5	1.34	4
9	48.78	4	150.17	7	-2.06	5	1.42	4	0.33	3	1.47	4	0.29	3	1.2	5
10	25.57	3	149.47	8	-9.33	4	2.24	3	0.32	2	1.42	2	0.28	4	4.2	2

Table C.2: Rank summary table of performance across different clustering indices.

Clustering Index Ranking Methods:

The following provides brief descriptions of clustering heuristics used to evaluate K in K-medoids clustering.

For more detail, see Malika et al. (2014).

- **Hartigan**: Choose value K with maximum index difference between K and K-1.
- **CH**: Choose maximum value among orders of K considered.
- **Beale**: Choose minimum value of K such that the critical value of the index is less than alpha = 0.05. Other values whose critical value is less than alpha are ranked in order of significance.
- **KL**: Choose maximum value among orders of K considered.
- **Cindex**: Choose minimum value among orders of K considered.
- **DB** (Davies and Bouldin): Choose minimum value among orders of K considered.
- **Silhouette**: Choose maximum value among orders of K considered.
- **Duda**: Choose minimum value of K such that the critical value of the index is less than alpha = 0.05. Other values whose critical value is less than alpha are ranked in order of significance.

	Native perennial	F. perennis - B.hordeaceous	Invasive Annual	A. fatua - B. diandrus
Native perennial	95	8	7	29
F. perennis				
B.hordeaceous	10	50	30	29
Invasive Annual	25	11	115	22
A. fatua				
B. diandrus	19	21	7	76

Table C.3: Contingency table of observed transitions between state assignments between 2008-2018. For each plot observation of a state assignment in year t (rows), data shows the frequency of state assignments (columns) of the same plot in a subsequent year (t + 1). Diagonal values represent the frequency of a given state retaining its assignment (persistence), while off-diagonal values represent transitions in state assignment. Changes in assignment frequency were highly non-random ($\chi^2 = 392.017$, df = 9, $P < 0.001$).

Model	DF	Priority	1 Year SPEI	2 Year SPEI	3 Year SPEI	deltaAIC	AIC
1	12					35.31	1289.98
2	24	X				6.16	1260.83
3	24		X			31.82	1286.49
4	24			X		31.76	1286.43
5	24				X	28	1282.67
6	36	X	X			0	1254.67
7	36	X		X		3.92	1258.59
8	36	X			X	0.25	1254.92

Table C.4: AIC model comparison used to select the best fit multi-state model from a series of candidates. Covariates include "Priority Effects" – the effect of initial seeding mixture representation of indicator species correlated with cluster assignments – and "1-", "2-", and "3-year SPEI" – a standardized measure of drought stress computed over 1, 2, and 3 cumulative water year intervals, respectively. DF corresponds to the number of parameters estimated within the transition matrix, including baseline transition probabilities and effects of covariates.

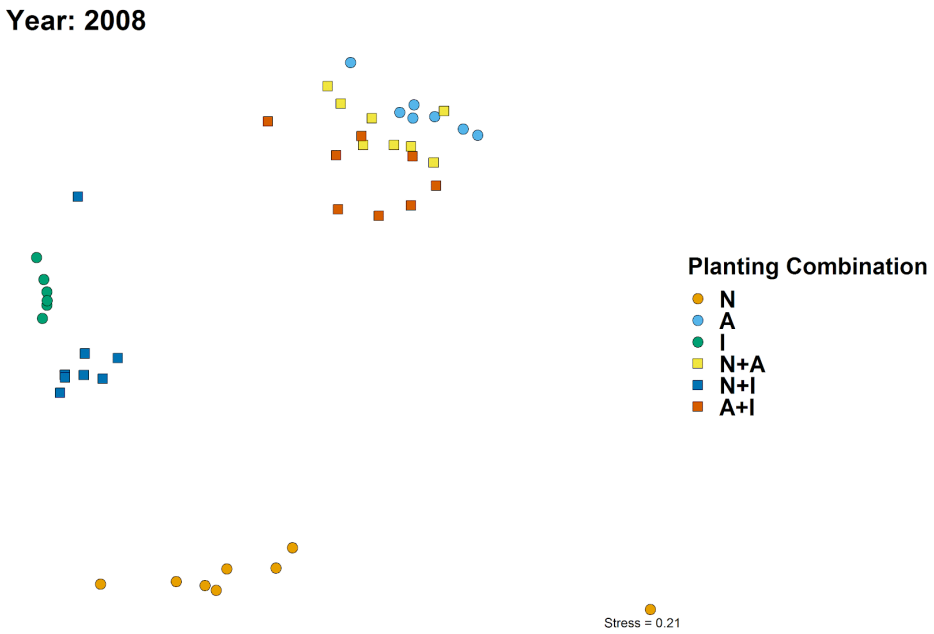

Figure C.1: Visualization of clustering assignments following K-medoids clustering. Non-metric multidimensional scaling (NMDS) ordination was conducted on all community observations from 2008 – 2018 (n=560). Pairwise community distance was calculated using Bray-Curtis dissimilarity index. Species vectors correspond to taxa that were found to be significantly associated ($p < 0.05$) with state assignments using indicator species analysis.

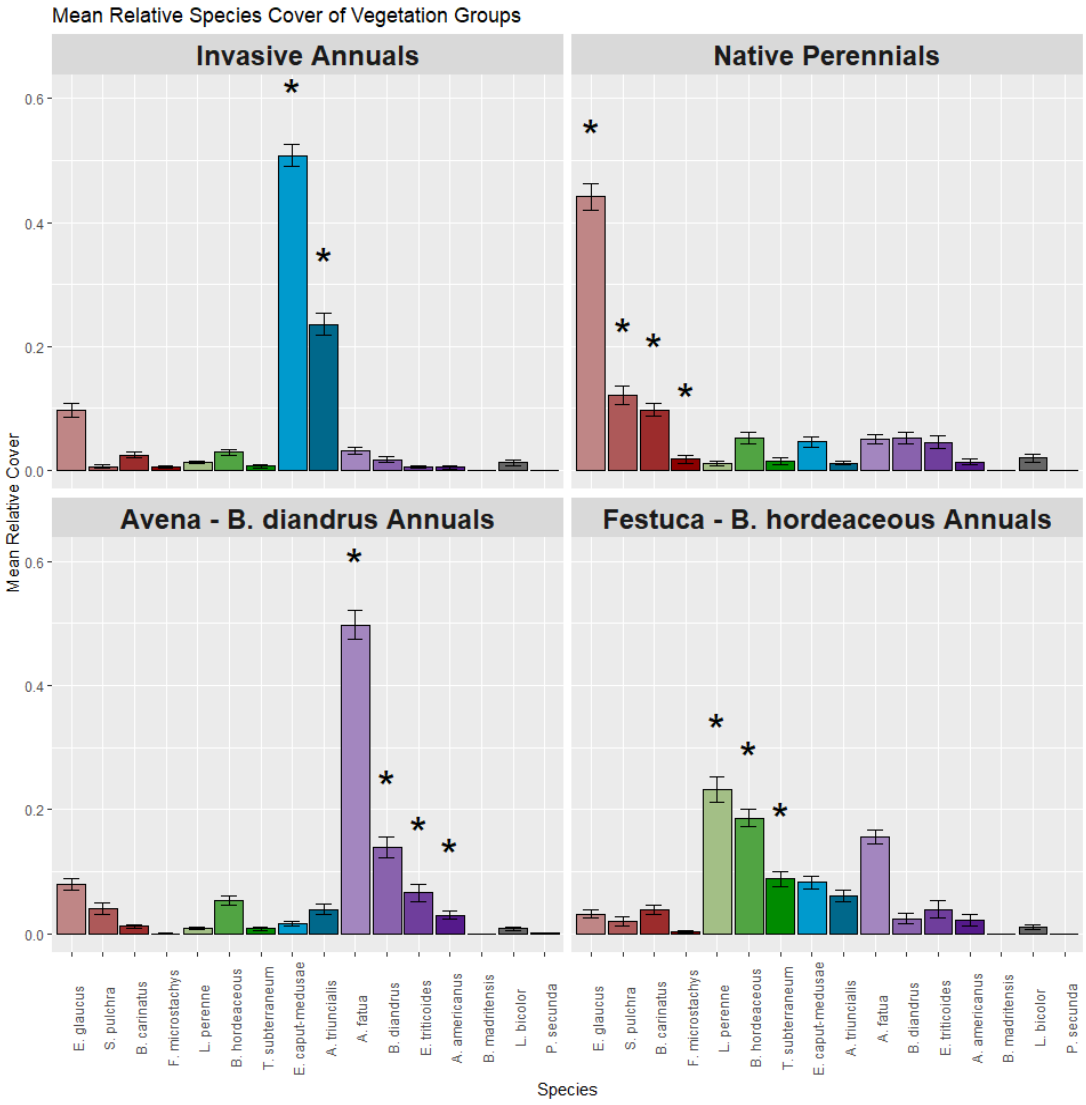

Figure C.2: Relative abundance of species across vegetation state assignments. Values refer to the average abundance of each species (+/- standard error) for observed communities assigned to each state. Species that served as significant ($P < 0.05$) indicators of each state type are highlighted using "*" and colored by representative state. On average, indicator species of each vegetation state accounted for 75% of the cumulative relative abundance of observed communities.

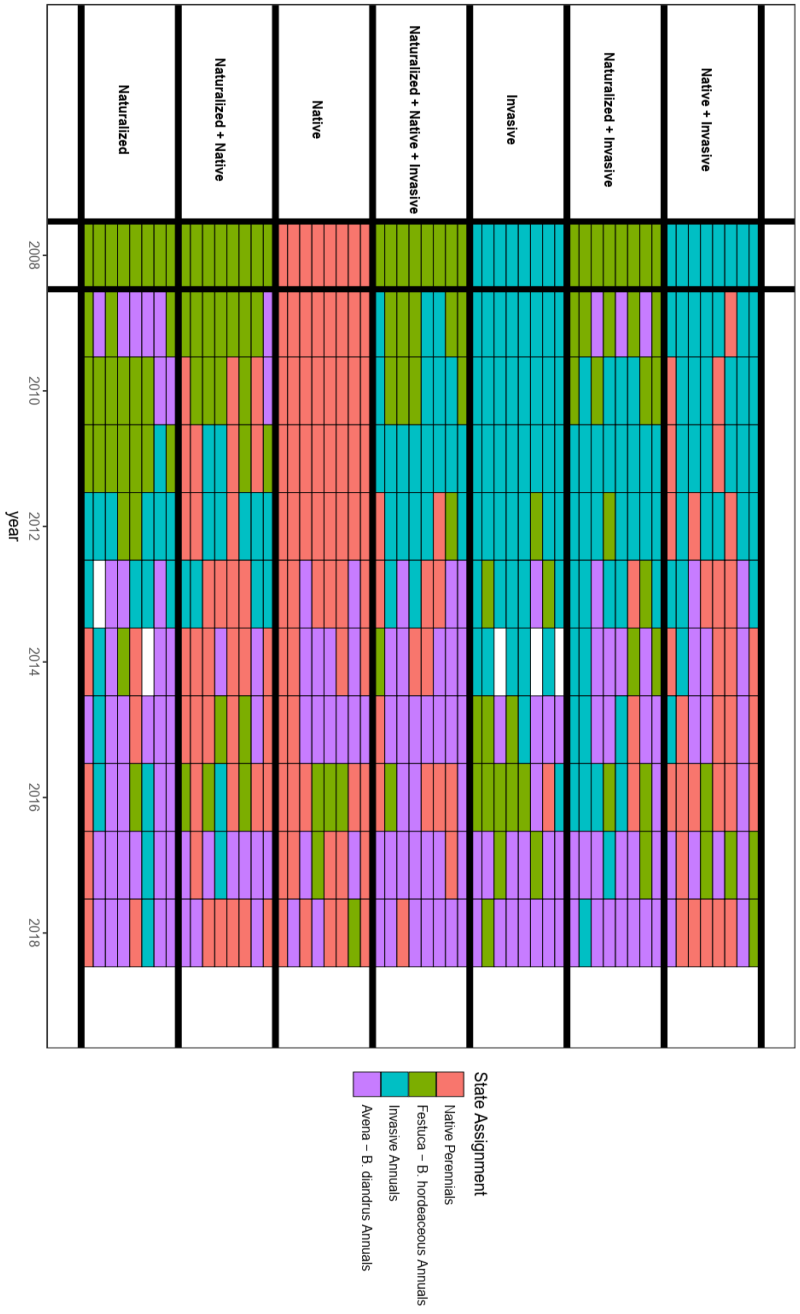

Figure C.3: Plot-level shifts in state assignment over time. For each observed community (grid cell), the state assignment of a community is presented as a function of initial seeding treatment (row) and time (column).

References

Adler, P. B., J. HilleRisLambers, P. C. Kyriakidis, Q. Guan, and J. M. Levine. 2006. Climate variability has a stabilizing effect on the coexistence of prairie grasses. Proceedings of the National Academy of Sciences of the United States of America 103:12793–12798.

Alexander, J. M., J. M. Diez, and J. M. Levine. 2015. Novel competitors shape species' responses to climate change. Nature 525:515–518.

Allen-Diaz, B., and J. W. Bartolome. 1998. Sagebrush – Grass Vegetation Dynamics : Comparing Classical and State-Transition Models. Ecological Applications 8:795–804.

Amatangelo, K. L., J. S. Dukes, and C. B. Field. 2008. Responses of a california annual grassland to litter manipulation. Journal of Vegetation Science 19:605–612.

Anderson, M. J., K. E. Ellingsen, and B. H. McArdle. 2006. Multivariate dispersion as a measure of beta diversity. Ecology Letters 9:683–693.

Angert, A. L., T. E. Huxman, P. Chesson, and D. L. Venable. 2009. Functional tradeoffs determine species coexistence via the storage effect. Proceedings of

the National Academy of Sciences of the United States of America 106:11641–11645.

Ågren, G. I. 2004. The C:N:P stoichiometry of autotrophs - Theory and observations. Ecology Letters 7:185–191.

Ågren, G. I. 2008. Stoichiometry and nutrition of plant growth in natural communities. Annual Review of Ecology, Evolution, and Systematics 39:153–170.

Barbour, M. G., T. Keeler-Wolf, and A. A. Schoenherr, editors. 2007. Terrestrial Vegetation of California. University of California Press.

Bartolome, J. W. 1979. Germination and seedling establishment in california annual grassland. Journal of Ecology 67:273–281.

Bartolome, J. W., B. Allen-Diaz, and R. D. Jackson. 2008. Developing Data-Driven Descriptive Models for Californian Grasslands. Pages 124–135 *in* R. J. Hobbs and K. N. Suding, editors. New models for ecosystem dynamics and restoration. Island Press, Washington, D.C.

Bates, D., M. Mächler, B. Bolker, and S. Walker. 2015. Fitting Linear Mixed-Effects Models Using lme4. Journal of Statistical Software 67:1–48.

Beguería, S., S. M. Vicente-Serrano, F. Reig, and B. Latorre. 2014. Standardized precipitation evapotranspiration index (SPEI) revisited: Parameter fitting, evapotranspiration models, tools, datasets and drought monitoring. International Journal of Climatology 34:3001–3023.

Bestelmeyer, B. T., J. R. Brown, K. M. Havstad, R. Alexander, G. Chavez, and J. E. Herrick. 2003. Development and use of state-and-transition models for

rangelands. Journal of Range Management 56:114–126.

Bobbink, R. 1991. Effects of Nutrient Enrichment in Dutch Chalk Grassland. The Journal of Applied Ecology 28:28.

Bobbink, R., K. Hicks, J. Galloway, T. Spranger, R. Alkemade, M. Ashmore, M. Bustamante, S. Cinderby, E. Davidson, F. Dentener, B. Emmett, J. W. Erisman, M. Fenn, F. Gilliam, A. Nordin, L. Pardo, and W. Vries. 2010. Global assessment of nitrogen deposition effects on terrestrial plant diversity: A synthesis. Ecological Applications 20:30–59.

Borer, E. T., E. W. Seabloom, D. S. Gruner, W. S. Harpole, H. Hillebrand, E. M. Lind, P. B. Adler, J. Alberti, T. M. Anderson, J. D. Bakker, and others. 2014. Herbivores and nutrients control grassland plant diversity via light limitation. Nature 508:517–520.

Brauer, V. S., M. Stomp, and J. Huisman. 2012. The nutrient-load hypothesis: Patterns of resource limitation and community structure driven by competition for nutrients and light. American Naturalist 179:721–740.

Butchart, S. H. M., M. Walpole, B. Collen, A. Strien, J. P. W. Scharlemann, R. E. A. Almond, J. E. M. Baillie, B. Bomhard, C. Brown, J. Bruno, K. E. Carpenter, G. M. Carr, J. Chanson, A. M. Chenery, J. Csirke, N. C. Davidson, F. Dentener, M. Foster, A. Galli, J. N. Galloway, P. Genovesi, R. D. Gregory, M. Hockings, V. Kapos, J.-F. Lamarque, F. Leverington, J. Loh, M. A. McGeoch, L. McRae, A. Minasyan, M. H. Morcillo, T. E. E. Oldfield, D. Pauly, S. Quader, C. Revenga, J. R. Sauer, B. Skolnik, D. Spear, D. Stanwell-Smith, S. N. Stuart, A. Symes, M. Tierney, T. D. Tyrrell, J.-C. Vie, and R. Watson. 2010. Global

biodiversity: Indicators of recent declines. Science 328:1164–1168.

Canfield, D. E., A. N. Glazer, and P. G. Falkowski. 2010. The evolution and future of earth's nitrogen cycle. Science 330:192–196.

Cardinale, B. J., H. Hillebrand, W. S. Harpole, K. Gross, and R. Ptacnik. 2009. Separating the influence of resource 'availability' from resource 'imbalance' on productivity-diversity relationships. Ecology Letters 12:475–487.

Chalcraft, D. R., S. B. Cox, C. Clark, E. E. Cleland, K. N. Suding, E. Weiher, and D. Pennington. 2008. Scale-dependent responses of plant biodiversity to nitrogen enrichment. Ecology 89:2165–2171.

Chapin, F. S., B. H. Walker, R. J. Hobbs, D. U. Hooper, J. H. Lawton, O. E. Sala, and D. Tilman. 1997. Biotic control over the functioning of ecosystems. Science 277:500–504.

Chapin, F. S., E. S. Zavaleta, V. T. Eviner, R. L. Naylor, P. M. Vitousek, H. L. Reynolds, D. U. Hooper, S. Lavorel, O. E. Sala, S. E. Hobbie, M. C. Mack, and S. Díaz. 2000. Consequences of changing biodiversity. Nature 405:234–242.

Chase, J. M., and T. M. Knight. 2013. Scale-dependent effect sizes of ecological drivers on biodiversity: Why standardised sampling is not enough. Ecology Letters 16:17–26.

Chase, J. M., B. J. McGill, D. J. McGlinn, F. May, S. A. Blowes, X. Xiao, T. M. Knight, O. Purschke, and N. J. Gotelli. 2018. Embracing scale-dependence to achieve a deeper understanding of biodiversity and its change across communities. Ecology Letters 21:1737–1751.

Chesson, P. 2000. Mechanisms of maintenance of species diversity. Annual Review of Ecology and Systematics 31:343–66.

Clark, A. T., C. Lehman, and D. Tilman. 2018. Identifying mechanisms that structure ecological communities by snapping model parameters to empirically observed tradeoffs. Ecology Letters 21:494–505.

Corbin, J. D., A. R. Dyer, and E. W. Seabloom. 2007. Competitive Interactions. *in* J. D. Corbin, M. R. Stromberg, and C. M. D'Antonio, editors. California grasslands: Ecology and management. First Edition. University of California Press, Berkeley; Los Angeles, California.

Crawley, M. J., A. E. Johnston, J. Silvertown, M. Dodd, C. De Mazancourt, M. S. Heard, D. F. Henman, and G. R. Edwards. 2005. Determinants of species richness in the park grass experiment. American Naturalist 165:179–192.

DeMalach, N., and R. Kadmon. 2017. Light competition explains diversity decline better than niche dimensionality. Functional Ecology 31:1834–1838.

Demalach, N., H. Saiz, E. Zaady, and F. T. Maestre. 2019. Plant species – area relationships are determined by evenness , cover and aggregation in drylands. Global Ecology and Biogeography 28:290–299.

DeMalach, N., E. Zaady, and R. Kadmon. 2017. Light asymmetry explains the effect of nutrient enrichment on grassland diversity. Ecology Letters 20:60–69.

DiTomaso, J. M., G. B. Kyser, M. R. George, M. P. Doran, and E. A. Laca. 2008. Control of Medusahead (Taeniatherum caput-medusae) Using Timely Sheep Grazing. Invasive Plant Science and Management 1:241–247.

Díaz, S., and M. Cabido. 2001. Vive la différence: Plant functional diversity matters to ecosystem processes. Trends in Ecology and Evolution 16:646–655.

Díaz, S., J. Kattge, J. H. C. Cornelissen, I. J. Wright, S. Lavorel, S. Dray, B. Reu, M. Kleyer, C. Wirth, I. Colin Prentice, E. Garnier, G. Bönisch, M. Westoby, H. Poorter, P. B. Reich, A. T. Moles, J. Dickie, A. N. Gillison, A. E. Zanne, J. Chave, S. Joseph Wright, S. N. Sheremet Ev, H. Jactel, C. Baraloto, B. Cerabolini, S. Pierce, B. Shipley, D. Kirkup, F. Casanoves, J. S. Joswig, A. Günther, V. Falczuk, N. Rüger, M. D. Mahecha, and L. D. Gorné. 2016. The global spectrum of plant form and function. Nature 529:167–171.

Dudney, J., L. M. Hallett, L. Larios, E. C. Farrer, and N. Erica. 2017. Lagging behind: Have we overlooked previous-year rainfall effects in annual grasslands? Journal of Ecology 105:484–495.

Dwyer, J. M., and D. C. Laughlin. 2017. Constraints on trait combinations explain climatic drivers of biodiversity: the importance of trait covariance in community assembly. Ecology Letters 20:872–882.

Dybzinski, R., and D. Tilman. 2007. Resource use patterns predict long-term outcomes of plant competition for nutrients and light. American Naturalist 170:305–318.

Elmendorf, S. C., and S. P. Harrison. 2009. Temporal variability and nestedness in california grassland species composition. Ecology 90:1492–1497.

Elser, J. J., M. E. S. Bracken, E. E. Cleland, D. S. Gruner, W. S. Harpole, H. Hillebrand, J. T. Ngai, E. W. Seabloom, J. B. Shurin, and J. E. Smith. 2007. Global analysis of nitrogen and phosphorus limitation of primary producers in

freshwater, marine and terrestrial ecosystems. Ecology Letters 10:1135–1142.

Emery, S. M., and K. L. Gross. 2007. Dominant species identity, not community evenness, regulates invasion in experimental grassland plant communities. Ecology 88:954–964.

Englund, G., and S. D. Cooper. 2003. Scale effects and extrapolation in ecological experiments. Advances in Ecological Research 33:161–213.

Eskelinen, A., and S. Harrison. 2015. Erosion of beta diversity under interacting global change impacts in a semi-arid grassland. Journal of Ecology 103:397–407.

Eviner, V. T., and M. K. Firestone. 2007. Mechanisms determining patterns of nutrient dynamics. Pages 94–106. *in* J. D. Corbin, M. R. Stromberg, and C. M. D'Antonio, editors. California grasslands: Ecology and management. First Edition. University of California Press, Berkeley; Los Angeles, California.

Eviner, V. T., and C. V. Hawkes. 2012. The Effects of Plant–Soil Feedbacks on Invasive Plants: Mechanisms and Potential Management Options. Pages 122–141 *in* Invasive plant ecology and management: Linking processes to practice. First Edition. CABI, Cambridge, Massachusetts.

Fay, P. A., D. M. Kaufman, J. B. Nippert, J. D. Carlisle, and C. W. Harper. 2008. Changes in grassland ecosystem function due to extreme rainfall events: Implications for responses to climate change. Global Change Biology 14:1600–1608.

Fay, P. A., S. M. Prober, W. S. Harpole, J. M. H. Knops, J. D. Bakker, E. T. Borer, E. M. Lind, A. S. MacDougall, E. W. Seabloom, P. D. Wragg, P. B.

Adler, D. M. Blumenthal, Y. M. Buckley, C. Chu, E. E. Cleland, S. L. Collins, K. F. Davies, G. Du, X. Feng, J. Firn, D. S. Gruner, N. Hagenah, Y. Hautier, R. W. Heckman, V. L. Jin, K. P. Kirkman, J. Klein, L. M. Ladwig, Q. Li, R. L. McCulley, B. A. Melbourne, C. E. Mitchell, J. L. Moore, J. W. Morgan, A. C. Risch, M. Schütz, C. J. Stevens, D. A. Wedin, and L. H. Yang. 2015. Grassland productivity limited by multiple nutrients. Nature Plants 1:1–5.

Felton, A. J., and M. D. Smith. 2017. Integrating plant ecological responses to climate extremes from individual to ecosystem levels. Philosophical Transactions of the Royal Society B: Biological Sciences 372.

Fry, E. L., E. S. Pilgrim, J. R. B. Tallowin, R. S. Smith, S. R. Mortimer, D. A. Beaumont, J. Simkin, S. J. Harris, R. S. Shiel, H. Quirk, K. A. Harrison, C. S. Lawson, P. J. Hobbs, and R. D. Bardgett. 2017. Plant, soil and microbial controls on grassland diversity restoration: a long-term, multi-site mesocosm experiment. Journal of Applied Ecology 54:1320–1330.

Fukami, T. 2015. Historical Contingency in Community Assembly: Integrating Niches, Species Pools, and Priority Effects. Annual Review of Ecology, Evolution, and Systematics 46:1–23.

Funk, J. L., E. E. Cleland, K. N. Suding, and E. S. Zavaleta. 2008. Restoration through reassembly: Plant traits and invasion resistance. Trends in Ecology & Evolution 23:695–703.

Galatowitsch, S. M. 2012. Diagnosis and Goal Setting. Pages 31–75. Sinauer, Sunderland, Massachusetts.

Germain, R. M., S. Y. Strauss, and B. Gilbert. 2017. Experimental dispersal reveals characteristic scales of biodiversity in a natural landscape. Proceedings of the National Academy of Sciences of the United States of America 114:4447–4452.

Gilbert, B., and J. M. Levine. 2013. Plant invasions and extinction debts. Proceedings of the National Academy of Sciences of the United States of America 110:1744–1749.

Goldberg, D. E., and T. E. Miller. 1990. Effects of different resource additions on species diversity in an annual plant community. Ecology 71:213–225.

Gotelli, N. J., and R. K. Colwell. 2001. Quantifying biodiversity: Procedures and pitfalls in the measurement and comparison of species richness. Ecology Letters 4:379–391.

Grace, J. B., T. M. Anderson, E. W. Seabloom, E. T. Borer, P. B. Adler, W. S. Harpole, Y. Hautier, H. Hillebrand, E. M. Lind, M. Pärtel, J. D. Bakker, Y. M. Buckley, M. J. Crawley, E. I. Damschen, K. F. Davies, P. A. Fay, J. Firn, D. S. Gruner, A. Hector, J. M. H. Knops, A. S. MacDougall, B. A. Melbourne, J. W. Morgan, J. L. Orrock, S. M. Prober, and M. D. Smith. 2016. Integrative modelling reveals mechanisms linking productivity and plant species richness. Nature 529:390–393.

Griffin-Nolan, R. J., D. M. Blumenthal, S. L. Collins, T. E. Farkas, A. M. Hoffman, K. E. Mueller, T. W. Ocheltree, M. D. Smith, K. D. Whitney, and A. K. Knapp. 2019. Shifts in plant functional composition following long-term drought in grasslands. Journal of Ecology 107:2133–2148.

Grime, J. P. 2006. Plant strategies, vegetation processes, and ecosystem properties. Second Edition. John Wiley & Sons, New York, New York.

Grime, J. P. 1974. Vegetation classification by reference to strategies. Nature 250:26–31.

Güsewell, S. 2004. N:P ratios in terrestrial plants: Variation and functional significance. New Phytologist 164:243–266.

Hallett, L. M., L. G. Shoemaker, C. T. White, and K. N. Suding. 2019. Rainfall variability maintains grass-forb species coexistence. Ecology Letters 22:1658–1667.

Handreck, K. A. 1997. Phosphorus requirements of Australian native plants. Australian Journal of Soil Research 35:241–289.

Harpole, W. S., L. L. Sullivan, E. M. Lind, J. Firn, P. B. Adler, E. T. Borer, J. Chase, P. A. Fay, Y. Hautier, H. Hillebrand, A. S. MacDougall, E. W. Seabloom, J. D. Bakker, M. W. Cadotte, E. J. Chaneton, C. Chu, N. Hagenah, K. Kirkman, K. J. La Pierre, J. L. Moore, J. W. Morgan, S. M. Prober, A. C. Risch, M. Schuetz, and C. J. Stevens. 2017. Out of the shadows: multiple nutrient limitations drive relationships among biomass, light and plant diversity. Functional Ecology 31:1839–1846.

Harpole, W. S., L. L. Sullivan, E. M. Lind, J. Firn, P. B. Adler, E. T. Borer, J. Chase, P. A. Fay, Y. Hautier, H. Hillebrand, A. S. MacDougall, E. W. Seabloom, R. Williams, J. D. Bakker, M. W. Cadotte, E. J. Chaneton, C. Chu, E. E. Cleland, C. D'Antonio, K. F. Davies, D. S. Gruner, N. Hagenah, K. Kirkman, J. M. H. Knops, K. J. La Pierre, R. L. McCulley, J. L. Moore,

J. W. Morgan, S. M. Prober, A. C. Risch, M. Schuetz, C. J. Stevens, and P. D. Wragg. 2016. Addition of multiple limiting resources reduces grassland diversity. Nature 537:93–96.

Harpole, W. S., and D. Tilman. 2007. Grassland species loss resulting from reduced niche dimension. Nature 446:791–793.

Harrison, S., and M. LaForgia. 2019. Seedling traits predict drought-induced mortality linked to diversity loss. Proceedings of the National Academy of Sciences of the United States of America 116:5576–5581.

Harrison, S. P., E. S. Gornish, and S. Copeland. 2015a. Climate-driven diversity loss in a grassland community. Pages 8672–8677 *in* Proceedings of the national academy of sciences.

Harrison, S. P., E. S. Gornish, and S. Copeland. 2015b. Climate-driven diversity loss in a grassland community. Proceedings of the National Academy of Sciences of the United States of America 112:8672–8677.

Harrison, S. P., M. L. LaForgia, and A. M. Latimer. 2018. Climate-driven diversity change in annual grasslands: Drought plus deluge does not equal normal. Global Change Biology 24:1782–1792.

Hart, S. P., J. Usinowicz, and J. M. Levine. 2017. The spatial scales of species coexistence. Nature Ecology & Evolution 1:1066–1073.

Hautier, Y., P. Niklaus, and A. Hector. 2009. Competition for light causes plant biodiversity loss after eutrophication. Science 324:636–638.

Hautier, Y., E. Vojtech, and A. Hector. 2018. The importance of competition for light depends on productivity and disturbance. Ecology and Evolution 8:10655–10661.

He, F., and S. P. Hubbell. 2011. Species-area relationships always overestimate extinction rates from habitat loss. Nature 473:368–371.

Heady, H. F. 1958. Vegetational changes in the California annual type. Ecology 39:402–416.

Hector, A., and R. Bagchi. 2007. Biodiversity and ecosystem multifunctionality. Nature 448:188–190.

Hill, M. O. 1973. Diversity and evenness : A unifying notation and its consequences. Ecology 54:427–432.

Hillebrand, H., B. Blasius, E. T. Borer, J. M. Chase, J. A. Downing, B. K. Eriksson, C. T. Filstrup, W. S. Harpole, D. Hodapp, S. Larsen, A. Lewandowska, E. W. Seabloom, D. B. Van de Waal, and A. B. Ryabov. 2018. Biodiversity change is uncoupled from species richness trends: Consequences for conservation and monitoring. Journal of Applied Ecology 55:169–184.

Hillerislambers, J., S. G. Yelenik, B. P. Colman, and J. M. Levine. 2010. California annual grass invaders: the drivers or passengers of change? Journal of Ecology 98:1147–1156.

Hobbs, R. J., S. Arico, J. Aronson, J. S. Baron, P. Bridgewater, V. A. Cramer, P. R. Epstein, J. J. Ewel, C. A. Klink, A. E. Lugo, D. Norton, D. Ojima, D. M. Richardson, E. W. Sanderson, F. Valladares, M. Vilà, R. Zamora, and M. Zobel. 2006. Novel ecosystems: Theoretical and management aspects of the

new ecological world order. Global Ecology and Biogeography 15:1–7.

Hobbs, R. J., E. Higgs, and J. A. Harris. 2009. Novel ecosystems: implications for conservation and restoration. Trends in Ecology and Evolution 24:599–605.

Hobbs, R. J., S. Yates, and H. A. Mooney. 2007. Long-term data reveal complex dynamics in grassland in relation to climate and disturbance. Ecological Monographs 77:545–568.

Hoover, D. L., A. K. Knapp, and M. D. Smith. 2014. Resistance and resilience of a grassland ecosystem to climate extremes. Ecology 95:2646–2656.

Hylander, K., and J. Ehrlén. 2013. The mechanisms causing extinction debts. Trends in Ecology and Evolution 28:341–346.

IPCC. 2014. Synthesis report. Contribution of working groups i ii and iii to the fifth assessment report of the intergovernmental panel on climate change. Geneva, Switzerland.

Isbell, F., D. Craven, J. Connolly, M. Loreau, B. Schmid, C. Beierkuhnlein, T. M. Bezemer, C. Bonin, H. Bruelheide, E. De Luca, A. Ebeling, J. N. Griffin, Q. Guo, Y. Hautier, A. Hector, A. Jentsch, J. Kreyling, V. Lanta, P. Manning, S. T. Meyer, A. S. Mori, S. Naeem, P. A. Niklaus, H. W. Polley, P. B. Reich, C. Roscher, E. W. Seabloom, M. D. Smith, M. P. Thakur, D. Tilman, B. F. Tracy, W. H. Van Der Putten, J. Van Ruijven, A. Weigelt, W. W. Weisser, B. Wilsey, and N. Eisenhauer. 2015. Biodiversity increases the resistance of ecosystem productivity to climate extremes. Nature 526:574–577.

Jackson, C. 2011. Multi-state models for panel data: The msm package for r. Journal of Statistical Software 38.

Jackson, R. D., and J. W. Bartolome. 2002. A state-transition approach to understanding nonequilibrium plant community dynamics in Californian grasslands. Plant Ecology 162:49–65.

Jackson, S. T., and D. F. Sax. 2010. Balancing biodiversity in a changing environment: Extinction debt, immigration credit and species turnover. Trends in Ecology and Evolution 25:153–160.

Jost, L. 2006. Entropy and diversity. Oikos 113:363–375.

Jost, L. 2007. Partitioning diversity into independent alpha and beta components. Ecology 88:2427–2439.

Keeler-Wolf, T., J. M. Evens, A. I. Solomeshch, V. L. Holland, and M. G. Barbour. 2007. Community classification and nomenclature. Pages. Pages 21–34 *in* M. R. Stromberg, J. Corbin, and C. M. D'Antonio, editors. California grasslands ecology and management. First Edition. University of California Press, Berkeley; Los Angeles, California.

Kimball, S., A. L. Angert, T. E. Huxman, and D. L. Venable. 2010. Contemporary climate change in the Sonoran Desert favors cold-adapted species. Global Change Biology 16:1555–1565.

Komatsu, K. J., M. L. Avolio, N. P. Lemoine, F. Isbell, E. Grman, G. R. Houseman, S. E. Koerner, D. S. Johnson, K. R. Wilcox, J. M. Alatalo, J. P. Anderson, R. Aerts, S. G. Baer, A. H. Baldwin, J. Bates, C. Beierkuhnlein, R. T. Belote, J. Blair, J. M. G. Bloor, P. J. Bohlen, E. W. Bork, E. H. Boughton, W. D. Bowman, A. J. Britton, J. F. Cahill, E. Chaneton, N. R. Chiariello, J. Cheng, S. L. Collins, J. H. C. Cornelissen, G. Du, A. Eskelinen, J. Firn, B. Foster,

L. Gough, K. Gross, L. M. Hallet, X. Han, H. Harmens, M. J. Hovenden, A. Jagerbrand, A. Jentsch, C. Kern, K. Klanderud, A. K. Knapp, J. Kreyling, W. Li, Y. Luo, R. L. McCulley, J. R. McLaren, J. P. Megonigal, J. W. Morgan, V. Onipchenko, S. C. Pennings, J. S. Prevéy, J. N. Price, P. B. Reich, C. H. Robinson, F. L. Russell, O. E. Sala, E. W. Seabloom, M. D. Smith, N. A. Soudzilovskaia, L. Souza, K. Suding, K. B. Suttle, T. Svejcar, D. Tilmand, P. Tognetti, R. Turkington, S. White, Z. Xu, L. Yahdjian, Q. Yu, P. Zhang, and Y. Zhang. 2019. Global change effects on plant communities are magnified by time and the number of global change factors imposed. Proceedings of the National Academy of Sciences of the United States of America 116:17867–17873.

Kraft, N. J. B., O. Godoy, and J. M. Levine. 2015. Plant functional traits and the multidimensional nature of species coexistence. Proceedings of the National Academy of Sciences of the United States of America 112:797–802.

Kramer-Walter, K. R., P. J. Bellingham, T. R. Millar, R. D. Smissen, S. J. Richardson, and D. C. Laughlin. 2016. Root traits are multidimensional: specific root length is independent from root tissue density and the plant economic spectrum. Journal of Ecology 104:1299–1310.

Kreyling, J., A. Jentsch, and C. Beierkuhnlein. 2011. Stochastic trajectories of succession initiated by extreme climatic events. Ecology Letters 14:758–764.

Kuussaari, M., R. Bommarco, R. K. Heikkinen, A. Helm, J. Krauss, R. Lindborg, E. Öckinger, M. Pärtel, J. Pino, F. Rodà, C. Stefanescu, T. Teder, M. Zobel, and I. Steffan-Dewenter. 2009. Extinction debt: A challenge for biodiversity conservation. Trends in Ecology and Evolution 24:564–571.

Kuznetsova, A., P. B. Brockhoff, and R. H. B. Christensen. 2017. lmerTest Package: Tests in Linear Mixed Effects Models. Journal of Statistical Software 82.

LaForgia, M. L., S. P. Harrison, and A. M. Latimer. 2020. Invasive species interact with climatic variability to reduce success of natives. Ecology 101:1–10.

LaForgia, M. L., M. J. Spasojevic, E. J. Case, A. M. Latimer, and S. P. Harrison. 2018. Seed banks of native forbs, but not exotic grasses, increase during extreme drought. Ecology 99:896–903.

Lan, Z., G. D. Jenerette, S. Zhan, W. Li, S. Zheng, and Y. Bai. 2015. Testing the scaling effects and mechanisms of n-induced biodiversity loss: Evidence from a decade-long grassland experiment. Journal of Ecology 103:750–760.

Larios, L., R. J. Aicher, and K. N. Suding. 2013. Effect of propagule pressure on recovery of a California grassland after an extreme disturbance. Journal of Vegetation Science 24:1043–1052.

Leibold, M. A., M. Holyoak, N. Mouquet, P. Amarasekare, J. M. Chase, M. F. Hoopes, R. D. Holt, J. B. Shurin, R. Law, D. Tilman, M. Loreau, and A. Gonzalez. 2004. The metacommunity concept: A framework for multi-scale community ecology. Ecology Letters 7:601–613.

Lepš, J. 2014. Scale- and time-dependent effects of fertilization, mowing and dominant removal on a grassland community during a 15-year experiment. Journal of Applied Ecology 51:978–987.

Lind, E. M., E. Borer, E. Seabloom, P. Adler, J. D. Bakker, D. M. Blumenthal, M. Crawley, K. Davies, J. Firn, D. S. Gruner, W. Stanley Harpole, Y. Hautier, H.

Hillebrand, J. Knops, B. Melbourne, B. Mortensen, A. C. Risch, M. Schuetz, C. Stevens, and P. D. Wragg. 2013. Life-history constraints in grassland plant species: A growth-defence trade-off is the norm. Ecology Letters 16:513–521.

Loreau, M., S. Naeem, P. Inchausti, J. Bengtsson, J. P. Grime, A. Hector, D. U. Hooper, M. A. Huston, D. Raffaelli, B. Schmid, D. Tilman, and D. A. Wardle. 2001. Biodiversity and ecosystem functioning: Current knowledge and future challenges. Science 294:804–808.

Maechler, M., P. Rousseeuw, A. Struyf, M. Hubert, and K. Hornik. 2019. Finding groups in data: Cluster analysis extended. R Packag. version 2.0 6.

Malika, C., N. Ghazzali, V. Boiteau, and A. Niknafs. 2014. NbClust: An r package for determining the relevant number of clusters in a data set. Journal of Statistical Software 61:1–36.

Mattson, D. A., and W. J. Herms. 1992. The dilemma of plants: To grow or defend. The Quarterly Review of Biology 67:283–335.

McGlinn, D. J., X. Xiao, F. May, N. J. Gotelli, T. Engel, S. A. Blowes, T. M. Knight, O. Purschke, J. M. Chase, and B. J. McGill. 2019. Measurement of biodiversity (mob): A method to separate the scale-dependent effects of species abundance distribution, density, and aggregation on diversity change. Methods in Ecology and Evolution 10:258–269.

McKey, D. 1994. Legumes and nitrogen: The evolutionary ecology of a nitrogen-demanding lifestyle. Advances in Legume Systematics 5: The Nitrogen Factor 5:211–228.

Nippert, J. B., A. K. Knapp, and J. M. Briggs. 2006. Intra-annual rainfall variability and grassland productivity: Can the past predict the future? Plant Ecology 184:65–74.

Ogden, J. C., S. M. Davis, K. J. Jacobs, T. Barnes, and H. E. Fling. 2005. The use of conceptual ecological models to guide ecosystem restoration in South Florida. Wetlands 25:795–809.

Oksanen, J., F. G. Blanchet, M. Friendly, R. Kindt, P. Legendre, D. McGlinn, P. R. Minchin, R. O'hara, G. L. Simpson, P. Solymos, and others. 2016. Vegan: Community ecology package. R package version 2.4-3. Vienna: R Foundation for Statistical Computing.

Pacala, S. W., and M. Rees. 1998. Models suggesting field experiments to test two hypotheses explaining successional diversity. The American Naturalist 152:729–737.

Passarge, J., S. Hol, M. Escher, and J. Huisman. 2006. Competition for nutrients and light: Stable coexistence, alternative stable states, or competitive exclusion? Ecological Monographs 76:57–72.

Pitt, M. D., and H. F. Heady. 1978. Responses of annual vegetation to temperature and rainfall patterns in northern California. Ecology 59:336–350).

Porensky, L. M., K. J. Vaughn, and T. P. Young. 2012. Can initial intraspecific spatial aggregation increase multi-year coexistence by creating temporal priority? Ecological Applications 22:927–936.

Powell, K. I., J. M. Chase, and T. M. Knight. 2013. Invasive plants have scale-dependent effects on diversity by altering species-area relationships.

Prugh, L. R., N. Deguines, J. B. Grinath, K. N. Suding, W. T. Bean, R. Stafford, and J. S. Brashares. 2018. Ecological winners and losers of extreme drought in California. Nature Climate Change 8:819–824.

Reich, P. B. 2014. The world-wide 'fast-slow' plant economics spectrum: A traits manifesto. Journal of Ecology 102:275–301.

Sala, O. E., L. A. Gherardi, L. Reichmann, E. Jobbágy, and D. Peters. 2012. Legacies of precipitation fluctuations on primary production: Theory and data synthesis. Philosophical Transactions of the Royal Society B: Biological Sciences 367:3135–3144.

Sandel, B., and E. M. Dangremond. 2012. Climate change and the invasion of California by grasses. Global Change Biology 18:277–289.

Sax, D. F., and S. D. Gaines. 2003. Species diversity: From global decreases to local increases. Trends in Ecology and Evolution 18:561–566.

Scheiner, S. M. 2003. Six types of species-area curves. Global Ecology and Biogeography 12:441–447.

Schuler, M. S., J. M. Chase, and T. M. Knight. 2015. More individuals drive the species energy-area relationship in an experimental zooplankton community. Oikos 124:1065–1070.

Seabloom, E. W., O. N. Bjørnstad, B. M. Bolker, and O. J. Reichman. 2005. Spatial signature of environmental heterogeneity, dispersal, and competition in successional grasslands. Ecological Monographs 75:199–214.

Seabloom, E. W., E. T. Borer, V. L. Boucher, R. S. Burton, K. L. Cottingham, L. Goldwasser, W. K. Gram, B. E. Kendall, and F. Micheli. 2003a. Competition, seed limitation, disturbance, and reestablishment of California native annual forbs. Ecological Applications 13:575–592.

Seabloom, E. W., E. T. Borer, and L. L. Kinkel. 2018. No evidence for trade-offs in plant responses to consumer food web manipulations. Ecology 99:1953–1963.

Seabloom, E. W., W. S. Harpole, O. J. Reichman, and D. Tilman. 2003b. Invasion, competitive dominance, and resource use by exotic and native California grassland species. Proceedings of the National Academy of Sciences of the United States of America 100:13384–9.

Seastedt, T. R., R. J. Hobbs, and K. N. Suding. 2008. Management of novel ecosystems: Are novel approaches required? Frontiers in Ecology and the Environment 6:547–553.

Slette, I. J., A. K. Post, M. Awad, T. Even, A. Punzalan, S. Williams, M. D. Smith, and A. K. Knapp. 2019. How ecologists define drought, and why we should do better. Global Change Biology 25:3193–3200.

Smith, M. D. 2011. An ecological perspective on extreme climatic events: A synthetic definition and framework to guide future research. Journal of Ecology 99:656–663.

Smith, M. D., and A. K. Knapp. 2003. Dominant species maintain ecosystem function. Ecology Letters 6:509–517.

Smith, M. D., K. J. La Pierre, S. L. Collins, A. K. Knapp, K. L. Gross, J. E. Barrett, S. D. Frey, L. Gough, R. J. Miller, J. T. Morris, L. E. Rustad, and J.

Yarie. 2015. Global environmental change and the nature of aboveground net primary productivity responses: insights from long-term experiments. Oecologia 177:935–947.

Smith, M. D., J. C. Wilcox, T. Kelly, and A. K. Knapp. 2004. Dominance not richness determines invasibility of tallgrass prairie. Oikos 106:253–262.

Soons, M. B., M. M. Hefting, E. Dorland, L. P. M. Lamers, C. Versteeg, and R. Bobbink. 2017. Nitrogen effects on plant species richness in herbaceous communities are more widespread and stronger than those of phosphorus. Biological Conservation 212:390–397.

Stampfli, A., and M. Zeiter. 2004. Plant regeneration directs changes in grassland composition after extreme drought: A 13-year study in southern Switzerland. Journal of Ecology 92:568–576.

Stein, C., W. S. Harpole, and K. N. Suding. 2016. Transitions and invasion along a grazing gradient in experimental California grasslands. Ecology 97:2319–2330.

Stevens, M. H., and W. P. Carson. 1999. Plant density determines species richness along an experimental fertility gradient. Ecology 80:455–465.

Stringham, T. K., W. C. Krueger, and P. L. Shaver. 2003. State and Transition Modeling: An Ecological Process Approach. Journal of Range Management 56:106.

Stromberg, M. R., C. M. D'Antonio, T. P. Young, J. Wirka, and P. Kephart. 2007. California Grassland Restoration. *in* M. R. Stromberg, J. D. Corbin, and C. M. D'Antonio, editors. California grasslands ecology and management. First Edition. University of California Press, Berkeley; Los Angeles, California.

Stuble, K. L., E. P. Zefferman, K. M. Wolf, K. J. Vaughn, and T. P. Young. 2017. Outside the envelope: Rare events disrupt the relationship between climate factors and species interactions. Ecology 98:1623–1630.

Suding, K. N., S. L. Collins, L. Gough, C. Clark, E. E. Cleland, K. L. Gross, D. G. Milchunas, and S. Pennings. 2005. Functional- and abundance-based mechanisms explain diversity loss due to N fertilization. Proceedings of the National Academy of Sciences of the United States of America 102:4387–4392.

Suttle, K. B., M. A. Thomsen, and M. E. Power. 2007. Species Interactions Reverse Grassland Responses to Changing Climate. Science 315:640–642.

Tilman, D. 1982a. Resource competition and community structure. Princeton University Press.

Tilman, D. 1982b. Resource competition and community structure. First Edition. Princeton University Press, Princeton, New Jersey.

Tilman, D. 1987. Secondary succession and the pattern of plant dominance along experimental nitrogen gradients. Ecological Monographs 57:189–214.

Tilman, D. 1994. Competition and Biodiversity in Spatially Structured Habitats. Ecology 75:2–16.

Tilman, D., and C. Lehman. 2001. Human-caused environmental change: impacts on plant diversity and evolution. Proceedings of the National Academy of Sciences 98:5433–5440.

Tilman, G. D. 1984. Plant Dominance Along an Experimental Nutrient Gradient. Ecology 65:1445–1453.

Tjørve, E., W. E. Kunin, C. Polce, and K. M. Tjørve. 2008. Species-area relationship: Separating the effects of species abundance and spatial distribution. Journal of Ecology 96:1141–1151.

Tylianakis, J. M., R. K. Didham, J. Bascompte, and D. A. Wardle. 2008. Global change and species interactions in terrestrial ecosystems. Ecology Letters 11:1351–1363.

Uricchio, L. H., S. C. Daws, E. R. Spear, and E. A. Mordecai. 2019. Priority Effects and Nonhierarchical Competition Shape Species Composition in a Complex Grassland Community. The American Naturalist 193:213–226.

Vellend, M., and L. Baeten. 2013. Global meta-analysis reveals no net change in local-scale plant biodiversity over time 110:19456–19459.

Vicente-Serrano, S. M., S. Beguería, and J. I. López-Moreno. 2010. A multiscalar drought index sensitive to global warming: The standardized precipitation evapotranspiration index. Journal of Climate 23:1696–1718.

Vitousek, P. M., J. D. Aber, R. W. Howarth, G. E. Likens, P. A. Matson, D. W. Schindler, W. H. Schlesinger, and D. G. Tilman. 1997a. Human alteration of the global nitrogen cycle: Sources and consequences. Ecological Applications 7:737–750.

Vitousek, P. M., and R. W. Howarth. 1991. Nitrogen limitation on land and in the sea: How can it occur? Biogeochemistry 13:87–115.

Vitousek, P. M., H. A. Mooney, J. Lubchenco, and J. M. Melillo. 1997b. Human domination of Earth's ecosystems. Science 277:494–499.

Vitousek, P. M., S. Porder, B. Z. Houlton, and O. A. Chadwick. 2010. Terrestrial phosphorus limitation: Mechanisms, implications, and nitrogen-phosphorus interactions. Ecological Applications 20:5–15.

Wainwright, C. E., E. M. Wolkovich, and E. E. Cleland. 2012. Seasonal priority effects: Implications for invasion and restoration in a semi-arid system. Journal of Applied Ecology 49:234–241.

Wilcox, K. R., S. E. Koerner, D. L. Hoover, A. K. Borkenhagen, D. E. Burkepile, S. L. Collins, A. M. Hoffman, K. P. Kirkman, A. K. Knapp, T. Strydom, and others. 2020. Rapid recovery of ecosystem function following extreme drought in a south african savanna grassland. Ecology 101:e02983.

Williams, J. W., and S. T. Jackson. 2007. Novel climates, no-analog communities, and ecological surprises. Frontiers in Ecology and the Environment 5:475–482.

Wilson, S. D., and D. Tilman. 1991. Components of Plant Competition Along an Experimental Gradient of Nitrogen Availability Author. Ecology 72:1050–1065.

Wright, I. J., P. B. Reich, M. Westoby, D. D. Ackerly, Z. Baruch, F. Bongers, J. Cavender-Bares, T. Chapin, J. H. C. Cornellssen, M. Diemer, J. Flexas, E. Garnier, P. K. Groom, J. Gulias, K. Hikosaka, B. B. Lamont, T. Lee, W. Lee, C. Lusk, J. J. Midgley, M. L. Navas, Ü. Niinemets, J. Oleksyn, H. Osada, H. Poorter, P. Pool, L. Prior, V. I. Pyankov, C. Roumet, S. C. Thomas, M. G. Tjoelker, E. J. Veneklaas, and R. Villar. 2004. The worldwide leaf economics spectrum. Nature 428:821–827.

Yoon, J. H., S. Y. Wang, R. R. Gillies, B. Kravitz, L. Hipps, and P. J. Rasch. 2015. Increasing water cycle extremes in California and in relation to ENSO

cycle under global warming. Nature Communications 6.

Young, J. A. 1992. Ecology and management of medusahead (Taeniatherum caput-medusae ssp. asperum Melderis). Great Basin Naturalist 52:242–252.

Young, T. P., K. L. Stuble, J. A. Balachowski, and C. M. Werner. 2017. Using priority effects to manipulate competitive relationships in restoration. Restoration Ecology 25:S114–S123.

Young, T. P., E. P. Zefferman, K. J. Vaughn, and S. Fick. 2014. Initial success of native grasses is contingent on multiple interactions among exotic grass competition, temporal priority, rainfall and site effects. AoB Plants 7:plu081.

Zavaleta, E. S., M. R. Shaw, N. R. Chiariello, B. D. Thomas, E. E. Cleland, C. B. Field, and H. A. Mooney. 2003. Grassland responses to three years of elevated temperature, CO 2, precipitation, and N deposition. Ecological Monographs 73:585–604.